THE AMERICAN JOURNAL OF PATHOLOGY

VOLUME XXXIX AUGUST, 1961 NUMBER 2

SILICONE EMBOLIZATION DURING CLINICAL AND EXPERIMENTAL HEART SURGERY EMPLOYING A BUBBLE OXYGENATOR

DONALD A. B. LINDBERG, M.D.*; FRED V. LUCAS, M.D.*; JOHN SHEAGREN, B.A., AND JAMES R. MALM, M.D.

From the Department of Pathology and the Department of Surgery, Columbia University College of Physicians and Surgeons and the Presbyterian Hospital, New York, N.Y.

Several techniques have been developed to replace the function of the heart and lungs during the performance of open-heart surgery.[1-3] These generally necessitate oxygenation of the blood outside the body. Such artificial pump-oxygenators have the inherent danger of embolization of various materials, viz., fibrin, air, and silicone antifoaming compound.[4-7] This report includes our experience with one pump-oxygenator unit and illustrates the problem of embolization of silicone antifoaming material both in man and in experimental animals.

MATERIAL AND METHODS

Oxygenation

A DeWall type bubble oxygenator[2] was utilized at this institution from 1956 through 1959 for open-heart operations. This unit maintains the extracorporeal circulation through the use of finger-type Sigma motor pumping units at the arterial and venous ends of the circuit. Oxygen is forced through a ceramic plate into a vertical column of blood which constitutes the oxygenator. The frothy mixture then passes into a defoaming unit containing plastic or steel wool pads and into a helical debubbling unit. Here the gases are permitted to escape into the open reservoir and thence to the outside. The silicone antifoam agent (Antifoam A, Dow Corning Corp., Midland, Michigan) [8,9] was applied to all inner plastic surfaces of the upper end of the oxygenator column, the debubbling chamber, and the upper end of the helix. Every effort was made to apply the antifoam emulsion as thinly as possible, and all excess was removed prior to autoclaving. In addition, small quantities of silicone antifoam were sprayed into the cardiotomy reservoir when required to control

Accepted for publication, March 29, 1961.

* Present address: Department of Pathology, University of Missouri, Columbia, Mo.

foaming. The silicone emulsion was also applied to the plastic or steel wool sponges within the defoaming unit by baking so as to reduce excess of silicone.

Surgical Procedure

Venous blood was withdrawn by cannulation of the inferior vena cava. After oxygenation, as already described, the blood was returned to an iliac artery and forced upward into the aorta. The coronary arteries derived their flow from blood which had passed upward through the aorta.

Ten of the cases reported had open-heart surgery and were treated in the manner just described. In two additional patients, operations were performed for thoracic aneurysm, utilizing a left atrial-femoral by-pass technique. The aorta in these cases was clamped above and below the aneurysm. Thus, the contracting left ventricle sent blood to the carotid arteries and great vessels arising proximal to the upper aortic clamp. The renal arteries and such vessels as arose below the distal aortic clamp were perfused by artificial means. For this purpose the left atrium was cannulated, and blood, oxygenated in the lungs, was continuously removed, drawn into the pumps, and forced upward into a femoral artery to perfuse the lower aorta and its branches.

Experiments of analogous type were performed on 14 dogs. In 6 of these, silicone or air bubbles were injected directly into the renal arteries or the left ventricles of intact animals. In 8 dogs a simulated open-heart operation was performed. In all 8, the blood from the venae cavae was oxygenated artificially as described and was then returned under pressure to the iliac artery.

Anatomic Observations

All 12 human cases had necropsy examinations. In only one case was the brain not investigated. Necropsies were performed on all experimental animals. Samples of major organs of the dogs and of some of the patients were fixed under reduced pressure after the method of Heimbecker.[10] In both groups microscopic preparations of all viscera were stained with hematoxylin and eosin and examined under bright field illumination. In addition, unstained sections were viewed under phase contrast illumination.

Results

The role of silicone embolization is best illustrated by considering in detail a human case. Following this illustration is a summary of all 12 patients and also the results observed in experimental dogs.

Case Report

Case 1 was a patient who had total cardiopulmonary by-pass with the DeWall pump-oxygenator.

A 35-year-old white man had a ventricular septal defect and severe pulmonic stenosis. Cardiac catheterization also suggested a possible atrial septal defect. Preoperative laboratory determinations were normal with respect to hemoglobin, hematocrit, blood urea nitrogen, urinalysis, and serum electrolytes. Open-heart surgery was performed with total cardiopulmonary by-pass at normothermia at a perfusion rate of 75 ml. per kg. of body weight for a period of 140 minutes. Elective cardiac arrest was induced by perfusion of the coronary arteries with 40 ml. of 2½ per cent potassium citrate, after clamping the proximal portion of the aorta. Through a right ventriculotomy incision the ventricular septal defect was closed with interrupted sutures and the valvular pulmonic stenosis relieved by direct fracture. A cleft medial tricuspid leaflet was repaired through the atrial incision. The operation lasted 5 hours. Following the operation, satisfactory cardiac beat could not be maintained, and for 4 days the heart beat was maintained by an electrical pacemaker through wires inserted in the myocardium. Because of the progressive accumulation of blood in the

left hemithorax, the patient was re-explored 9 hours postoperatively. A small branch of the left coronary artery was found to have been lacerated and was ligated. A tracheostomy was performed. Blood pressure throughout the 4 days averaged 70/50 despite vasopressor infusion. The patient never regained consciousness and on 2 occasions had grand mal seizures. Urine output was 900 ml. over the 4-day period, including a mere 81 ml. during the terminal 24 hours. The blood urea nitrogen (BUN) had risen to 90 mg. per hundred cc. on the third postoperative day. The patient died 91 hours after the initial operation.

At necropsy, the prosthetic patch totally obliterated the interventricular septal defect. The pulmonic infundibulum was stenotic. A congenital cleft in the anterior leaflet of the tricuspid valve had been repaired satisfactorily. Nonetheless, 4/5 of the myocardium, including that of the left and right ventricles and interventricular septum, was the seat of total infarction as judged both grossly and microscopically. This degree of infarction was vastly greater than that ordinarily seen in association with mere manipulation of the heart. Moreover, it far exceeded the area of distribution of the lacerated branch of the coronary artery. The lungs and viscera were congested. Necrotizing tracheitis and esophagitis were present as a result of intubation. A single large pale kidney was located; the second kidney was congenitally absent.

Microscopic Examination

Microscopic examination of the kidney revealed dilated capillary loops in the glomeruli (Fig. 1). The capillaries at first glance seemed empty. Nevertheless, careful inspection showed the existence of finely granular material in some of the dilated capillary loops, suggesting the presence of small, nearly transparent emboli. The endothelial nuclei were flattened and often assumed an extra-luminal position. Occasionally, intracapillary erythrocytes appeared flattened against the vessel walls. Evidence of emboli in dilated capillary loops was present in about 50 per cent of the glomeruli in sections stained with hematoxylin and eosin. Frequently more than one capillary loop in each glomerulus was affected. Because of the transparent nature of the microscopic emboli, it was assumed that they might represent silicone. Various special stains were employed, but in no case were the refractile granules stained. Frozen sections stained with Sudan IV showed a layer of dye adhering to the periphery of the round emboli or stringing through the material (Fig. 2). The presence of the refractile silicone emboli was accentuated by examination of unstained sections under phase contrast illumination (Fig. 3), or by greatly reducing the intensity of ordinary illumination for stained sections.

The brain contained multiple small areas of fresh encephalomalacia in the cerebral and cerebellar white matter. These were largely perivascular. Also there were petechial hemorrhages in the perivascular regions of these areas in the basal ganglia and brain stem. Refractile emboli were demonstrated in these regions on examination with phase contrast illumination (Figs. 4 and 5). We shall present evidence that this material was silicone antifoam.

TABLE I

SUMMARY OF CASES

Case no.	Age and sex	Lesion	Operation	Duration, perfusion (min.)	Duration, elective arrest (min.)	Survival (hr.)
1	35 M	Defect of interventricular septum, pulmonary infundibulum, tricuspid valve	Right ventriculotomy; repair septum	140	58	91
2	31 F	Interatrial septal defect	Right atriotomy; prosthetic patch; exploratory right ventriculotomy	59	32 K+ citrate	36
3	33 F	Mitral stenosis	Mitral commissurotomy; prosthetic patch to aortic leaflet	95	K+ citrate	91
4	45 M	Left atrial myxoma	Right atriotomy; trans-septal resection of myxoma	125	87 K+ citrate	6
5	17 F	Interatrial septal defect	Right ventriculotomy; suture septal defect	55	31 K+ citrate	36
6	45 M	Calcific aortic stenosis	Aortotomy; dilate aortic valve; remove some calcium	99	None	0
7	44 F	Interatrial septal defect	Right atriotomy; prosthetic patch to septum	120	None	9
8	15 M	Tetralogy of Fallot	Right ventriculotomy; patch to ventricular septum; excise portion of pulmonary valve and outflow tract	120 *	Chilled	20
9	17 F	Tetralogy of Fallot	Right ventriculotomy; suture septal defect; patch to pulmonary outflow tract; excise portion of pulmonary infundibulum	120 *	None	13
10	43 F	Interatrial septal defect	Right atriotomy; apply prosthetic patch to septal defect	45	None	0
11	59 F	Dissecting aortic aneurysm	Left thoracotomy; re-entry fenestration of aneurysm	45 †	None	35
12	67 M	Dissecting aortic aneurysm	Left thoracotomy; resection of thoracic aneurysm	90 †	None	0

* Perfusion rate severely reduced during septal closure.
† Partial perfusion without oxygenation.

TABLE II

TABLE II

SUMMARY OF POSTOPERATIVE FUNCTION OF THE HEART, KIDNEYS AND BRAIN

Case no.	Blood pressure (mm. Hg)	Cardiac rhythmicity	Urine output	Urinalysis or BUN	Level of consciousness	Pertinent autopsy findings
1	70/50	Electrical pacemaker maintenance	900 ml. in 4 days	BUN = 90 mg. % on 3rd day	Unconscious; grand mal seizures	Massive infarction of right and left ventricles; multiple areas of acute encephalomalacia and petechial hemorrhages in brain; silicone emboli in above regions and in 60% of glomeruli
2	70/60	Regular rhythm	15 ml./hr. at best	BUN = 31 mg. %	Unconscious	Infarction of 4/5 of right and left ventricles; recent encephalomalacia of cerebral cortex and white matter; silicone emboli in myocardium, cerebral cortex, 55% of glomeruli
3	70/40	Regular rhythm	Oliguric	3–4+ protein, BUN = 85 mg. % K+ = 5.8 mEq/l.		Massive infarction of left and right ventricles; silicone emboli in myocardium and 60% of glomeruli *
4	75/40	Regular rhythm	Anuric		Unconscious	Massive infarction of right and left ventricles; multiple areas of acute encephalomalacia in cerebral cortex and white matter, corpora striata, cerebellar dentate nuclei; silicone emboli in myocardium, cerebral cortex and white matter, 60% of glomeruli
5	100/70	Electrical pacemaker maintenance	100 ml. total	4+ protein, BUN = 110 mg. %	Conscious in 8 hr.	Fresh encephalomalacia in white matter of cerebrum and cerebellum; silicone emboli in myocardium, adrenal, white matter of cerebrum and cerebellum, and 25% of glomeruli
6		Ventricular fibrillation at end of operation				Bilateral hemothorax; focal interstitial hemorrhages in myocardium; silicone emboli in myocardium, cerebral cortex and 50% of glomeruli
7		Regular rhythm	Anuric		Conscious	Hypoplasia of aorta and aortic valve; silicone emboli in myocardium, cerebrum, cerebellum and 55% of glomeruli
8	70/40	Regular rhythm			Speaking	Ischemic necrosis of cerebral nerve cells and basal ganglia cells; silicone emboli in cerebral cortex and 50% of glomeruli
9	60	Electrical pacemaker maintenance	20 ml.	3+ protein, BUN = 30 mg. %	Unconscious	Focal necrosis of myocardium and cerebral cortex; silicone emboli in cerebrum, cerebellum, myocardium and 45% of glomeruli
10		Ventricular fibrillation at end of operation				Silicone emboli in 10% of glomeruli; brain normal
11	100/60–65/40	Regular rhythm	214 ml. in 1st 24 hr.		Semi-conscious	Dissecting aneurysm extending from aortic ring to iliac bifurcation; no silicone emboli
12		Ventricular fibrillation and dilatation at end of operation				Generalized arteriosclerosis; syphilitic aortitis; no silicone emboli

* Brain not examined.

The myocardial necrosis was indeed massive and had progressed to fragmentation of muscle fibers with the accumulation of segmented leukocytes (Fig. 6). Clear refractile emboli were demonstrated in the capillaries and arterioles of the heart, although not every field of necrotic fibers contained an embolus.

Observations

The case histories of the 9 other patients who had intracardiac surgery closely resembled that of case 1 presented in detail above. The same procedures of necropsy examination were followed, and the observations were in general identical. Specifically, silicone emboli were found in the kidneys, heart, and brain in all. Morphologically, the emboli were as described above. The cases are summarized in Tables I and II. Cases 1 to 10 constitute all persons who had open heart surgery with extracorporeal circulation who were necropsied at this hospital.

The ages of the patients who had heart operations ranged from 15 to 45 years. Both sexes were represented. The heart lesions were congenital in 7, and in 3 (cases 3, 4 and 6) the lesions were acquired. The durations of the operative procedures varied greatly, but only the durations of the actual extracorporeal perfusions are listed in Table I. Necropsy revealed multiple silicone emboli in the kidneys, brain, and heart in all 10 cases. Massive myocardial infarction was present in cases 1, 2 and 3, with involvement of the right as well as the left ventricle and interventricular septum.

The number of emboli was most easily evaluated from the kidney sections. The percentage of glomeruli which contained embolic material was estimated from multiple sections of both kidneys. Patients 1 and 2 were perfused for over an hour at normal flow rates and had 50 per cent or more of the glomeruli affected. Patients 5 and 10 were perfused for a lesser period of time and demonstrated emboli in only 10 and 25 per cent of the glomeruli. When the time of perfusion was prolonged but the rate of perfusion was markedly reduced (e.g., patients 8 and 9), the number of emboli in the kidneys was in the 50 per cent range.

Cases 11 and 12 (Table I) did not have extracorporeal oxygenation but had intrathoracic operations for aortic aneurysms. In these, it was necessary to cross-clamp and isolate a segment of aorta. For this reason extracorporeal circulation was employed during the operations. A cannula was introduced into the left atrium, and approximately 1,500 ml. of blood per minute was removed and shunted into the Sigma motor pumps. From the extracorporeal pump it was then returned through a cannula in an iliac artery. The body was thus perfused with blood oxygenated in the patients' own lungs, and the blood was not exposed at any time to

the siliconized defrothing chamber of the DeWall oxygenator. In these cases extracorporeal circulation was maintained for 45 and 90 minutes. Yet necropsy revealed no evidence of silicone embolization.

In Table II an attempt has been made to present whatever objective evidence was available relating to the postoperative function of the heart, kidneys, and brain. The postoperative urinalysis and BUN determination are reported if they were performed. Arterial blood pressure determinations were always multiple but are presented as one representative value.

All of the patients cited who had intracardiac operative manipulation had postoperative hypotension. Cardiac rhythmicity in 2 of these could be maintained only with the electrical pacemaker. Renal function in the period immediately following operation was also impaired in all cases, with oliguria or anuria appearing as a consistent finding. Three patients did not regain consciousness after operation. Patient 1 had repeated convulsions. None of the 10 patients survived longer than 91 hours, so that all these phenomena might be related merely to hypotension and major operative stress. Case 11 was a person who did not have contact with the siliconized apparatus and yet displayed oliguria and hypotension.

Experimental Perfusion Studies (Table III)

In group A, the left renal arteries of 2 mongrel dogs were perfused with a mixture of 100 ml. of autologous venous blood and 10 cc. of Dow Corning Antifoam B. Sections of the right kidneys and other major organs were normal. Sections of the left kidneys revealed many clusters of refractile emboli in the glomerular capillaries (Fig. 7). This presented a dramatic and exaggerated version of the human lesions. Associated with the emboli in these acute experiments was a heavy proteinaceous urine in the proximal and distal renal tubules.

TABLE III

ANTIFOAM IN EXPERIMENTAL DOGS

Group	No. of dogs	Procedure	Location of emboli
A	2	Silicone in renal artery	80% of glomeruli
B	2	Air in renal artery	No silicone emboli
C	2	Silicone in left ventricle	Lungs, 10% of glomeruli
D	2	Perfusion for 120 minutes	Heart, brain, 70% of glomeruli
	2	Perfusion for 75 minutes	Heart, brain, 60% of glomeruli
	2	Perfusion for 30 minutes	Heart, brain, 50% of glomeruli
E	2	Transfusion with priming blood	Brain, 20% of glomeruli

In group B, a second pair of dogs was subjected to perfusion of the left renal artery with 100 ml. of autologous blood. No antifoam was employed. The blood was first shaken with air to a foamy consistency before being perfused, in order to create the possibility of air embolization. The resultant renal lesions consisted largely of hemorrhages into Bowman's capsule and the proximal tubules and occasionally interstitial hemorrhages in the cortex and pyramids. Nothing resembling the silicone emboli was observed.

Two dogs in group C were subjected to percutaneous puncture of the left ventricle. Through a number 18 needle and syringe, 50 cc. of autologous venous blood and 2 cc. of silicone antifoam were introduced into the chamber of the left ventricle. The dogs did not survive this procedure, cardiac arrest occurring within 3 minutes after cardiac puncture. In scattered renal glomeruli, capillary loops were dilated and contained clear silicone emboli resembling those observed in the previous dogs and in the patients. Scattered emboli were noted in pulmonary alveolar capillaries. The total number identified was small. None were demonstrated in the vessels of the brain.

Dogs in group D were subjected to total cardiopulmonary by-pass with the use of the DeWall bubble oxygenator. Pairs of animals were perfused for 120, 75 and 30 minutes. The dogs' organs were grossly normal after perfusion, but microscopic sections revealed typical glomerular capillary emboli (Fig. 8). Clear emboli were present in capillaries of the white matter of cerebrum and cerebellum and capillaries of the heart. Encephalomalacia was not present, but none of the animals lived over 12 hours. The concentration of emboli was best judged in the kidney and appeared to decrease with shorter durations of perfusion. Urine formed during perfusion or within 12 hours thereafter gave a 3 to 4 plus reaction for protein on acidification and heating.

Dogs in group E were neither perfused nor operated upon. Instead, aliquots of blood were removed from the femoral artery, and equivalent volumes of homologous canine blood were instilled in the femoral vein. The homologous blood was obtained from the arterial reservoir of the DeWall oxygenator apparatus at the termination of a 60-minute perfusion. Thus the blood which was given intravenously to the dogs in group E had been circulated through the bubble oxygenator and thoroughly mixed with the silicone substances lining the apparatus. Yet the group E dogs were not themselves subjected to extracorporeal oxygenation. These animals had no contact with the oxygenator except for the fact that the blood they received had circulated through the machine for 2 hours. Silicone emboli were demonstrable in the kidneys of these animals. The number of emboli was significantly reduced; perhaps 2

of 10 renal glomeruli showed them. Few emboli were present in the brain. Encephalomalacia was not noted.

Discussion

The problems presented by this investigation center largely about the following areas: (a) the validity of the evidence that embolization of silicone occurs in open-heart surgery utilizing the oxygenator apparatus described; (b) the quantitative relationship between embolization and the manner of extracorporeal oxygenation; (c) the physiologic significance of embolization in various regions.

Evidence of Silicone Embolization

On theoretical grounds, the possibility of silicone embolization from the extracorporeal pump-oxygenator is apparent. The material is applied manually or from a compressed freon spray-can to the internal surface of all tubing through which the most turbulent blood flow is anticipated, specifically the oxygenation column and the spiral debubbler helix. This equipment is washed and autoclaved but cannot be subjected to heat sufficiently great to actually bake the silicone agent. In a 120-minute perfusion of a 70 kg. patient, approximately 630 l. of blood course through the oxygenator unit. Thus, there is ample opportunity for embolization to occur.

Microscopic preparations from all patients and dogs perfused on the DeWall pump-oxygenator demonstrated clear refractile intravascular material in dilated capillaries. The material appeared in focal distribution throughout the kidney, myocardium, and cerebrum. In addition, there were protein casts in distal renal tubules, focal interstitial myocardial hemorrhage, ischemic necrosis of cerebral cortical cells, and perivascular demyelination of the white matter of the brain. Intervening regions of these organs were apparently healthy, as in the case of ordinary bacterial or thrombotic embolization. These consistent and objective changes in human patients and experimental dogs speak strongly for the existence of embolic phenomena in the process of extracorporeal oxygenation.

What is the identity of the embolic material?

From a histologic standpoint, the differential diagnosis of the lesions in any single human case must include the possibility of air or fat embolism. The appearance of the foreign substance in the glomerular capillaries does not suggest a gas embolus. The material resembles refractile liquid droplets. To test further the possibility of air embolization, crude experiments were conducted in dogs in which gross bubbles of air were deliberately introduced into the renal artery. Lesions similar to

those in the human perfusion cases were not noted. Tissue samples of dogs perfused with the pump-oxygenator were fixed at reduced pressure in order to exaggerate the appearance of possible air emboli. None were demonstrated. Thus, it appeared that under the conditions in which perfusion was carried out in patients and dogs, no gas emboli occurred.

The presence of multiple clear refractile emboli following major surgical procedures immediately brings to mind fat embolization. The emboli in the glomeruli, however, did not give a positive reaction with Sudan IV fat stains. The dye accumulated at the periphery or occasionally bridged the droplets. The basis for this characteristic histologic feature may be the fact that fat stains are highly soluble in neutral fat whereas they are partially miscible in silicones. That the embolic droplets might be fat was ruled out on the ground that they did not stain with fat stains and that there was strong evidence to incriminate silicone antifoam under conditions which excluded the possibility of fat emboli.

Animal experiments were carried out in order to demonstrate that the complex variables of the human surgical problem could be eliminated —save for the antifoam compound—and typical embolic lesions still be produced (Table III). For this reason in group A, perfusion of a single renal artery in the dog was carried out, using a mixture of his own blood and antifoam. Renal emboli identical to those in the human open-heart cases were seen in the absence of either intracardiac surgery or extracorporeal oxygenation. Aside from autologous blood, antifoam was the only agent introduced into the vascular system, and presumably was the substance lodged in the renal glomeruli and brains. Celiotomy was excluded from blame for the emboli by the experiment in group C. Here typical emboli were seen following the introduction of autologous blood and antifoam into the chamber of the left ventricle by percutaneous needle puncture. Again the antifoam alone resulted in multiple clear emboli in capillaries of the glomeruli and lung.

It appeared reasonable to determine whether merely mixing silicone and blood in a syringe before administration was comparable with the hemodynamic factors acting on blood inside the turbulent DeWall oxygenator chamber. The two methods of obtaining silicone-blood mixtures were shown to be comparable in the group E dogs. In this experiment, blood was removed from the "dead space" of the pump-oxygenator after it had been used for an animal perfusion study. The tubing and helical debubbling chamber contained much thoroughly mixed blood. Samples were removed and perfused into the venous circulation of intact dogs in group E. Sections of the dogs' kidney, heart, lung, and adrenal revealed typical silicone emboli. Thus it was possible to show that the arbitrary

addition of antifoam liquid was not necessary to produce the emboli, but that the blood remaining in the oxygenator apparatus after thorough mixing contained enough suspended antifoam to produce easily recognizable emboli.

If the silicone embolization demonstrated in experimental dogs occurred also in human patients, certain predictions should be possible concerning its behavior. Emboli should always be present in the human subject when extracorporeal oxygenation had been carried out utilizing the oxygenator described. The silicone emboli should not be present when the oxygenator had not been employed. The number of emboli present in the human patient should be quantitatively related to the duration and extent of contact with the siliconized oxygenator.

These theoretical predictions do, in fact, hold true. All of the 10 human subjects who had oxygenation had multiple silicone emboli in many organ sections (cases 1 to 10). Furthermore, no emboli were present in the tissues of two persons who had extracorporeal circulation without oxygenation (cases 11 and 12).

Quantitative and Physiologic Considerations

In both human subjects and experimental dogs, prolonged perfusion and high flow rates tended to produce large numbers of silicone emboli in the renal glomeruli. In the human patients, low flow rates tended to reduce the number of emboli expected with prolonged perfusions. This is in consonance with the thesis that prolonged turbulent flow removes the antifoam compound from its tenuous grip on the internal walls of the oxygenator. The minimal duration of perfusion necessary to induce embolization of antifoam has not been established. We can only state that emboli were observed in patients after 45 minutes of perfusion and in dogs after 30 minutes. Further experiments to determine if a safe perfusion time exists should be conducted if it remains necessary to employ this oxygenator apparatus.

The physiologic consequences of embolization should be quantitatively related to the number of emboli thrown into the circulation. But here the present observations and experiments are not adequate for firm conclusions. Malfunction of the kidneys, myocardium, and cerebrum have been noted in the patients with intracardiac surgical procedures. Yet one cannot be certain that even without silicone emboli patients recovering from major operations might not have similar aberrations. Blood urea nitrogen elevation and heavy proteinuria could be the consequences of hypotension alone. That the heavy proteinuria observed was the result of embolic damage to the glomerular membrane was more strongly suggested in the experimental dog. Here urine was examined

both during and immediately after the perfusion. Heavy proteinuria was always observed, whereas oliguria was not present.

The significance of silicone emboli in the myocardial capillaries, especially those of humans with massive myocardial necrosis, is a compelling problem. Emboli were present in varying numbers in the hearts of all human patients and in many experimental animals. Yet massive infarction did not occur in the majority of human cases, being striking only in 3. It is extremely difficult to reconstruct the amount of handling of the heart required for any particular operation. Thus, it must be assumed that silicone emboli, if they play any role in myocardial infarction, play only a contributory one which is dwarfed by the effects of physical trauma to the heart and by the systemic hypotension.

Multiple small silicone emboli were present in sections of cerebellum and cerebrum in human patients and dogs and were associated with focal ischemic necrosis. Dogs perfused by bubble oxygenators of the sort used in these experiments have been reported by others to show gross neurologic manifestations of cerebral and cerebellar damage.[4–6] In their series, Giannelli and colleagues[5] postulated embolization as the cause for the brain dysfunction observed. We feel silicone embolization definitely affects the brain. In the present series the dogs did not survive long enough either for meaningful neurologic examinations or for acute encephalomalacia to have been recognized on microscopic examination. The human cases provided unequivocal evidence that multiple small areas of cerebral and cerebellar infarction and hemorrhage did in fact occur following open-heart perfusions. These were associated with silicone emboli in the local or adjacent capillaries. Postoperative neurologic examinations failed to reveal distinctive lesions.

Summary

In 10 human patients who died following open-heart surgical procedures and perfusion with the DeWall extracorporeal pump-oxygenator, clear refractile emboli were demonstrated in the capillaries of the kidney, brain and heart. Multiple areas of encephalomalacia and apparently reduced renal function were associated with these lesions. The emboli were identified as silicone antifoam, originating from the treated surface of the oxygenator column and helical debubbling chamber. Identification was based on the production of identical lesions in the kidneys of dogs perfused on the DeWall pump-oxygenator. The emboli had a characteristic appearance when stained with Sudan fat stains.

Addendum

Since the completion of this study, all extracorporeal perfusions have been carried out utilizing a rotating disc oxygenator. All glass surfaces

in contact with blood have a baked silicone resin coating. Silicone emboli have not been noted in animals perfused with this equipment, nor were they noted in one human subject who died following an open-heart operation.

References

1. Björk, V. O. Brain perfusions in dogs with artificially oxygenated blood. *Acta chir. scandinav.*, 1948, **96**, Suppl. 137, 1–122.
2. DeWall, R. A.; Warden, H. E.; Read, R. C.; Gott, V. L.; Ziegler, N. R.; Varco, R. L., and Lillehei, C. W. A simple, expendable, artificial oxygenator for open heart surgery. *S. Clin. North America*, 1956, **36**, No. 4, 1025–1034.
3. Cross, F. S.; Berne, R. M.; Hirose, Y.; Jones, R. D., and Kay, E. B. Evaluation of a rotating disc type reservoir-oxygenator. *Proc. Soc. Exper. Biol. & Med.*, 1956, **93**, 210–214.
4. Owens, G.; Adams, J. E.; Dawson, R. E.; Lance, E. M.; Sawyers, J. L., and Scott, H. W., Jr. Observed central nervous system responses during experimental employment of various pump-oxygenators. *Surgery*, 1958, **44**, 240–254.
5. Giannelli, S., Jr.; Molthan, M. F.; Best, R. J.; Dull, J. A., and Kirby, C. K. The effects produced by various types of pump-oxygenators during two-hour partial infusions in dogs. *J. Thoracic Surg.*, 1957, **34**, 563–569.
6. Yates, P. O.; Cassie, A. B.; Dark, J. F.; Jack, G. D., and Riddell, A. G. The detection of antifoam emboli following perfusion with a heart-lung machine. *Lancet*, 1959, **1**, 130.
7. Penry, J. K.; Cordell, A. R.; Johnston, F. R., and Netsky, M. G. Cerebral embolism by Antifoam A in a bubble oxygenator system: an experimental and clinical study. *Surgery*, 1960, **47**, 784–794.
8. McGregor, R. R. Silicones in Medicine and Surgery. Dow Corning Corp., Midland, Mich., 1957, 44 pp.
9. Barondes, R. deR.; Judge, W. D.; Towne, C. G., and Baxter, M. L. The silicones in medicine: new organic derivatives and some of their unique properties. *Mil. Surgeon*, 1950, **106**, 379–387.
10. Heimbecker, R. O. In: Extracorporeal Circulation. Allen, J. G. (ed.). Charles C Thomas, Springfield, Ill., 1958, pp. 312–314.

We are indebted to Dr. Harry P. Smith for his advice and patient criticism.

[*Illustrations follow*]

Legends for Figures

Fig. 1. Case 1. A 35-year-old man, perfused on the DeWall pump-oxygenator for 140 minutes. The capillaries of a renal glomerulus are dilated by clear silicone emboli. Hematoxylin and eosin stain. × 310.

Fig. 2. Case 1. An ovoid silicone embolus lies within a glomerular capillary. The fat stain has accumulated at its periphery rather than having dissolved homogeneously throughout the embolus. Sudan IV stain. × 390.

Fig. 3. Case 1. A glomerular capillary is dilated by a cylindrical, refractile silicone embolus. Unstained section, phase contrast illumination. × 320.

Fig. 4. Case 1. Cerebral cortex. A sausage-shaped silicone embolus lies within a dilated cerebral capillary. The surrounding brain shows gliosis and encephalomalacia. Unstained section, phase contrast illumination. × 390.

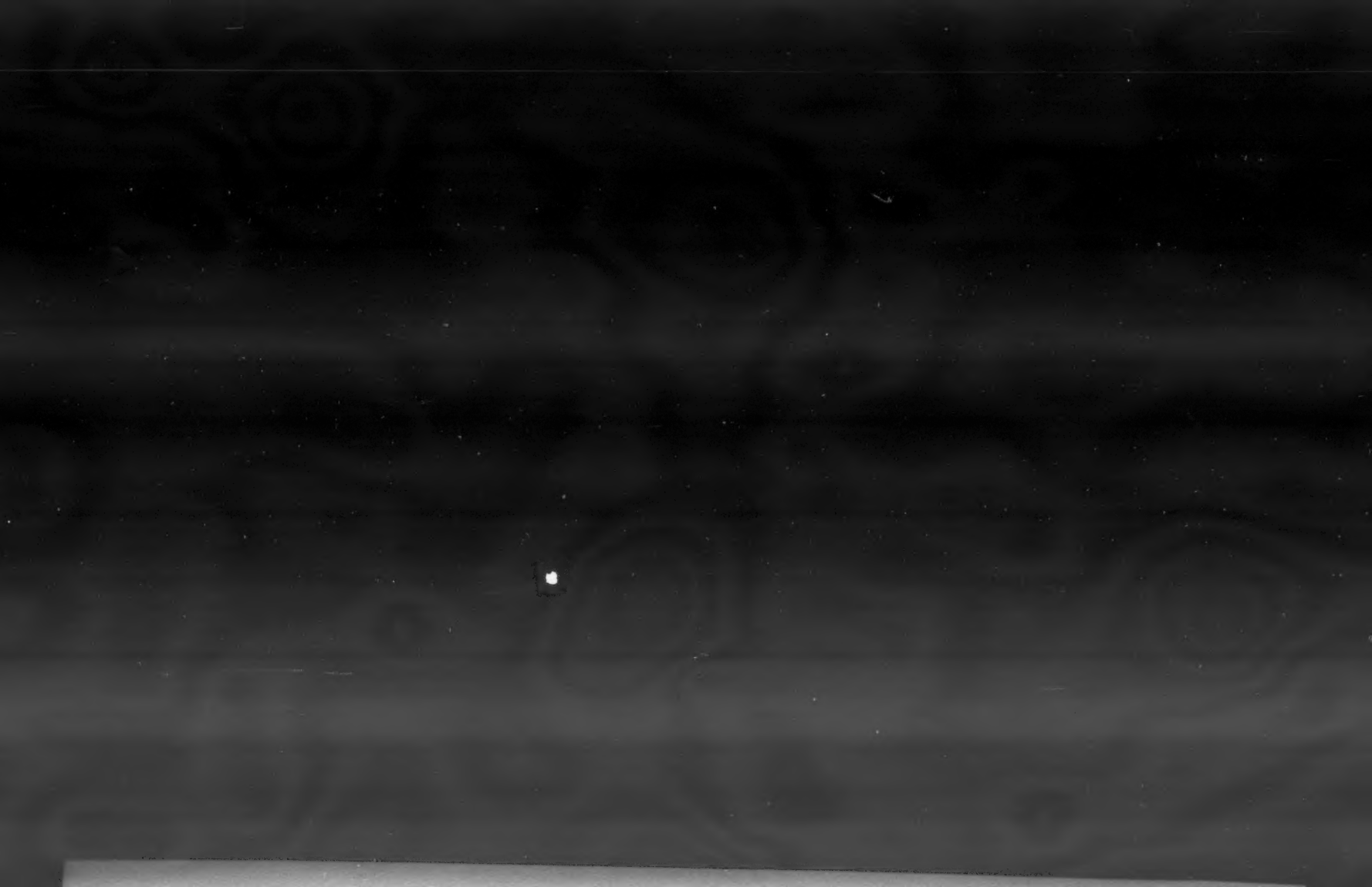


1
3

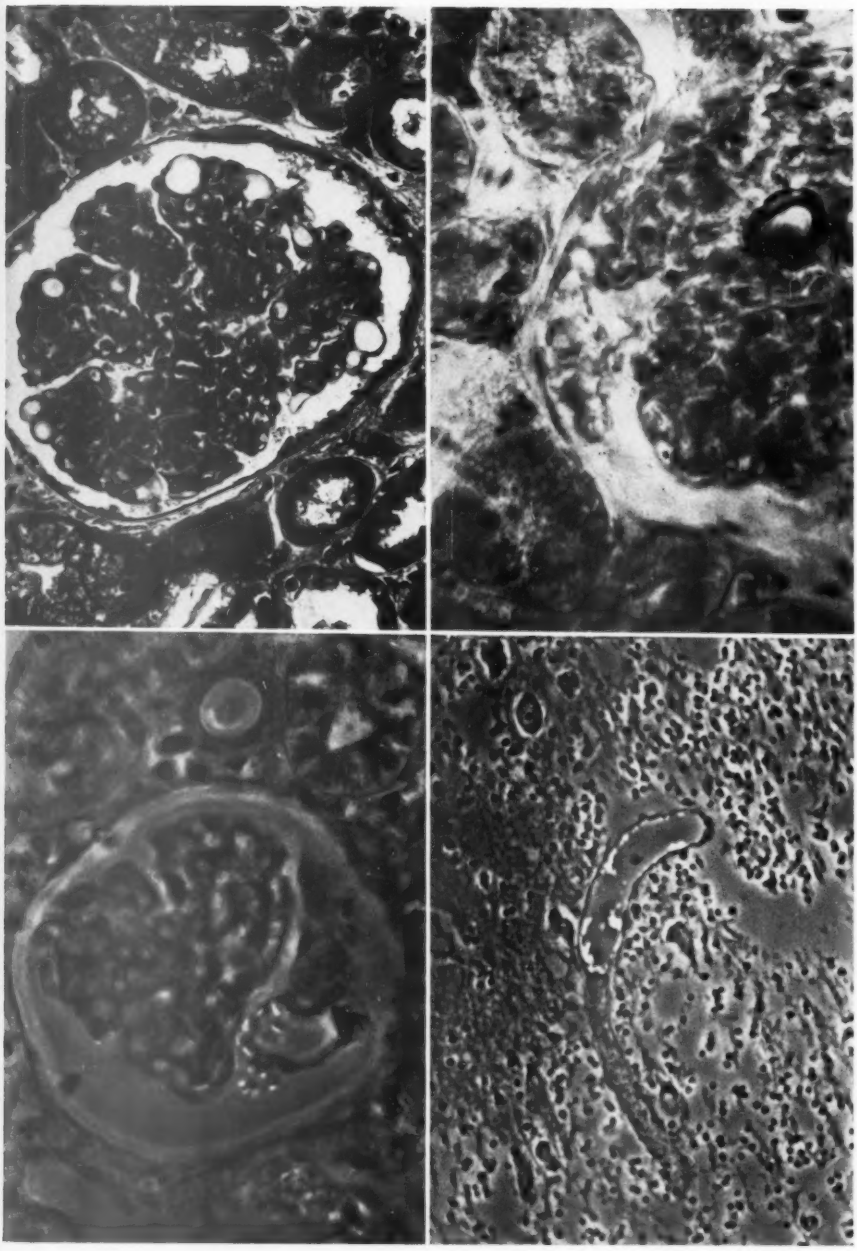

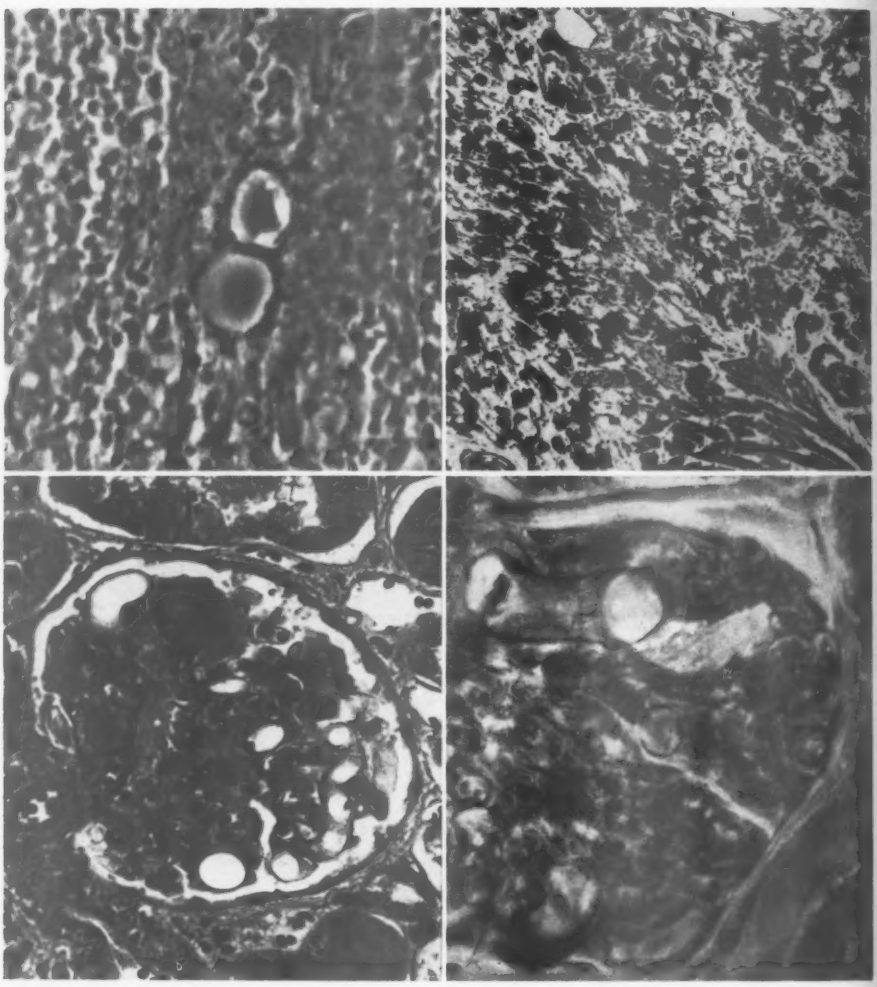

FIG. 5. Case 1. Basal ganglion. Two refractile silicone emboli are lodged in cerebral capillaries. The surrounding region shows acute encephalomalacia. Unstained; phase contrast illumination. × 440.

FIG. 6. Case 1. Myocardium of the left ventricle remote from surgical incisions. Coagulation necrosis of muscle fibers is present throughout much of the area. Fibers at the lower right are intact. No silicone emboli are present in this field. Hematoxylin and eosin stain. × 70.

FIG. 7. Dog from group A. The left renal artery was perfused by a mixture of autologous blood and DC Antifoam B. The glomerulus contains capillaries dilated by clear silicone emboli. Sections of the contralateral kidney were normal. Hematoxylin and eosin stain. × 312.

FIG. 8. Dog from group D. This dog was perfused on the DeWall pump-oxygenator for 30 minutes. A glomerulus contains a large, clear cylindrical silicone embolus. Beneath this are two smaller round emboli in cross sections of capillaries. Unstained; phase contrast illumination. × 440.

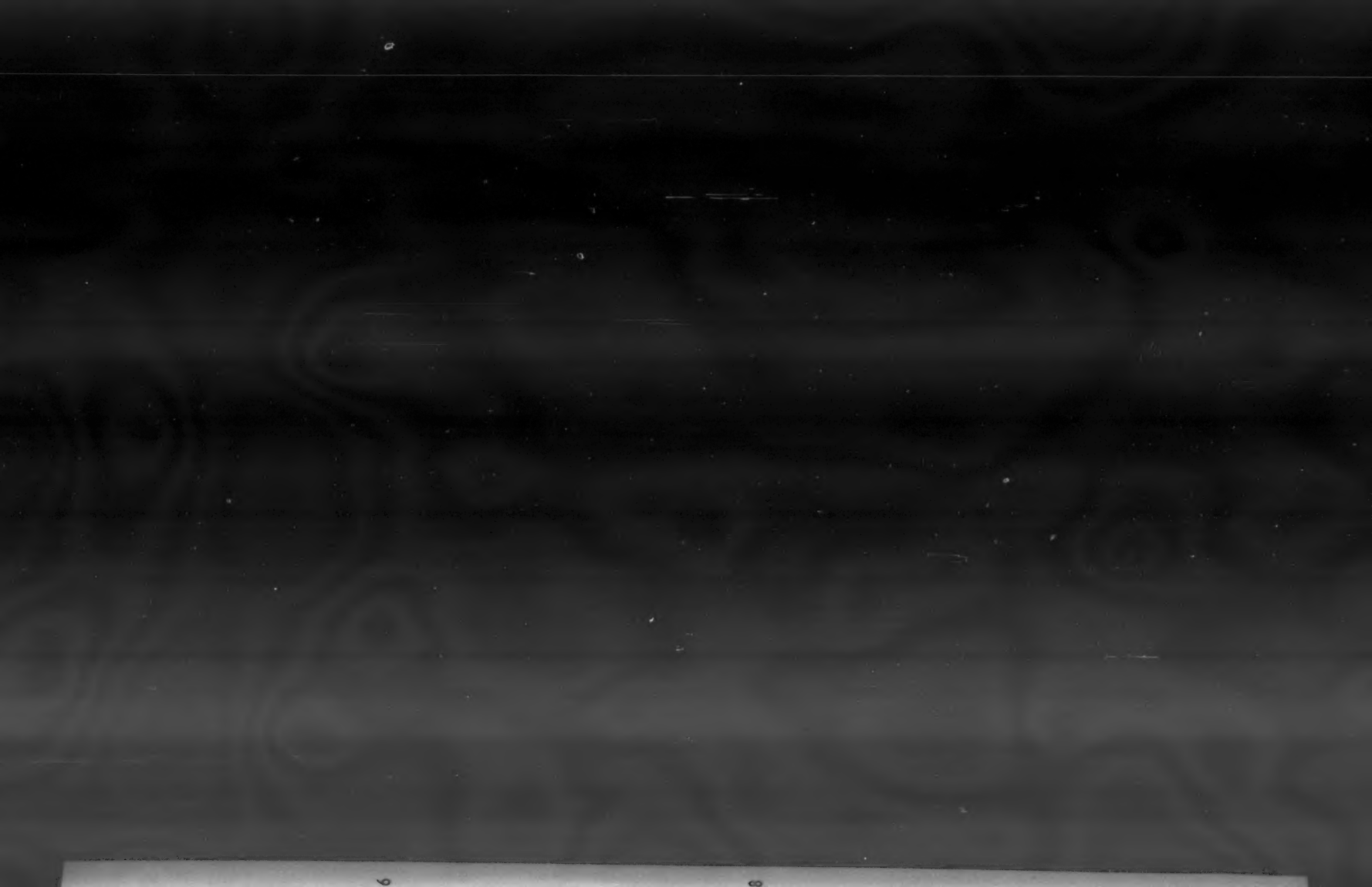

OCCLUSIVE INTRAPULMONARY VASCULAR ANOMALY IN THE NEWBORN

A Cause of Congenital Pulmonary Hypertension?

Emanuel Rubin, M.D.,* and Lotte Strauss, M.D.

From the Department of Pathology, Division of Pediatric Pathology, The Mount Sinai Hospital, New York, N.Y.

The rapid development of surgical techniques for the correction of cardiovascular defects has increasingly focused attention on the pulmonary vascular tree, the integrity of which is of fundamental importance in the long-term result of corrective surgery of the heart. Studies such as those of Civin and Edwards [1] and Edwards [2] have stimulated research into the structure of the pulmonary vascular tree in congenital heart disease. Occlusive vascular lesions in the lungs are known to occur in individuals with various acquired and congenital cardiovascular and pulmonary disorders. When present, these are usually recognized at varying intervals after the birth of the individual, and are rare in the very young. Consequently, in most instances, they are considered sequels of altered pulmonary hemodynamics. Nonthrombotic vascular obstructions in the newborn lung are little known, and where observed,[3] their significance has been a matter of speculation. Congenital "occlusive vascular disease" in the lung in a small series of newborns suffering from multiple congenital anomalies will be described and its nature and possible functional significance discussed.

Material and Methods

Five cases exhibiting unusual changes in the intrapulmonary vasculature form the basis of this study. The lungs were fixed in 10 per cent neutral formalin. Multiple sections of the lungs from as many as 8 tissue blocks were examined in each case. Serial sections were prepared in 3 cases. Alternate sections in each series were stained with hematoxylin and eosin and Weigert's elastica-van Gieson stains. Each series consisted of 100 sections, 5 μ in thickness. In 2 cases, additional staining methods were applied, such as Mallory's phosphotungstic acid-hematoxylin, Wilder's silver stain for reticulum fibers, Masson's trichrome stain, the periodic acid-Schiff technique, K-ferrocyanide for hemosiderin, Alcian blue, and Heidenhain's iron hematoxylin for myofibrils. Segments of formalin-fixed lung from 2 cases were treated with 1 per cent osmic acid for the demonstration of fat. Sections of lung tissue from an additional 71 necropsies were studied as controls. These included mostly newborn infants and stillborns and a few infants up to the age of 6 months. Forty-four of

* Supported in part by United States Public Health Service Research Training Grant 2G-115.

Presented at the Fifty-eighth Annual Meeting of the American Association of Pathologists and Bacteriologists, Chicago, Illinois, April 27, 1961.

Accepted for publication, March 20, 1961.

these were free from developmental defects. The remainder consisted of infants with congenital anomalies, especially of the cardiovascular apparatus. These included 10 newborns (22 to 40 weeks, gestational age) with isolated ventricular septal defect as the major anomaly; 9 infants (1 day to 6 months of age) with persistent common atrioventricular canal, and 8 additional cases of multiple anomalies of mesenchymal structures, including the cardiovascular system.

Case Abstracts (Table I)

Case 1

A white male infant was born after 37 weeks' gestation to a healthy 40-year-old mother. The pregnancy was uncomplicated, and labor and delivery proceeded normally. The birth weight was 2,650 gm. The infant did poorly from birth; he did not suck well and vomited frequently. Multiple congenital anomalies were evident. The child was pale; the hemoglobin was 11 gm. per hundred cc. Radiologic examination of the chest revealed a globular heart with right ventricular enlargement. An electrocardiogram showed right ventricular preponderance. The patient's condition deteriorated, and he died at the age of 19 days.

Necropsy Examination. The body was that of a white male infant weighing 2,000 gm. and measuring 48 cm. The heart was enlarged, weighing 27 gm. (normal, 19 gm.). The right ventricle was dilated and hypertrophied, measuring 0.6 cm. in thickness. An isolated 0.6 cm. defect was present high in the ventricular septum. The pulmonary artery was dilated. A single coronary artery arose from a normal right coronary ostium, giving off a left anterior descending branch, a left circumflex branch, and a posterior descending branch. The ductus arteriosus was patent. The lungs were of normal size and exhibited numerous subpleural hemorrhages and severe bilateral bronchopneumonia. Other anomalies included microphthalmus, micrognathia, right calcaneovalgus, left metatarsus varus, flexion deformities of all fingers, cleft upper lip, cleft uvula, incomplete rotation of mesentery, Meckel's diverticulum, undescended right testis, and multiple cortical cysts of the kidneys.

Case 2

A male fetus was born to a 30-year-old white woman, para 2, gravida 2, after 40 weeks' gestation. Vaginal bleeding had occurred in the first and second trimesters. Labor was induced by artificial rupture of the membranes with release of 3,000 cc. of amniotic fluid. During labor the fetal heart rate decreased, and 3 hours after onset of labor could no longer be heard.

Necropsy Examination. The body was that of an undersized white male fetus, weighing 1,400 gm. and measuring 40 cm. Multiple congenital anomalies included micrognathia, left choanal stenosis, flexion contractures of wrists and thumbs, esophageal atresia, malrotation of the intestines, atresia of the extrahepatic bile ducts, hypoplasia of the gallbladder, and a retro-esophageal right subclavian artery. A subarachnoid hemorrhage was found at the base of the brain. The heart weighed 15 gm. (normal, based on body weight, 11 gm.) and revealed no abnormalities. The foramen ovale and ductus arteriosus were patent. The lungs were of normal size.

Case 3

A male infant was born to a 42-year-old healthy white woman after 40 weeks' gestation. The pregnancy was uncomplicated. Labor was induced by artificial rupture of the membranes and proceeded uneventfully. From birth the infant was cyanotic and had a poor cry. Respirations were irregular. The cyanosis grew progressively more severe, and the patient expired on the second day of life.

Necropsy Examination. The body was that of a white male newborn, weighing 1,770 gm. and measuring 42 cm. The heart was enlarged, weighing 22 gm. (normal, 13 gm., based on body weight). The ventricles were of normal size, the right

TABLE I

SUMMARY OF CASES

Case	Gestation age (wk.)	Body wt. (gm.)	Sex	Age at death	Cardiovascular anomalies	Other anomalies
1	36	2650	M	19 days	Isolated I.V.S.D., single coronary artery, cardiac hypertrophy, dilatation of right heart and pulmonary artery	Microphthalmos; cleft lip; bifid uvula; flexion deformities of feet and fingers; deformed ears; malrotation; Meckel's diverticulum; cortical cysts of kidneys; undescended right testis
2	40	1400	M	Stillborn	Anomalous right subclavian artery	Esophageal atresia; horseshoe kidney with left double ureter; micrognathia; choanal stenosis; flexion contractures of wrists and thumbs; extrahepatic biliary atresia; malrotation
3	40	1770	M	2 days	Isolated I.V.S.D.; agenesis of right umbilical artery; deformities of aortic, pulmonary and mitral valves; cardiac enlargement	Cleft lip; flexion deformities of hands and feet (club feet); deformed ears; horseshoe kidneys; ectopic pancreatic tissue in duodenum and jejunum
4	38	2350	M	2 days	I.V.S.D.; atrial septal defect	Microphthalmos; polydactyly; micrognathia; congenital hydronephrosis; multiple cortical cysts of kidneys; omphalocele; malrotation
5	34	2430	M	10 days	Cardiomegaly with abnormal configuration; ostium II; dilation of pulmonary artery; absence of ductus venosus; drainage of umbilical vein into coronary sinus; chorioangioma of placenta	Hypoplasia of left lobe of liver; intrahepatic biliary atresia

ventricle measuring 0.3 cm. and the left, 0.4 cm. in thickness. A 1.4 cm. defect was present in the upper portion of the interventricular septum. The aortic and pulmonic valves were fenestrated. The foramen ovale and ductus arteriosus were patent. The pulmonary artery and the ductus arteriosus were dilated. The lungs were of normal size and showed bilateral severe bronchopneumonia. Other anomalies included bilateral cleft upper lip, right pes equinovarus, left pes calcaneovalgus, subluxation of the metacarpal-phalangeal articulations of both index fingers, horseshoe kidney with right crossed ectopia, bilateral undescended testes, bilateral low-set ears, aplasia of the left umbilical artery, hypoplastic left iliac artery, and epidermoid cysts of the prostate.

Case 4

A male child was born to a white woman, para 1, gravida 1, after an uncomplicated pregnancy of 38 weeks. Delivery was uneventful, and the baby breathed and cried spontaneously. Numerous congenital anomalies included microphthalmos and enophthalmos, slight micrognathia, low-set ears, omphalocele, 6 digits on all extremities, syndactyly of the right foot, and fusion of the penis with the scrotum. The omphalocele was repaired under local anesthesia on the first day of life, the baby tolerating the procedure well. On the following day he was found dead in bed.

Necropsy Examination. The body was that of a small white male infant, weighing 2,350 gm. and measuring 43 cm. The heart was of normal size, weighing 17 gm. (normal, 17.9 gm.). The ventricles were of normal size. An atrial septal defect was present, owing to shortness of the valve of the foramen ovale. High in the interventricular septum was an 0.5 cm. defect. The ductus arteriosus was patent and of normal caliber. The lungs were small, weighing 28 gm. together (normal, 39 gm.), but except for the subpleural petechiae, appeared normal. In addition to the anomalies found in life, necropsy revealed multiple minute cortical cysts of the kidneys, moderate hydronephrosis, intra-abdominal right testis, and nonrotation of the mesentery. Cultures of blood and spinal fluid were negative.

Case 5

A male child was born to a 23-year-old white woman, para 1, gravida 1, after 34 weeks' gestation. Pregnancy was uneventful, labor spontaneous and uncomplicated. The birth weight was 2,430 gm. The infant did not breathe until 5 minutes after delivery, after which respirations were grunting. The Moro reflex was absent, and the cry was whining. Generalized edema was noted. A diagnosis of congestive heart failure was made, and the infant received digitalis. The hemoglobin dropped to 11 gm. per hundred cc., necessitating the administration of packed red cells. On the second day of life a systolic murmur was heard and hepatosplenomegaly was present. Sclerema soon appeared, and the infant was treated with adrenocortical steroids. Because the baby had not passed a stool by the third day, a catheter was inserted into the rectum. A 6-inch meconium cast was ejected. The baby became severely icteric the following day. A Coombs test was negative. Roentgen examination of the chest showed a globular heart with a rounded contour on the right side. Purpura appeared, and the platelets were found to number 40,000 per cu. mm. Cultures of blood and urine were negative. as was a serum test for syphilis. The infant became increasingly weak and lethargic and expired on the eleventh day of life.

Necropsy Examination. The body was that of a poorly nourished, thin, icteric, white male infant, weighing 1,850 gm. and measuring 37 cm. Purpuric spots were present over the chest. The heart was enlarged, weighing 38 gm. (normal, 14 gm.), and was increased in transverse diameter; its apex was blunted. The umbilical vein emptied directly into the dilated coronary sinus without passing through a ductus venosus. The right atrium was dilated. The foramen ovale was patent, and two small fenestrations were noted in the interatrial septum. The interventricular septum was intact. The right ventricle was hypertrophied (0.4 cm.) as was the left ventricle

(0.5 cm.). The anterior leaflet of the mitral valve was hypoplastic. The pulmonary artery was dilated and thickened. The liver weighed 130 gm. (normal, 88 gm.). Its left lobe was very small. The extrahepatic bile ducts were patent and of normal caliber, and the common bile duct was traced to the duodenum. The spleen weighed 40 gm. (normal, 6 gm.). The remaining organs were not remarkable. Microscopic examination of the liver revealed atresia of the intrahepatic bile ducts.

Microscopic Observations

Structure of Normal Pulmonary Vessels

The arteries were classified by size, according to Brenner's classification.[4] In sections of lungs from normal subjects, the muscular arteries are provided with internal and external elastic membranes delimiting the media, which consists of a circular smooth muscle coat. The internal elastica is thinner and more delicate than the external membrane (Fig. 1). In the intima a single layer of endothelial cells is seen, resting upon the internal elastic membrane (Fig. 2). In the small muscular arteries, the lumen is somewhat larger than the combined thickness of the media and intima. The arterioles, defined as vessels of less than 100 μ external diameter, reveal a similar structure except that the media is larger in relation to the total thickness of the wall, and the lumen has about the same width as the vessel wall.

Anomalous Pulmonary Vessels

Since the structural anomalies in the intrapulmonary vessels are essentially similar in all 5 cases, differing mainly in extent from case to case, a separate description of each would be repetitious.

The elastic and the large muscular arteries did not differ significantly from normal controls except in cases 1 and 4. Striking changes were restricted to small muscular arteries and occasionally involved arterioles.

Intima. In many small muscular arteries and occasional arterioles, a pronounced intimal proliferation was found. In cross sections of the vessels the proliferation frequently assumed a papillary form or appeared as a cushion projecting into the lumen (Figs. 3, 7, 9, 11 and 14). Thus the caliber of the lumen was drastically reduced. The endothelial lining could always be distinguished as a single layer of cells covering the intimal cushion. In longitudinal sections the cellular proliferation was seen to be segmental, extending for 100 to 200 μ along the course of the vessel (Figs. 5, 6 and 8). The proliferation was most commonly located in the initial segment of a small muscular artery branching from a medium-sized vessel. Distally it formed a spur-like projection into the lumen rather than tapering off gradually (Fig. 5). The cells forming the cushions were plump, with abundant clear cytoplasm and round, occa-

sionally vesiculated nuclei; a delicate chromatin network was usually concentrated on the inner surface of the nuclear membrane. One or 2 nucleoli could be seen. The nuclei resembled those of smooth muscle cells in the vascular media. The cytoplasm took none of the stains utilized well. It did not appear to contain fat, glycogen or mucopolysaccharide. A feature which distinguished the intimal cells from those of the media was that they nowhere appeared elongated in cross or longitudinal section relative to the axis of the vessel. Myofibrils could not be demonstrated. Argyrophilic fibrils formed a delicate network surrounding the cells. Elastic and collagenous fibers were absent.

In some sections the cellular intimal tissue appeared to extend proximally for a short distance into the larger artery, surrounding the mouth of the smaller branch. In this location the intimal proliferation differed in that it contained a few elastic and collagenous fibers in addition to cells (Figs. 8 and 12).

Media. The arterial segments demonstrating proliferative intimal lesions were either lacking an internal elastic membrane or this was greatly attenuated or interrupted (Figs. 4, 9 and 11). In some vessels a very fine internal elastic membrane could be traced around a portion of the circumference, the remaining area being free of elastic fibers. At the site of branching of the small muscular artery, the internal elastic membrane became interrupted or deflected away from the lumen, and appeared to fuse with the external elastic membrane (Figs. 6 and 9). Consequently, where these changes were present in the initial portion of the small muscular branches, the adventitia and the intima were separated only by a single elastic membrane, without a recognizable intervening circular media. Where an incomplete or fragmented internal elastic membrane could be seen, the media tended to be quite thin, with attenuated circular muscle fibers (Fig. 9). In other vessels a normal media and internal elastic membrane were in contact with the cellular cushions. The abnormal media showed no inflammatory infiltration, scarring or hyalinization. Most of the arteries exhibiting occlusive changes continued abruptly into dilated and very thin-walled vessels (Fig. 5). These distal channels barely had a media and resembled veins because of their delicate structure. In serial sections these sinusoidal vessels could be traced into capillaries. When the affected vessels were arterioles, they frequently led into capillaries a short distance from the narrowed segment. Histologically, arteriovenous communications could not be demonstrated.

Adventitia. The adventitia of the narrowed small arteries could be as much as twice the usual thickness. It consisted mainly of collagenous fibers with a few elastic fibers admixed.

The intimal and medial changes were found in many of the small muscular arteries in cases 1, 2 and 3, and somewhat less frequently in case 4. In each section of case 5 a few affected arteries were found; however, the majority of the vessels appeared normal. In case 1 the vascular changes appeared most numerous and pronounced. This case, therefore, lent itself best to the study of the abnormal vessels. In cases 1 and 4, in addition to the changes in the small muscular arteries, defects of the internal elastic membrane of larger (elastic) arteries were noted. These were associated with small patches of fibrocellular intimal proliferation (Fig. 13); the patches contained elastic fibers. Although they tended to be located opposite sites of branching, some were unrelated to branching. In case 3 the normal elastic cushions at sites of branching tended to be exaggerated (Fig. 10). In case 1, fibroelastic intimal proliferation was seen in larger artery branches near the hilus. The veins were normal throughout.

It should be noted that a survey of the vessels of the systemic circulation (viscera) revealed no deviation from the normal structure.

Discussion

Segmental obliterative vascular anomalies in small muscular arteries were observed in the lungs at necropsy in 4 newborn infants from 1 to 19 days of age, suffering from cardiovascular and other anomalies of mesenchymal tissues. They were also encountered in one full-term fetus with a normal heart. In many areas the lesions were associated with partial or complete absence of the media in the narrowed or occluded segment of an artery, and attenuation of the media in the vessel immediately distal to the site of stenosis. The adventitia of the narrowed vessels was frequently thickened. The existence of these vascular lesions in the newly born indicates that they were present in intra-uterine life.

Intimal cushions have been described in cross sections of small pulmonary arteries in newborns by von Hayek.[3] He considered them normally occurring arteriovenous anastomoses designed to short-circuit the pulmonary blood flow into the systemic circulation. Arteriovenous anastomoses exist in the adult lung[5] and have recently been demonstrated in the fetal lung.[6] However, these shunts apparently are not associated with vascular structures of the type described here. In our cases, serial sections showed that the affected arteries eventually led into capillaries. These lesions were not found in lungs of normally developed newborns. Thus it appears unlikely that they represent normal devices for regulating pulmonary blood flow in fetal life.

The cells forming the intimal cushions between endothelium and circular media of small muscular arteries had a striking resemblance to

the so-called epithelioid muscle cells described in arteriovenous anastomoses such as occur in the finger tips or in the glomus coccygeum in man.[5] Similar structures have also been described in other species.[7] The cells are quite distinct from the endothelium, which forms a single layer of flattened elongated cells with spindle-shaped nuclei and scant cytoplasm, and from the circular muscle fibers of the media. It has been suggested that the swollen, vacuolated appearance of the cells may be due to histamine sensitivity.[3] Their morphologic peculiarities may have been responsible for labeling them as arteriovenous anastomoses. While the staining characteristics of the intimal cells are not distinctive, the possibility that they represent primitive muscle cells cannot be dismissed. In some pathologic states, subendothelial proliferation of smooth muscle in arteries has been described.[8]

Could these lesions have been caused by arteritis or thrombosis? Healed arteritis is usually accompanied by partial fibrous replacement of the media and intimal fibroelastic proliferation. One of the characteristics of the affected vessels was the absence of fibrous connective tissue in the intima and media. Inflammatory cells, usually found in acute arteritis, were conspicuously absent from the abnormal vessels in our cases. Their uniform size and location, together with the absence of fibroelastic activity, was evidence against a thrombotic origin. Thoma[9] advanced a theory of intimal proliferation following the slowing of blood flow which could not be compensated by contraction of the media. In view of the defective structure of the media in our cases, this theory merits consideration, especially since the intimal cushions were seen in locations where flow was usually slowed, i.e., at the sites of branching. On the other hand, attenuation of the smooth muscle of the vascular media can be observed in occluded or arteriosclerotic vessels or whenever intravascular pressure is reduced as a result of diminished flow. This is also evident in the vessel distal to an occluded segment.[10,11] This may account for the vein-like appearance of arteries distal to occlusive lesions in the pulmonary vascular tree, which may have led to their interpretation as arteriovenous shunts.[3,12]

Is it possible that the occlusive intimal lesions constitute a response to abnormal fetal pulmonary circulation? One would expect that this is effectively prevented by the shunting devices of the foramen ovale and ductus arteriosus.[13] However, our knowledge of circulatory physiology of the fetal lung and of developmental mechanics of the pulmonary vascular bed is too incomplete to evaluate this. The pulmonary circulation may be more important in later fetal life than commonly believed.[14] The pronounced right ventricular hypertrophy found in cases 1 and 5 lends support to this. In addition, although in the fetus the pressures in

the ventricles and great vessels are approximately equal,[15] the position of the interventricular septal defect suggests that a significant portion of the left ventricular output may have been directed into the pulmonary artery.[16] However, it must be remembered that case 2 had neither cardiac anomalies nor right ventricular hypertrophy. Proliferative changes in pulmonary arteries have been reported frequently as secondary to long-standing pulmonary hypertension. This has been noted in acquired cardiac lesions such as mitral stenosis,[17] in association with congenital heart disease,[1,2,18] or in "primary" pulmonary hypertension.[19] Support for this concept has come from the production of such lesions in experimental pulmonary hypertension in animals[20] and from the results of surgical pulmonary-systemic anastomoses in man.[21] These lesions have usually been recorded in older children and adults, but occasional reports have described intimal changes in very young children[22,23] and in infants as young as 6 and 9 months of age.[24,25] Wolman[26] reported pulmonary vascular changes in a 6-week-old and a newborn infant.

Intimal proliferation in association with pulmonary hypertension is almost invariably segmental. As in the cases in this study, the lesions are located at the origin of small muscular branches with a thin-walled dilated vessel distal to the narrowed segment.[27,28] The site of branching appears to be particularly vulnerable to other insults as well,[29] and elastic intimal cushions (stress cushions) are normally found at these sites in fetal pulmonary arteries.[30] In the specimens where the occlusive changes are particularly widespread, focal disruption of the elastic structure of larger arteries proximal to the occlusive changes is observed. This is associated with fibroelastic intimal thickening, which is distinct from the normal "stress cushions" of fetal pulmonary arteries. These changes may signify that increased intravascular pressure existed in the pulmonary circulation at the time of birth and probably *in utero*, perhaps secondary to widespread occlusive lesions in small arteries. Intimal plaques in larger arteries in 2 cases are morphologic evidence of increased intravascular pressure.

A similarity exists between the so-called "plexiform" or "glomus-like" lesions in the lungs of some subjects with pulmonary hypertension, and the vascular changes under discussion, particularly with respect to their location at the origin of small arterial branches.[31,32] Although plexiform lesions have not been observed in the fetus or newborn, it is possible that they represent a later stage of the lesion described here. In a case of pulmonary hypertension in a 15½-week-old infant recently reported,[33] pulmonary vascular changes resembled both the vessels described here and the glomus-like lesions in older subjects.[31]

It has been suggested that proliferative pulmonary vascular lesions

associated with "primary" pulmonary hypertension,[34] or with congenital heart disease [12,18] may not be secondary to hypertension but may represent an associated developmental defect. It is noteworthy that in each of our cases showing the pulmonary vascular anomaly, widespread developmental defects of mesenchymal tissues, including the cardiovascular system, existed. In addition, all but one had low birth weights, a reflection of stunted growth. Intimal proliferation may occur over the defective media, thus providing a device preventing overdistention of an artery provided with an inadequate musculature, by removing it from the circulation. Medial defects similar in appearance and location to those in our cases have been demonstrated in association with "primary" pulmonary hypertension in the adult [35] and in an 11-month-old infant with patent ductus arteriosus.[24] Evans described it in a woman, 22 years old, with patent ductus arteriosus and other congenital anomalies similar to those in our case 3. Gilmour and Evans [34] have suggested that primary pulmonary hypertension is caused by congenital aplasia or hypoplasia of the media of small pulmonary arteries. According to Evans, pulmonary hypertension caused by acquired intra- and extrapulmonary lesions is not accompanied by medial defects.[36] Observations in 3 siblings with "primary" pulmonary hypertension [37] also suggest that in some cases, pulmonary hypertension may have a basis in structural defects in the pulmonary vasculature.

The vascular changes described were of a type occasionally observed in association with pulmonary hypertension. Congenital lesions such as those reported may assume clinical importance in individuals surviving the perinatal period, in whom correction of congenital cardiac defects is contemplated. In some instances, the presence of congenital intrapulmonary vascular alterations may account for the failure of corrective operations to prevent the development or progression of pulmonary hypertension.

Summary

1. A segmental occlusive vascular anomaly characterized by cellular intimal proliferation and a defective media has been demonstrated in the small pulmonary arteries of 1 stillborn fetus and 4 infants who died in the neonatal period. The lesions were most commonly seen at the site of branching of small from medium-sized muscular arteries.

2. The pulmonary vascular anomaly was observed only in subjects with multiple congenital defects including intracardiac anomalies in 3. It is suggested that the alteration represents a developmental defect.

3. Congenital structural defects in the pulmonary vasculature may in some cases be responsible for the development of "primary" pul-

monary hypertension or pulmonary hypertension associated with congenital heart disease. This may explain why even early surgical repair of cardiac anomalies may at times fail to prevent or correct pulmonary hypertension.

References

1. Civin, W. H., and Edwards, J. E. Pathology of the pulmonary vascular tree; comparison of intrapulmonary arteries in the Eisenmenger complex and in stenosis of ostium infundibuli associated with biventricular origin of the aorta. *Circulation,* 1950, **2,** 545–552.
2. Edwards, J. E. Functional pathology of the pulmonary vascular tree in congenital cardiac disease. *Circulation,* 1957, **15,** 164–196.
3. Hayek, H. von. Die menschliche Lunge. Springer, Berlin, 1953, 289 pp.
4. Brenner, O. Pathology of vessels of the pulmonary circulation. *Arch. Int. Med.,* 1935, **56,** 211–237.
5. Clara, M. Die arterio-venösen Anastomosen; Anatomie, Biologie, Pathologie. Springer, Vienna, 1956, ed. 2, 315 pp.
6. Groniowski, J. Morphological investigations on pulmonary circulation in the neonatal period. *Am. J. Dis. Child.,* 1960, **99,** 516–523.
7. Benninghoff, A. In: Handbuch der mikroskopischen Anatomie des Menschen. Von Möllendorff, W. (ed.). Springer, Berlin, 1930, Vol. 6, p. 107.
8. Kaunitz, P. E. Origin of left coronary artery from pulmonary artery; review of literature and report of 2 cases. *Am. Heart J.,* 1947, **33,** 182–206.
9. Thoma, R. Ueber die compensatorische Endarteriitis. *Virchows Arch. path. Anat.,* 1888, **112,** 10–16.
10. Hueper, W. C. Arteriosclerosis: the anoxemia theory. Intravascular hydrostatic pressure. A. Decreased. *Arch. Path.,* 1945, **39,** 51–54.
11. Thoma, R. Quoted in: Handbuch der speziellen pathologischen Anatomie und Histologie. Henke, F. and Lubarsch, O. (eds.) Springer, Berlin, 1924, Vol. 2, Herz und Gefässe, p. 683.
12. Dammann, J. F., Jr.; Berthrong, M., and Bing, R. J. Reverse ductus; a presentation of the syndrome of patency of the ductus arteriosus with pulmonary hypertension and a shunting of blood flow from pulmonary artery to aorta. *Bull. Johns Hopkins Hosp.,* 1953, **92,** 128–150.
13. Dawes, G. S. The Pulmonary Circulation After Birth. In: Pulmonary Circulation: an International Symposium, 1958, sponsored by the Chicago Heart Association. Adams, W. R., and Veith, I. (eds.). Grune & Stratton, New York, 1959, pp. 199–203.
14. Sciacca, A., and Condorelli, M. Involution of the ductus arteriosus. A morphological and experimental study, with a critical review of the literature. Bibliotheca Cardiologica, Fasc. 10. Karger, Basel, 1959, 52 pp.
15. Hamilton, W. F.; Woodbury, R. A., and Woods, E. B. The relation between systemic and pulmonary blood pressures in the fetus. *Am. J. Physiol.,* 1937, 119, 206–212.
16. Taussig, H. B. Congenital Malformations of the Heart. The Commonwealth Fund, New York, 1947, p. 390.
17. Spain, D. M. Necrotizing and healing pulmonary arteritis with advanced mitral stenosis. *Arch. Path.,* 1956, **62,** 489–493.
18. Evans, W., and Short, D. S. Pulmonary hypertension in congenital heart disease. *Brit. Heart J.,* 1958, **20,** 529–551.

19. BERTHRONG, M., and COCHRAN, T. H. Pathological findings in nine children with "primary" pulmonary hypertension. *Bull. Johns Hopkins Hosp.*, 1955, **97**, 69–111.

20. FERGUSON, D. J., and VARCO, R. L. The relation of blood pressure and flow to the development and regression of experimentally induced pulmonary arteriosclerosis. *Circulation Res.*, 1955, **3**, 152–158.

21. WAGENVOORT, C. A.; DU SHANE, J. W., and EDWARDS, J. E. Hypertensive pulmonary arterial lesions as a late result of anastomosis of systemic and pulmonary circulations. *Proc. Staff Meet. Mayo Clin.*, 1960, **35**, 186–191.

22. CROSS, K. R., and KOBAYASHI, C. K. Primary pulmonary vascular sclerosis. Report of a case. *Am. J. Clin. Path.*, 1947, **17**, 155–162.

23. RUTISHAUSER, E., and BLANC, W. Anastomoses artério-veineuses glomiques du poumon avec syndrome d'insuffisance droite et cyanose. *Schweiz. Ztschr. allg. Path.*, 1950, **13**, 61–65.

24. ZUR LINDEN, W. Isolierte Pulmonalsklerose im jüngsten Kindesalter. *Virchows Arch. path. Anat.*, 1924, **252**, 229–239.

25. WÄTJEN, D. Zur Kenntnis der Pulmonalsklerose im Säuglingsalter. *Verhandl. deutsch. path. Ges.*, 1926, **21**, 259–266.

26. WOLMAN, M. Hypertrophy of the branches of the pulmonary artery and its possible relationship with so-called primary pulmonary arteriosclerosis in 2 infants with hypertrophy of the right heart. *Am. J. M. Sc.*, 1950, **220**, 133–143.

27. DAMMANN, J. F., JR., and FERENCZ, C. The significance of the pulmonary vascular bed in congenital heart disease. III. Defects between ventricles or great vessels in which both increased pressure and blood flow may act upon the lungs and in which there is common ejectile force. *Am. Heart J.*, 1956, **52**, 210–231.

28. HEATH, D. Structural Alterations of Pulmonary Vessels in Response to Pulmonary Hypertension. In: Pulmonary Circulation: an International Symposium, 1958, sponsored by the Chicago Heart Association. ADAMS, W. R., and VEITH, I. (eds.). Grune & Stratton, New York, 1959, pp. 122–125.

29. BRAUNSTEIN, H. Periarteritis nodosa limited to the pulmonary circulation. *Am. J. Path.*, 1955, **31**, 837–857.

30. ROBERTSON, J. H. Stress zones in foetal arteries. *J. Clin. Path.*, 1960, **13**, 133–139.

31. NAEYE, R. L., and VENNART, G. P. The structure and significance of pulmonary plexiform structures. *Am. J. Path.*, 1960, **36**, 593–605.

32. MOSCHCOWITZ, E.; RUBIN, E., and STRAUSS, L. Hypertension of the pulmonary circulation due to congenital glomoid obstruction of the pulmonary arteries. *Am. J. Path.*, 1961, **39**, 75–93.

33. HRUBAN, Z., and HUMPHREYS, E. M. Congenital anomalies associated with pulmonary hypertension in an infant. *Arch. Path.*, 1960, **70**, 766–779.

34. GILMOUR, J. R., and EVANS, W. Primary pulmonary hypertension. *J. Path. & Bact.*, 1946, **58**, 687–697.

35. EVANS, W. Congenital pulmonary hypertension. *Proc. Roy. Soc. Med.*, 1951, **44**, 600–608.

36. EVANS, W. The less common forms of pulmonary hypertension. *Brit. Heart J.*, 1959, **21**, 197–217.

37. COLEMAN, P. N.; EDMUNDS, A. W. B., and TREGILLUS, J. Primary pulmonary hypertension in three sibs. *Brit. Heart J.*, 1959, **21**, 81–88.

[*Illustrations follow*]

Legends for Figures

Fig. 1. A normal small muscular artery from the lung of a full-term infant. Note the internal and external elastic membranes and the well-developed media. Elastica-van Gieson stain. × 640.

Fig. 2. A normal small muscular artery from the lung of a full-term infant, showing a single layer of intimal cells and a well-developed media. Hematoxylin and eosin stain. × 640.

Fig. 3. Case 1. A small pulmonary artery with its lumen narrowed by intimal cushions. Hematoxylin and eosin stain. × 640.

Fig. 4. Case 1. An elastic tissue stain of the same artery shown in Figure 3. Note the absence of an internal elastic membrane. Weigert's elastica stain. × 640.

Fig. 5. Case 1. Longitudinal section of a small pulmonary artery demonstrating segmental intimal proliferation with a valve-like projection into a thin-walled, dilated, distal channel. Hematoxylin and eosin stain. × 160.

Fig. 6. Case 1. Longitudinal section of an arterial branch with segmental intimal proliferation. Note the interruption of the internal elastic membrane. Weigert's elastica stain. × 640.

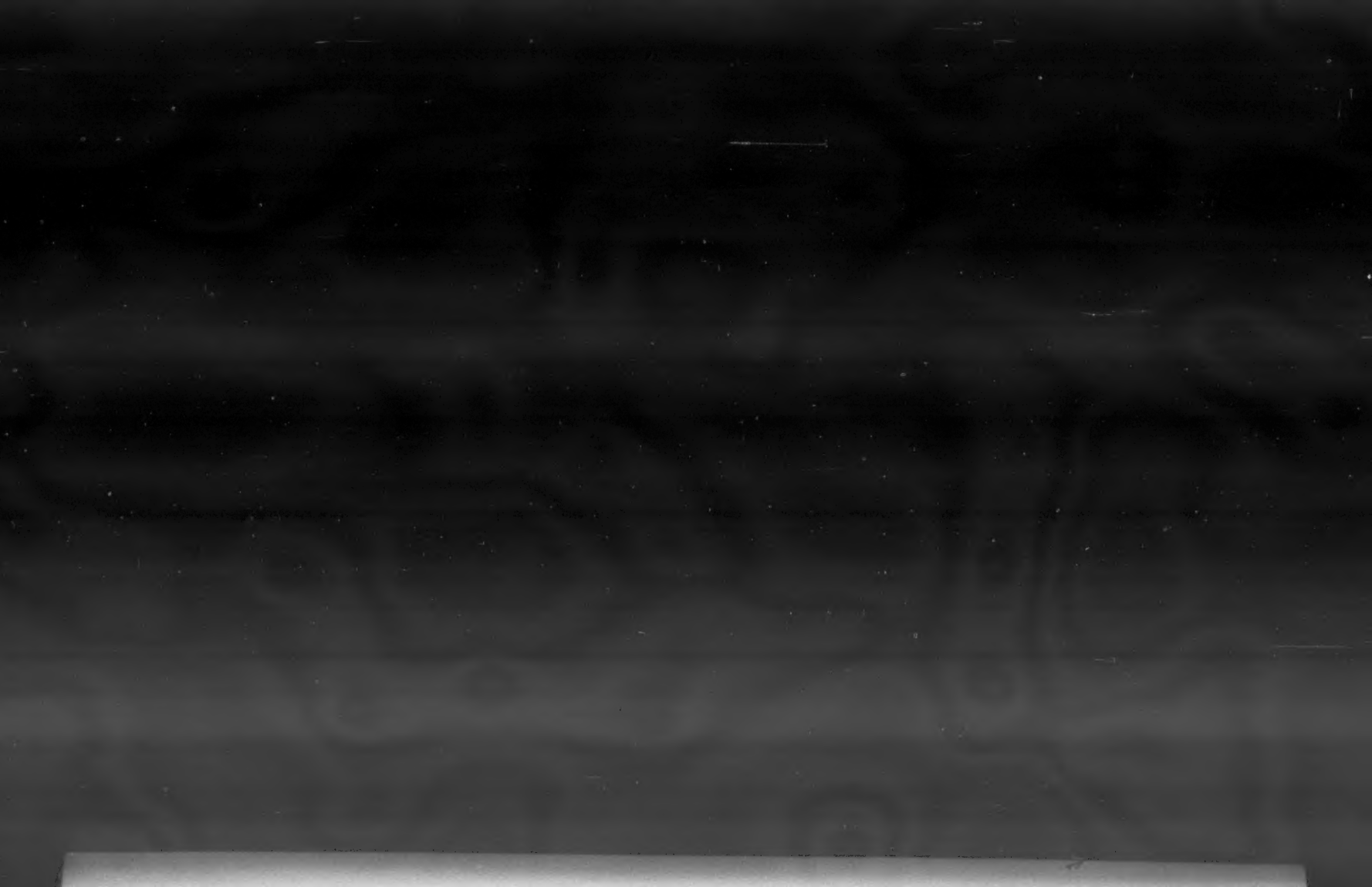


1
3
5

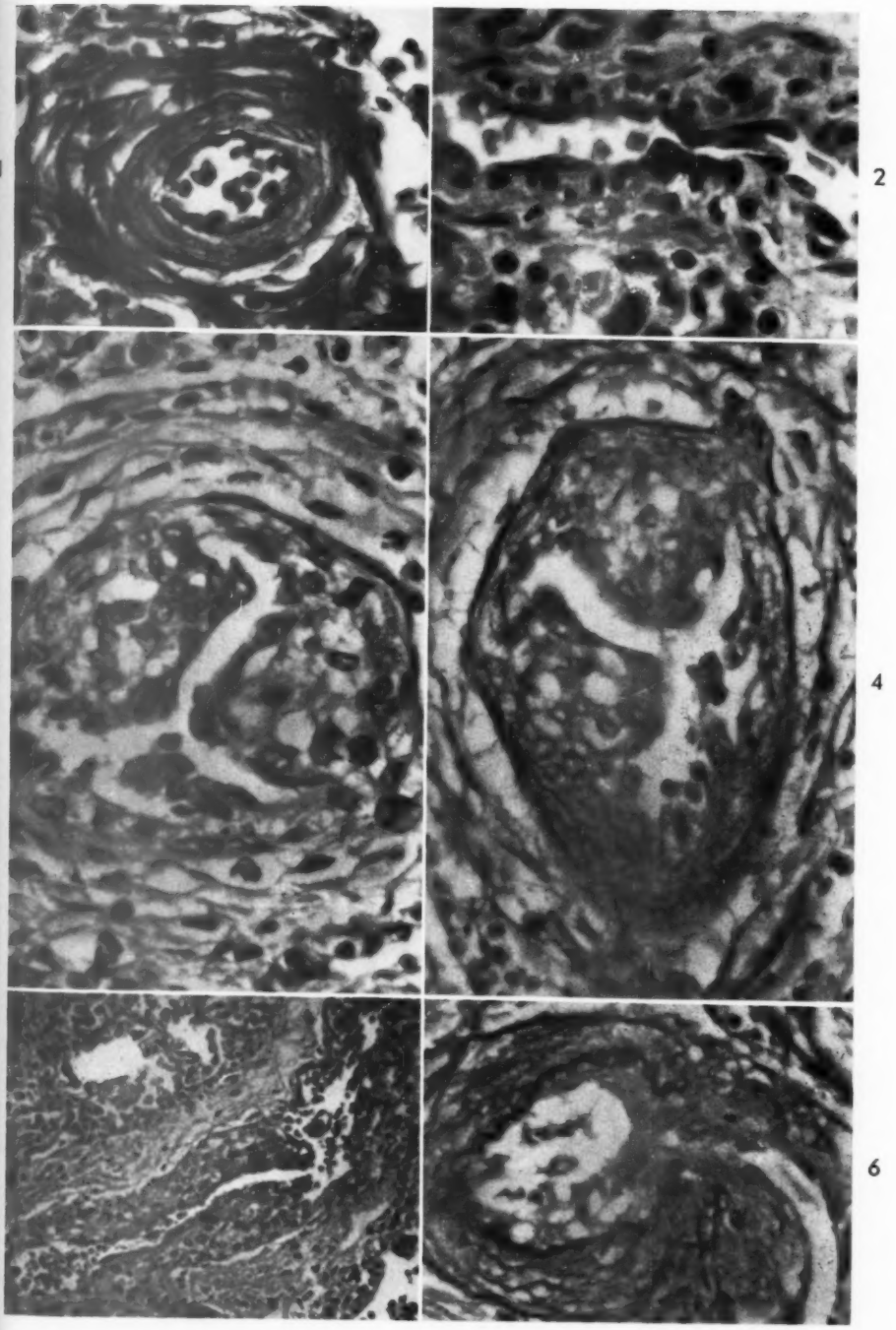
1
2
3
4
5
6

FIG. 7. Case 2. A small pulmonary artery with its lumen narrowed by intimal proliferation. Hematoxylin and eosin stain. × 640.

FIG. 8. Case 2. Cellular intimal proliferation in a small arterial branch. The two opposing fibroelastic cushions at the mouth of the smaller artery are considered normal. Weigert's elastica stain. × 160.

FIG. 9. Case 3. A small pulmonary artery showing a hypoplastic media and intimal proliferation. Internal and external membranes fuse at one point (arrow). Elastica-van Gieson stain. × 640.

FIG. 10. Case 3. An elastic artery showing exaggerated fibro-elastic cushions at the site of arterial branching (stress cushions). Elastica-van Gieson stain. × 100.

FIG. 11. Case 4. A small pulmonary artery with hypoplastic media and papillary intimal proliferation. Elastica-van Gieson stain. × 640.

FIG. 12. Case 4. An arterial branch showing interruption of the internal elastic membrane (arrows). Note the cellular proliferation in a smaller branch distal to this point. Elastica-van Gieson stain. × 640.

FIG. 13. Case 4. Fibroelastic intimal cushion in an elastic artery with focal interruption of the internal elastic membrane. This probably is the site of branching. Elastica-van Gieson stain. × 160.

FIG. 14. Case 5. A small pulmonary artery with its lumen narrowed by cellular intimal proliferation. Hematoxylin and eosin stain. × 640.

7

9

11

13

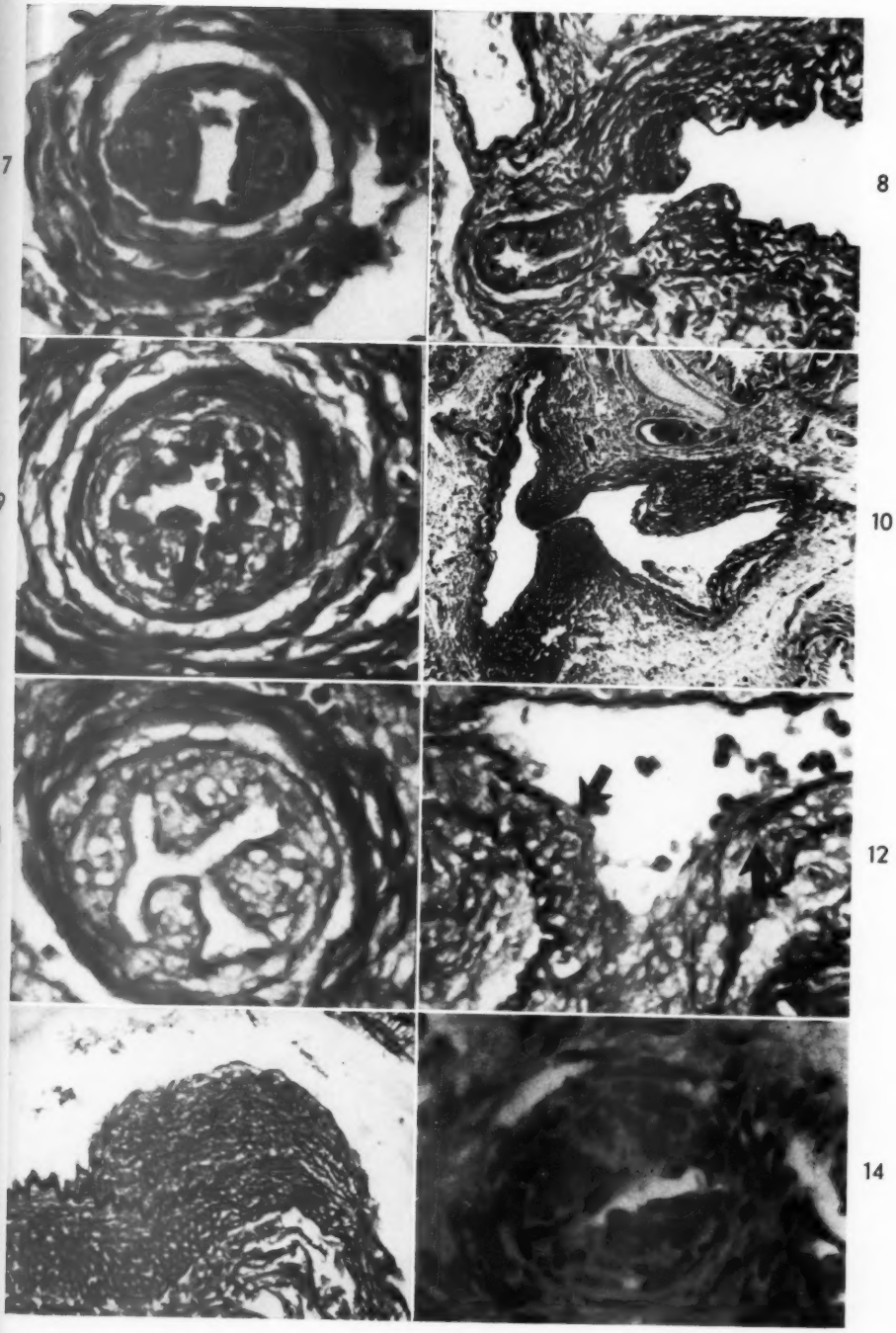
7
8
9
10
11
12
13
14

THE ANATOMIC CHARACTER OF THE VASCULAR ANOMALIES ASSOCIATED WITH ANENCEPHALY

With Consideration of the Role of Abnormal Angiogenesis in the Pathogenesis of the Cerebral Malformation

F. Stephen Vogel, M.D.

From the Department of Pathology, The New York Hospital—Cornell Medical Center, New York, N.Y.

Previous studies have provided cogent evidence that in anencephaly the anlage of the neuroectoderm is not intrinsically defective, that the encephalon develops normally through at least the first 6 or 7 weeks of fetal life, and that abnormal angiogenesis occurs in close association with the cerebral malformation.[1,2] At this early stage of embryonic development, a cardinal event in angiogenesis is the integration of the primordial vascular bed, that has formed *in situ* within the encephalon, into the systemic circulation by union with the major cephalic vessels. The observations cited above have raised the question of whether this union and integration occur in encephalons that later manifest the characteristic malformations of anencephaly. To obtain further information on this matter, detailed studies have been made of the anatomic characters of the vasculature within the malformed cerebrum, on the one hand, and of the major cephalic arteries and veins, on the other. Particular consideration has been given to the interrelations between these two vasculatures. Additional information has been provided about the pathogenesis of anencephaly.

Material and Methods

In 3 anencephalic monsters, the topographic anatomy of the major cephalic arteries and veins was studied in detail by the vinyl casting technique.[3] Only a few of the vessels within the cephalic masses were filled by this procedure; therefore, they were investigated in 7 additional cases by detailed examinations of serial histologic sections and by reconstruction of paraffin models.

Vinyl Casting Technique

The sternum of each anencephalic monster was removed and, with the organs *in situ*, more than a liter of kerosene was injected under moderate pressure into an isolated segment of the aortic arch and then into the superior vena cava with the purpose of flushing blood and blood clots from the cephalic arteries and veins. Red vinyl acetate (Ward's Biological Supplies, Rochester, New York), diluted with acetone to the consistency of blood, was then injected into the isolated aortic arch

This investigation was supported by a research grant from the National Institute of Neurological Disease and Blindness of the National Institutes of Health, United States Public Health Service.

Accepted for publication, March 27, 1961.

at an approximate pressure of 100 mm. of Hg. Yellow vinyl acetate, similarly diluted, was introduced in retrograde manner through the superior vena cava. The vinyl hardened promptly. Visceral tissues were fixed in formalin for histologic examinations; the cephalic soft tissues were digested with 20 per cent KOH.

Histologic and Paraffin Reconstruction Techniques

The deformed cerebrums of 7 anencephalic monsters were sectioned in their entirety in coronal or horizontal planes and embedded in celloidin. Sections of these tissues were then cut at 10 μ for staining by hematoxylin and eosin, Masson's trichrome method, Nissl's cresyl violet method, Giemsa's method, Wilder's method for reticulum, and by the Verhoeff method for elastic tissue. Selected blocks were serially sectioned at thicknesses of 50 μ and stained by Masson's trichrome method. Companion areas were photographed in consecutive serial sections at a magnification of 25 times. The colored photographs were projected upon a translucent screen with an enlargement of approximately 3.5 times. The outline of each individual vessel was marked upon tracing paper and then upon a sheet of paraffin, 15 by 15 cm. by 1.5 mm. (Mizzy Inc., Clifton Forge, Virginia). The sheet was cut to the specific size that would provide a uniform 3-dimensional enlargement of structures in the histologic sections. The areas covered by the vessels were then carefully excised, together with such connecting strips as were necessary to maintain the proper anatomic relations. The wax model of the vasculature in the first histologic section was secured to a sheet of wax, and those of subsequent sections were consecutively superimposed upon this. In the model described herein and illustrated in Figure 2, the spatial relationships were maintained by orientation to two straight arteries that traversed all histologic sections and lay in dense fibrous tissue tangential to the island of neural tissue under study. After each layer of the model was secured, the intravascular attachments, except when essential for support of isolated vessels, were removed with a warmed scalpel. The outer surface of each vessel was colored red with oil paint.

Observations

Summary of Vinyl Injection Studies in 3 Cases of Anencephaly

The cerebral deformities were grossly characteristic in all 3 cases. The calvarias were absent and the cerebral hemispheres were regularly replaced by diminutive, hemorrhagic, friable, discoid masses, closely applied to the flattened base of the skull and secured principally by hair-bearing skin that lapped over the peripheral margins of these masses. A craniorachischisis in one of the cases was characterized, in addition to the craniocerebral deformity, by an absence of the skin over a "V" shaped area that extended downwards from the acrania to the lower cervical region, a lack of union and marked lateral displacement of the posterior bony processes of the cervical spines, and exposure of the imperfectly formed cervical segment of the spinal cord (Figs. 3 and 4).

The vinyl arterial castings of this case clearly showed that the major cephalic vessels took origin from the aortic arch in normal positions and with approximately normal sizes. The vertebral arteries arose from the arches of the subclavian vessels and ascended through the vertebral foramens. They emerged at the posterior lip of the base of the skull and passed across this bony plateau in a straight anterior and medial course to

anastomose in a "V" formation, producing the basilar artery. Small arteries originated from the terminal portions of the vertebral vessels. Two passed caudad and, with anastomosis in the mid-line, assumed the distribution of the anterior spinal artery. Small, tortuous vessels extended laterally, simulating the posterior inferior cerebellar arteries. The basilar artery was moderate in size and lay in the mid-line of the skull, coursing almost to the anterior edge of the bony plateau before bifurcating to form laterally-directed tortuous vessels that resembled the posterior communicating arteries in distribution. One extremely slender vessel passed through the base of the skull, uniting the right terminal branch of the basilar artery and the terminals of the right internal carotid artery. The vertebral-carotid vessels were all closely applied to the bony plateau, and very few tributaries extended cephalad into the overlying cerebral mass.

The common carotid arteries took origin in normal positions from the right innominate artery and the arch of the aorta. The lateral aspects of the face were generously supplied by large external carotid branches whose terminals anastomosed freely in the orbital cavity and also supplied the skin at the peripheral margins of the cephalic mass. The internal carotid arteries were of moderate size and formed dense plexuses of large vessels in the proximal regions of the carotid siphons. Many large branches passed anteriorly into the orbital sockets, where they anastomosed freely with equally large terminals of the external carotid system.

The superior vena cava was distended with vinyl, and entering it were large left innominate and right subclavian vessels. The internal jugular veins joined these, and in their retrograde courses passed cephalad through foramens at the posterior edge of the bony skull. Extremely dense plexuses of freely anastomotic vessels emptied into the jugular veins. These racemose formations were closely applied to the anterior aspects of the exposed spinal canal, descending as lingular structures throughout the cervical regions. They also ascended over the posterior lip of the bony skull, then curved laterally and formed dense networks on the periphery of the bony plateau and ended above the orbital cavities. These plexuses lay beneath the cephalic mass, but did not receive major tributaries from it (Fig. 1).

The deformities of the cephalic vasculature of two other anencephalic monsters were notably similar and conformed closely with those described above. In each instance, the carotid and vertebral arteries arose in normal anatomic positions from the arch of the aorta, the innominate artery, and the subclavian arteries. The common carotid arteries were approximately normal in size and, upon bifurcation, yielded large ex-

ternal carotid vessels and smaller internal ones. Both sent rich anastomotic plexuses into the orbital sockets but, as in the previous case, united with the vertebral-basilar system by only slender branches. In one case, the union was unilateral on the left; in the other, bilateral, by extremely slender vessels that penetrated the base of the skull. In both cases the vertebral and basilar arteries closely approximated the normal in their sizes and distributions, and together constituted the major vasculature on the bony plateau of the skull. As in the previous case, only a few slender tributaries arose from these vessels and entered the overlying cerebral masses.

The jugular and innominate veins and the superior vena cava were not notably abnormal. However, the vessels that drained into the jugular veins at the base of the skull were plexiform and bizarre in distribution. Only a few venous channels drained from the deformed cerebrums.

Summary of the Histologic and Paraffin Reconstruction Studies in 7 Cases of Anencephaly

The necropsy observations in the 7 cases of anencephaly have been described previously,[2] being characterized in each case by a craniocephalic deformity, hypoplasia of the adrenal cortices, and hyperplasia of the thymus glands. Proptosis of both eyes was regularly present, but all had well-formed and well-preserved retinas and often rudimentary segments of optic nerves.

Detailed examinations of the cephalic masses in serial sections made it clear that they regularly contained islands of neural tissue formed of undifferentiated neurons and glial cells in disorderly or moderately well-ordered architectural arrangements. Between these islands there were abundant quantities of dense fibrous tissue and cysts partially lined by ependyma and frequently occupied by choroid, but most conspicuous within the neural islands and elsewhere were multitudes of vascular channels which were regularly lined by endothelium. Their walls were thin and most often devoid of muscular, elastic, or notable amounts of fibrous tissue. Many lay side by side with little intervening stroma. A few, principally within the fibrous stroma, had thick muscular medias and fibrous adventitias. Attempts to follow individual or racemose groups of vessels through serial sections made it abundantly clear that these channels were so extremely circuitous and serpentine that it was often impossible to envision their courses through consecutive histologic sections. Many ended abruptly; others arose without detectable anastomoses.

The paraffin reconstruction models of the vascular sinusoids within the globoid islands of neural tissue showed them to form incongruous networks of ill-proportioned, large and small, bizarre channels that

richly anastomosed and frequently formed blind tributaries. Approximately one half of the volume of the neural islands was composed of the sinusoidal vessels. By contrast, the few arteries that were present and had thick muscular walls anastomosed sparsely, as did those used for fixation points in the paraffin model (Figs. 2 and 5).

In the histologic sections of all cases, there were dense, focal agglomerations of cells in juxta-thelial and intrasinusoidal positions. Many of these cells had rounded nuclei, prominent nucleoli, and relatively abundant cytoplasm. They were occasionally in mitotic division and closely resembled blastic forms of the erythroid and myeloid series. Smaller cells with contracted, hyperchromatic nuclei and more abundant cytoplasm resembled normoblasts, whereas lesser numbers of cells had faintly granular cytoplasm and the lobulated nuclei of myelocytes (Fig. 6).

Discussion

The presence in anencephaly of well-formed and well-preserved structures derived from migratory neuroblasts,[2] notably the retina and cranial nerve ganglia, makes it plain that the initial formation of the encephalon is generally normal through at least the first 6 or 7 weeks of fetal life, for it is at this time that the optic vesicles assume independence from the lateral portions of the diencephalon. It is noteworthy that by this migration these neuroblasts acquire vascular autonomy through a dual blood supply. The presence of large tributaries from the internal and external carotid systems, as regularly demonstrated in the orbital cavities by the injection technique, indicates that this bipotential vascular supply is advantageously utilized in the development of the eyes.

Although the cephalic masses with their remnants of neuroectoderm and mesenchyma are endowed with a rich intrinsic vasculature, the injection studies have shown plainly that few of these vessels are in continuity with the major cephalic arteries and veins. Furthermore, the paraffin reconstruction models make it clear that these vessels are sinusoidal and are arranged as anfractuous networks that course serpiginously through the tissues, anastomose freely, and end abruptly and blindly, like sluggish bogs that meander, branch, and re-form; not like fast-flowing mountain streams that take direct and undeviating courses. It is well known that the primordial vessels in the encephalon are derived *in situ* from differentiation of mesenchymal cells gathered about the initial pools and flows of fluid in the neuroectoderm.[5] This primordial maze of channels notably exceeds the number of vessels present in the fully developed cerebrum, the pattern of the latter being governed by subsequent tissue demands and mechanical factors. There is consider-

able evidence that the amount of blood flowing through these primitive channels determines whether a given vessel within the meshwork atrophies, remains a capillary, or enlarges to form an arteriole or venule.[5] There is also much evidence that differentiation of adventitial cells into the smooth muscle of the media is notably influenced by the intrinsic blood pressure.[6] Under normal conditions, the ultimate thickness of the vessel walls thus depends largely upon pressure imparted to the primordial bed by integration with the systemic circulation. Since in anencephaly these cerebral vessels retain a plexiform architecture and many have delicate, nonmuscular walls, these anatomic features strongly attest to low intravascular pressure and failure of union with the systemic circulation.

Hematopoiesis is conspicuous in the cephalic tissues in anencephaly. It is well known that hematopoietic cells, as well as endothelium, are derived from mesenchyma, aggregated as blood islands in association with the primitive vascular sinuses.[7] Although there remains doubt whether erythropoiesis is stimulated by the oxygen content and capacity of the blood or oxygen tension and saturation,[8] the presence of hematopoiesis in the cerebrum at the neonatal period provides strong inferential evidence of marked and prolonged stimulation by anoxia. Since these changes are confined to the cerebrum, they again bespeak local interference in circulation. It remains speculative whether this *in situ* hematopoiesis suffices to fill the cephalic sinusoids with blood or whether minute anastomoses not demonstrable by the techniques employed exist with the systemic system.

The present observations conform closely to previous observations.[1,2] Taken together they provide strong evidence that the cerebral abnormalities of anencephaly in human beings occur during or shortly after 6 or 7 weeks of fetal development as a result of failure of union between the primordial cerebral vessels and the major systemic arteries and veins, with a lack of integration of the cerebral vasculature into the somatic circulation.

Summary

Vinyl injection studies showed marked vascular anomalies of the major cephalic arteries and veins in close anatomic relation with the cerebral deformities in 3 anencephalic monsters. Nevertheless, detailed histologic examinations of the deformed cerebral masses in 7 additional cases showed rich intrinsic vasculatures. However, notably few of these vessels filled by the injection technique, and in paraffin reconstruction models they appeared as anfractuous networks of branching and anastomotic sinusoids. They were regularly lined by endothelium, but many

were devoid of muscular or adventitial coats. Active hematopoiesis was present about and within them.

The topographic pattern and the muscular development of the mature cerebral blood vessels, in derivation from the meshwork of thin-walled primordial channels, is governed largely by blood flow and blood pressure. The lack of these vascular developments in anencephaly, when considered together with other anatomic features, provides cogent evidence that the cerebral abnormalities of anencephaly in human beings occur during or shortly after the first 6 or 7 weeks of fetal development as a result of failure of integration of the primordial cerebral vessels into the systemic circulation. Notable features were the manifestations of cerebral anoxia reflected by the presence of hematopoiesis, and retarded differentiation of neurons, the paucity of filling of the cerebral vessels by the vinyl injection technique, and the presence of well-formed and well-preserved structures derived from migratory neuroblasts.

References

1. Vogel, F. S., and McClenahan, J. L. Anomalies of major cerebral arteries associated with congenital malformations of the brain; with specific reference to the pathogenesis of anencephaly. *Am. J. Path.*, 1952, **28**, 701–723.
2. Vogel, F. S. The association of vascular anomalies with anencephaly. A postmortem study of nine cases in one of which unilateral anencephaly was present in a conjoined double monster. *Am. J. Path.*, 1958, **34**, 169–183.
3. Liebow, A. A.; Hales, M. R.; Lindskog, G. E., and Bloomer, W. E. Plastic demonstrations of pulmonary pathology. *J. Tech. Methods*, 1947, **27**, 116–129.
4. Clark, E. R., and Clark, E. L. Microscopic observations on the growth of blood capillaries in the living mammal. *Am. J. Anat.*, 1939, **64**, 251–301.
5. Clark, E. R. Studies on the growth of blood-vessels in the tail of the frog larva—by observation and experiment on the living animal. *Am. J. Anat.*, 1918, **23**, 37–88.
6. Clark, E. R., and Clark, E. L. Microscopic observations on the extra-endothelial cells of living mammalian blood vessels. *Am. J. Anat.*, 1940, **66**, 1–49.
7. Goss, C. M. Experimental removal of the blood island of *Amblystoma punctatum* embryos. *J. Exper. Zool.*, 1928–1929, **52**, 45–63.
8. Grant, W. C., and Root, W. S. The relation of O_2 in bone marrow blood to post-hemorrhagic erythropoiesis. *Am. J. Physiol.*, 1947, **150**, 618–627.

The technical assistance of Miss Hannelore Singer is gratefully acknowledged.

[*Illustrations follow*]

Legends for Figures

FIG. 1. The cephalic arteries of the anencephalic monster shown in Figures 3 and 4 have been filled with red vinyl, the veins with yellow. The vertebral, basilar, and ophthalmic vessels are clearly shown. Racemose networks of anastomotic veins line the cervical canal and cover the lateral portions of the plateau of the bony skull. A fuller description of the vessels is given in the text.

FIG. 2. A paraffin reconstruction model of the intracerebral vasculature shows it to be a network of tortuous, anastomotic sinuses with tributaries that end blindly. The straight muscular arteries that coursed through the fibrous tissue are shown arising from the green background.

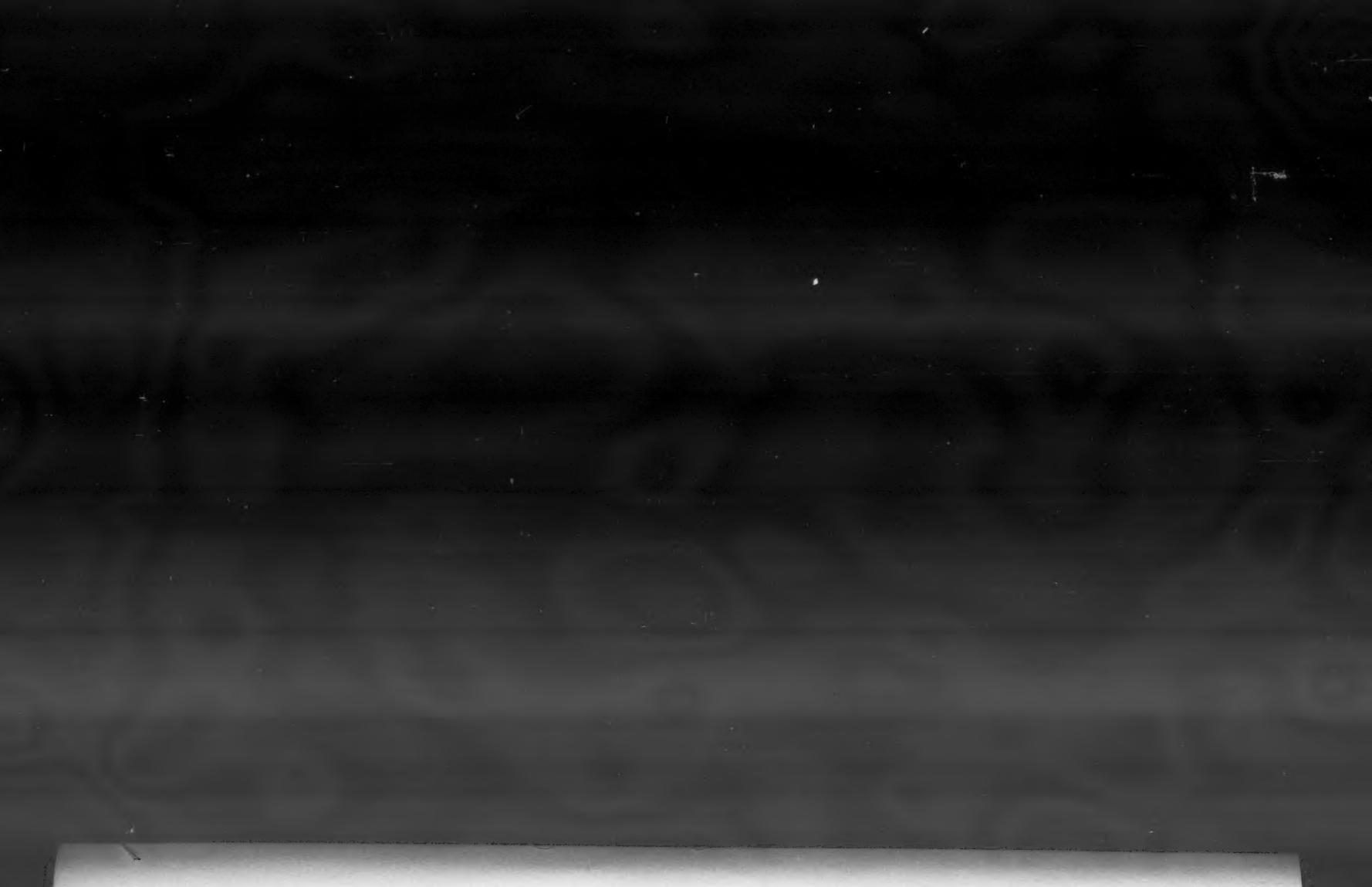

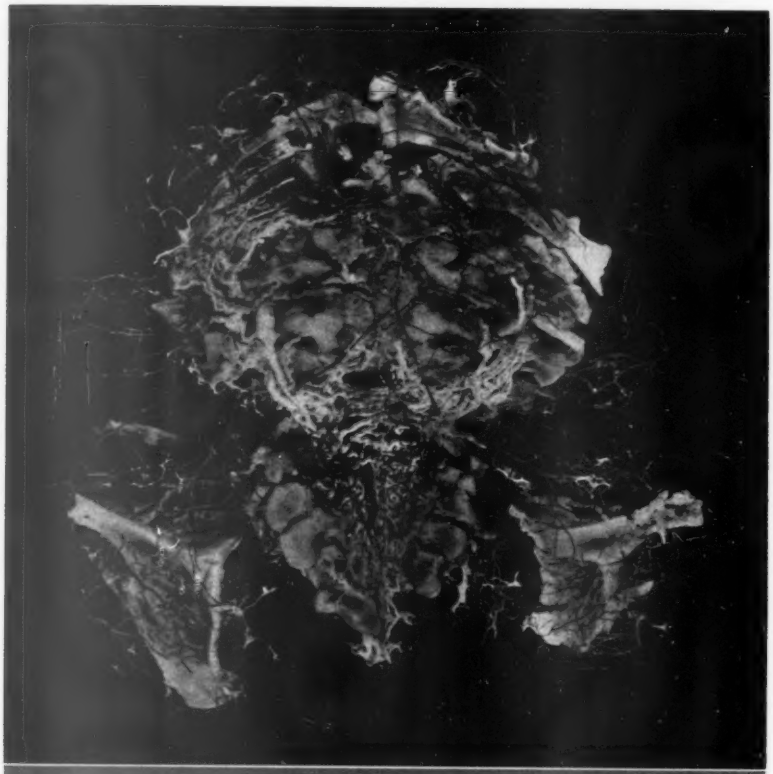

1

2

FIG. 3. An anencephalic monster with a deformity characterized by an absence of the calvaria, replacement of the cerebrum by a diminutive mass of hemorrhagic tissue, proptosis, and a cervical rachischisis.

FIG. 4. A posterior-superior view of the cephalic deformity positioned as in Figure 1.

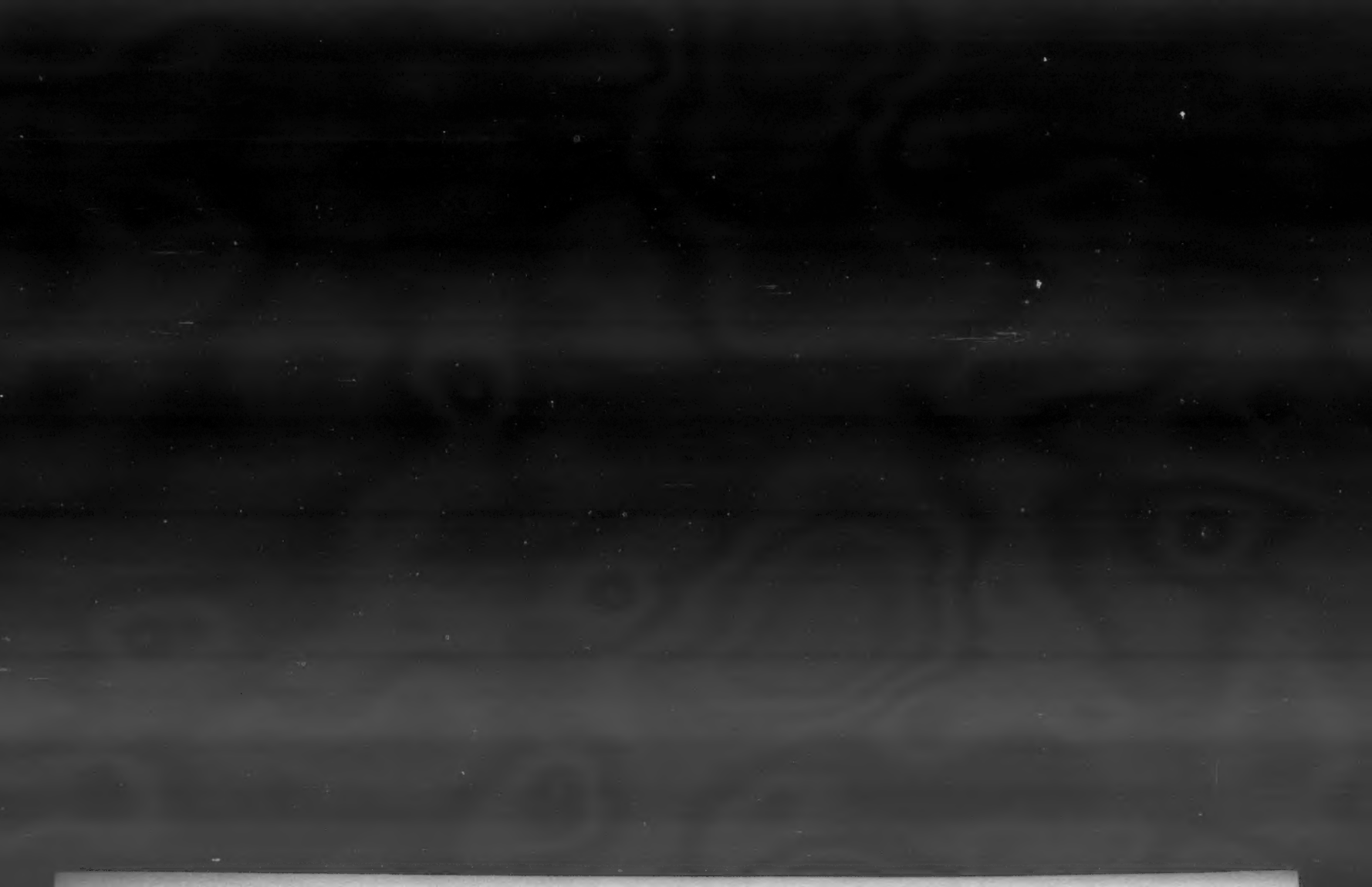

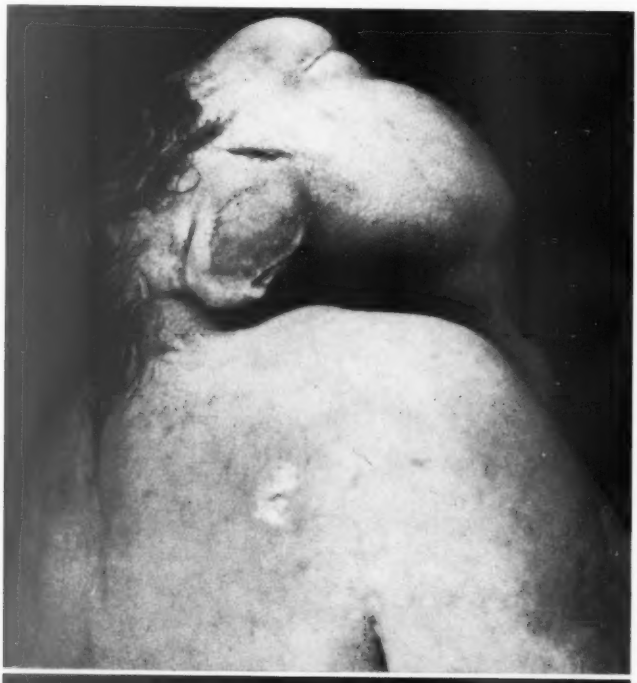

3

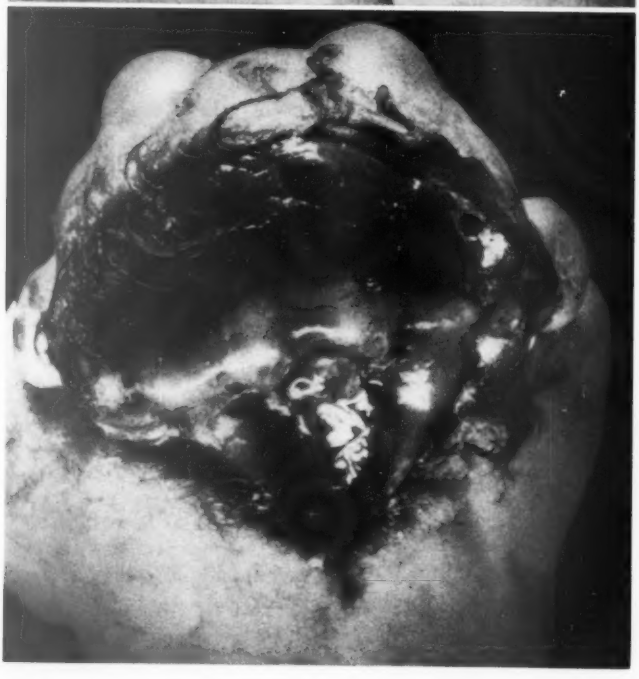

4

5

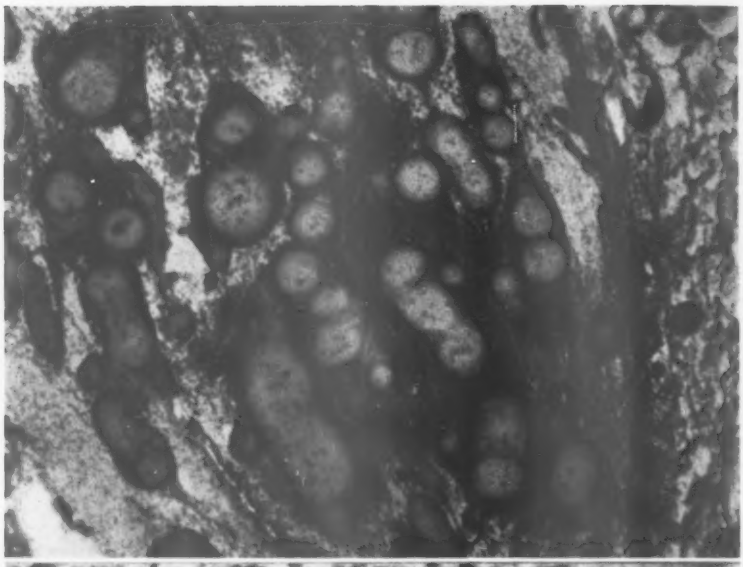

6

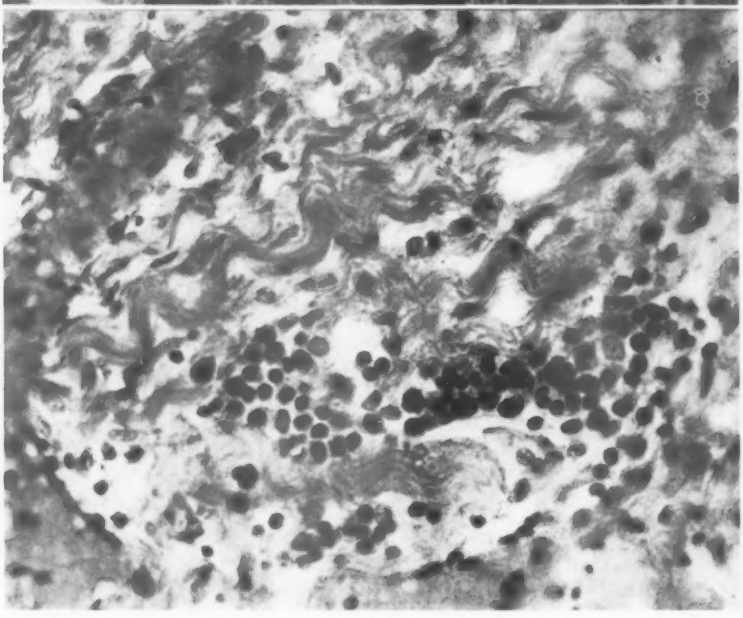

FIG. 5. A histologic section used in the preparation of the paraffin model. The vessels within the neural island are large and tortuous. The two arteries used for points of fixation are shown in the fibrous tissue on the right. The section is 50 μ thick. Masson's trichrome stain. × 60.

FIG. 6. An accumulation of cells in a juxta-thelial position to the cerebral sinusoids is composed of erythroblastic or myeloblastic elements, normoblasts and myelocytes. Hematoxylin and eosin stain. × 200.

A HISTOCHEMICAL STUDY OF SWELLING AND VACUOLATION OF PROXIMAL TUBULAR CELLS IN SUCROSE NEPHROSIS IN THE RAT

DAVID T. JANIGAN, M.D.,* AND ARMANDO SANTAMARIA, M.D.

From the Department of Pathology and Oncology, University of Kansas Medical Center, Kansas City, Kans.

Swelling and vacuolation of cells in response to various toxic agents generally are attributed to an increase in intracellular water. [1,2] The renal tubular alterations produced by sucrose and glucose [3–15] are similarly explained,[8,9,11,13,15] the cytologic changes being referred to as hydropic swelling; the over-all histologic lesion is termed "osmotic nephrosis." [9] While there have been various proposals as to the nature of the osmotic disturbance in sucrose nephrosis,[8,9,11,13,15] the role of pinocytosis has been largely overlooked. There are conflicting opinions concerning tubular epithelial vacuoles in "osmotic nephrosis." Zingg,[10] Lanz and Zollinger,[12] and Morard [13] suggested a mitochondrial origin, while Rouiller and Modjtabai [14] believed that they arose from a confluence of distended intracytoplasmic membranes. An electron microscopic study of sucrose nephrosis in the mouse, by Yolac,[15] could not confirm either theory.

There has been increasing evidence that the activation or release of intracellular acid hydrolases plays a prominent role in the phenomena of intracellular digestion, autolysis and necrosis.[16–29] The pathogenesis of the cytologic alterations in sucrose nephrosis was therefore reinvestigated in terms of changes in intracellular sites of acid phosphatase activity. In the rat kidney, sites of acid phosphatase activity can be demonstrated histochemically as well-defined droplets in tubular epithelium. It is presumed that these droplets correspond to those referred to as "phagosomes" [19] and isolated by Straus [30–32] from the rat kidney. These contain a number of other acid hydrolases.[31] Cytochrome oxidase, succinic dehydrogenase and diphosphopyridine nucleotide reductase activities were also investigated and changes in these oxidative enzymes compared with those in acid phosphatase activity.

MATERIAL AND METHODS

Sixty-eight male and female Sprague-Dawley rats, with an average body weight of 220 gm. (range, 119 to 300 gm.) were utilized. During light ether anesthesia the

This investigation was supported in part by a research training grant, 2G-125, Division of Research Grants, and research grant H-2922, National Heart Institute, United States Public Health Service.

Accepted for publication, April 5, 1961.

* Present address. Department of Pathology, Postgraduate Medical School, Ducane Road, London, England.

animals received a single intraperitoneal injection of 50 per cent sucrose in water (1.46 molal). The sucrose dosage ranged from 2 to 6 ml., and animals were killed by decapitation at 12, 18, 20 and 24 hours after injection; a few animals were killed at 3, 6, 36 and 40 hours. Control animals were also anesthetized but did not receive injections. After the injections, food and drinking water were withheld from both groups.

Tissues were fixed in 10 per cent calcium-formalin at 2 to 4° C.[33] Paraffin and frozen sections were stained with hematoxylin and eosin and oil red O respectively. The periodic acid-Schiff stain (PAS) was applied to tissue fixed in absolute ethanol. Some tissues were quenched in propane cooled to −175° C. and dehydrated by freeze substitution in acetone.[34] The methanol-PAS technique [35] was applied to these tissues after paraffin embedding.

The following enzyme studies were carried out: (1) Nonspecific acid phosphatase. Since biochemical evidence has indicated that much of the acid phosphatase in the kidney is localized within the phagosomes, it seemed desirable to employ a histochemical method which would best yield consistent and discrete localization without diffuse cytoplasmic or nuclear staining. Prior to the experiments, a number of the azo dye techniques were surveyed and were found to be less satisfactory than the following method: After 12 to 16 hours' fixation in cold calcium-formalin at 2 to 4° C., 10 μ frozen sections were cut, floated on slides from cold water and incubated in a freshly prepared and stored metal precipitate medium of Gomori.[36] Sodium glycerophosphate, containing the beta and alpha isomers in a 60 to 40 per cent ratio, was the substrate employed. Later the 100 per cent beta salt was used concomitantly for comparison [37] but showed no significant differences. Incubation times varied from 20 to 40 minutes, but within this time range, sections from both control and experimental animals were incubated together in the same media and for the same length of time. After incubation, the slides were rinsed in 0.5 per cent acetic acid in water for 30 seconds. They were then rinsed again in water and placed in a dilute solution of ammonium sulfide (3 to 4 drops in 50 ml. of water) for only 30 to 60 seconds. The omission of the substrate from the incubation medium served as the histochemical control.

(2) Nonspecific alkaline phosphatase activity was demonstrated by Gomori's technique [36] in frozen sections cut at 10 μ from cold calcium-formol fixed tissues. Incubation time was 20 to 30 minutes.

(3) Oxidate enzymes: Unfixed sections, 4 to 8 μ, were cut in a cryostat at −20° C., mounted on cover slips and used within 1 to 2 hours. Cytochrome oxidase activity was demonstrated by Burstone's method, using p-aminodiphenylamine and p-methoxyaminodiphenylamine as substrates.[38] Cryostat sections from 20 experimental animals were incubated for the demonstration of diphosphopyridine nucleotide (DPN) reductase [39] and succinic dehydrogenase,[40] utilizing nitro-BT [2,2′-di-p-nitrophenyl-5,5′-diphenyl-3,3′-(3,3′-dimethoxy-4,4′-biphenylene)-ditetrazolium chloride] as the tetrazolium salt.

The urine from 26 rats was collected for biochemical measurement of acid phosphatase at 12, 18, and 24 hours after injection. The animals were placed in metabolism cages, and small bottles were taped to the drain of each cage. The bottles were placed in Dewar flasks containing dry ice. In this way the urine was immediately frozen.

Morphologic Base Line and Artifacts of Acid Phosphatase Activity in the Rat Kidney

Topographically, the cortex of the rat kidney is divided into two zones. The outer cortical zone contains the convoluted portions of the

proximal tubules, the distal tubules and glomeruli. With the metal precipitate method of Gomori,[36] the acid phosphatase activity in the cells of the convoluted proximal tubules was localized in discrete sites of predominantly spherical shape (Figs. 2 and 3). These sites have been referred to as "droplets,"[24, 37, 41] which vary from 0.5 μ to 2.5 μ in diameter, the majority in the range of 1.5 to 2 μ. They were often distributed uniformly throughout the cell although most were located in the middle and basal zones. The acid phosphatase droplets in the distal tubules were smaller (about 0.5 μ) and more sparse.

The inner cortical zone is made up chiefly of the straighter, terminal portions of the proximal tubules along with the ascending limbs of Henle and collecting tubules. The acid phosphatase droplets in the cells of the terminal proximal tubules were smaller (about 0.5 to 1 μ), more uniform in size and less numerous than those in the convoluted portions. The other tubules in this zone, as well as those in the medulla, contained very few and faintly active droplets which were of about the same size as those found in the distal tubules.

Because of the nature of the changes in the acid phosphatase droplets occurring in the experimental lesions, certain artifacts that occasionally occurred must be described. Nuclear and diffuse light brown cytoplasmic staining sometimes was observed in control sections. In the experimental kidneys, these two features were always present in varying degrees, even though the sections were incubated in a fresh medium and with sections from control animals in which these features were absent. One of the induced changes noted in the experimental kidneys was the aggregation of droplets, later forming large irregular masses. These were distinguished from the occasional aggregation of 2 or 3 droplets noted in control sections (Fig. 3). The nonspecific deposition of small lead sulfide precipitates was also distinguished from the experimentally induced alterations. These granular precipitates were recognized by their angular shapes, often with sharp edges, and the difference in focal plane.

Results

The tubular lesions in sucrose nephrosis have been described in various species,[3–10,15] and a detailed account only of the alterations occurring in the convoluted segment of the proximal tubules will be reported. The time of onset or severity of the changes could not be correlated with the amount of sucrose injected, the size of the animal, or the time of injection—i.e., morning or evening. However, it was possible to trace and grade the progression of the alterations in the following order: (a) early changes; (b) vesicular swelling; and (c) vacuole formation.

Early Changes

The early changes consisted of homogeneous and often granular cytoplasmic swelling of proximal tubular cells. Alterations in the acid phosphatase droplets were minimal, confined to a greater frequency of small aggregates of droplets than noted in controls. The aggregates were almost always juxtanuclear and associated with slight acid phosphatase activity in the adjacent nucleus and cytoplasm.

Multiple small, sudanophilic globules were arranged in a linear manner along the basal portions of the proximal tubular cells in both control and experimental animals. This was particularly the case after 18 to 30 hours of fasting. No obvious changes in the activity of alkaline phosphatase, cytochrome oxidase, succinic dehydrogenase, or DPN reactivities were apparent. The methanol-PAS staining of freeze-substituted tissues showed small PAS-stained bodies in the control proximal tubular epithelium (Fig. 1); no changes in these were observed at this stage.

Vesicular Swelling

This stage was characterized by swollen proximal tubular epithelium containing multiple tiny vesicles imparting a foamy, reticulated appearance to the affected cell (Fig. 4). The vesicles varied in size in a given cell, with the larger ones near the basement membrane. While the alterations were sometimes patchy, they tended to affect all proximal convoluted tubules, often including the straight portions. Not all cells in a plane section of any one tubule were involved in similar manner. Proximal tubular epithelium within and lining Bowman's capsule showed similar features.

At this stage a number of changes were noted in the acid phosphatase droplets which appeared as large irregular and heavily stained masses filling most of the swollen cells and obscuring the nuclei (Fig. 5). The appearance of these masses indicated that they had resulted from the aggregation and apparent fusion of individual droplets. Some of the latter could be discerned around the periphery of the masses. Invariably, some of the masses were situated in the apical zone of swollen cells and were extruded into the lumen. Smaller aggregates of enlarged droplets were also seen. These were surrounded by cytoplasm showing both fine and coarse stippling of enzyme reactivity. Occasionally, no distinct droplets were found, there being only a diffuse and coarse staining of the cytoplasm (Fig. 6). In some instances there appeared, singly or in small numbers, enlarged droplets, occasionally with irregular margins. Nuclear staining was always present.

In contrast to the alterations of acid phosphatase droplets, cyto-

chrome oxidase activity was only slightly reduced and was sharply localized to sites where mitochondria were known to be found (Fig. 12). There was no obvious decrease in the number, or alterations in the shapes of the activity sites. There were slight reductions in DPN and succinic dehydrogenase activities. Alkaline phosphatase and PAS staining of brush borders were decreased in proportion to the amount of cellular damage. Some of the PAS-positive cytoplasmic bodies were found within vesicles, but the latter contained no lipid.

Vacuolar Changes

The formation of large vacuoles was regarded as the most advanced lesion. These were formed near the base of cells and arose through a confluence of small vesicles (Fig. 7). As they enlarged, remnants of vesicle membranes were found in and between the vacuoles. Again, not all cells in the plane of section of any one tubule contained the large vacuoles, early swelling or vesicular changes persisting in adjacent cells. The nuclei of the vacuolated cells were smaller and the nuclear outlines often wrinkled or crenated.

The over-all acid phosphatase activity was reduced markedly, many nephrons showing complete loss of reactivity. Not infrequently, however, the margins of many vacuoles were surrounded by irregular rims of both lightly and heavily stained cytoplasm (Figs. 8 to 11) and occasionally by a few faintly reactive droplets. Within some vacuoles, small collections of finely particulate cytoplasmic debris with small amounts of enzyme activity were observed; there was also some nuclear staining (Figs. 10 and 11). Tubular casts exhibiting acid phosphatase activity were occasionally found lower in the nephron. There was also a diffuse light and often dark brown staining of glomeruli, the inner cortex, and the medulla (Fig. 16).

Accompanying vacuolar changes was an over-all decrease of cytochrome oxidase activity, but the cytologic sites of activity were still discrete (Fig. 13). There was also a somewhat greater loss of succinic dehydrogenase (Figs. 14 and 15) and DPN reactivities. Little or no alkaline phosphatase activity remained in the brush borders. The vacuoles contained no sudanophilic or PAS-positive material.

In all stages there was reproducible correlation between the morphologic and histochemical alterations in about ⅔ of the animals. In the remainder, the chief variation was a striking loss of acid phosphatase activity at the stage of vesicular swelling. In such instances the large droplet aggregates and irregular masses were found only in a few nephrons.

While the number of measurements of urinary acid phosphatase was

small, the results indicated large increases in the excretion of this enzyme in experimental animals (Table I).

Discussion

In rat liver cells, a number of acid hydrolases, including acid phosphatase, are known to be associated with a new group of cytoplasmic organelles, termed "lysosomes."[17] According to de Duve, "lysosome" indicates "what is believed to be a morphologically distinct entity, defined on the basis of purely biochemical data."[29] When freshly isolated in isotonic sucrose, lysosomes are almost devoid of enzyme activity since a lipoprotein membrane physically prevents access of substrates to their respective enzymes. Membrane damage induced by physical or chemical injuries results in activation and release of the enzymes.[17,20,21,29] The enzyme content and behavior in hypotonic media of phagosome droplets isolated from the rat kidney by Straus[30,31] are almost identical to those in the liver lysosomes of de Duve.

There is increasing evidence[28] that hepatic lysosomes might be represented histochemically by the peribiliary bodies with acid phosphatase activity and ultrastructurally by cytoplasmic peribiliary bodies or microbodies. In the rat kidney there is inconclusive evidence suggesting that histochemically demonstrable tubular acid phosphatase droplets and certain cytoplasmic bodies seen with the electron microscope might correspond to the phagosomes. As indicated above, there were wide differences in the size of acid phosphatase droplets demonstrated by Gomori's technique in the various nephron segments of the rat renal cortex.

Table I

URINARY EXCRETION OF ACID PHOSPHATASE

	12 hours	18 hours	24 hours
Controls	0.21 u.* (3)†	0.23 u. (3)	0.9 u. (7)
Sucrose nephrosis	2.4 u. (5)	3.7 u. (3)	2.6 u. (5)

* Mean values are expressed in Bodansky units.
† Number of animals in each group is indicated in parentheses.

Moreover, Straus also recorded wide variations in the size of droplets (phagosomes) isolated from the rat kidney.[31] Further, in a combined histochemical and electron microscopic study of experimental hydronephrosis, Novikoff[24] described acid phosphatase staining of membrane-limited and granule-containing vacuoles in the proximal tubular cells. Additional evidence relating membrane-limited cytoplasmic bodies seen with the electron microscope to the acid phosphatase droplets has been accumulated in the course of this study and will be published at a later date.[42]

While the accumulated evidence indicates that the tubular acid phosphatase droplets may represent the phagosomes, two discrepancies exist in their histochemical characterization. First, nonspecific esterases are not among known phagosomal enzymes as determined biochemically. On the other hand, the histochemical activity of these enzymes in the proximal tubules of the rat kidney is confined to sites somewhat similar in appearances to the acid phosphatase droplets (phagosomes).[43] The significance of this fact is not known. Secondly, while beta glucuronidase is isolated biochemically in phagosomes, it is not possible to obtain precise histochemical localization as in the case of acid phosphatase droplets. However, with improved techniques, Pearse has observed discrete intracellular localization of this enzyme in tubular epithelium.[44]

Vesicular Swelling

The changes in the acid phosphatase droplets which accompany vesicular swelling of tubular epithelium consisted of aggregation and apparent fusion, with the formation of large irregular acid phosphatase masses, followed by a diffuse and coarse reactivity in the surrounding cytoplasm. These results suggest that with vesicular swelling, droplet disruption occurs and there is an intracellular release of acid phosphatase. The observation of acid phosphatase activity in tubular casts and elevated levels of this enzyme in the urine would tend to support the belief that the enzyme is actually released from the altered droplets. If, as the evidence suggests, these droplets correspond to the phagosomes, then on the basis of the changes in the acid phosphatase-staining of the droplets, and the utilization of this enzyme as a "marker," it is possible that release of other acid hydrolases occurs with the alterations in the droplets.

The alterations in the acid phosphatase droplets accompanying vesicular swelling coincides with enlargement and rupture of membrane-limited bodies seen with the electron microscope.[42] It would seem then, that structural alterations in the phagosomes constitute the early morphologic features in sucrose nephrosis. The apparent release of acid phosphatase, and possibly other acid hydrolases, would be expected to accompany such structural alterations.[24] Release or activation of acid hydrolases is known to occur in tissues during autolytic, toxic and ischemic cell damage.[16,20,21,23,27] Novikoff has observed the formation of large irregular acid phosphatase masses from droplets in degenerating renal tubular epithelium of the rat after ureteral ligation.[24] In a histochemical study of the ischemic rat kidney, 30 to 60 minutes after ligation of the vascular pedicle or renal vein alone, the formation of large and irregular acid phosphatase masses from droplets was observed in greatly swollen proximal tubular cells[42] (Fig. 17).

Although it is possible that the structural alterations of the phagosomes or activation of intracellular hydrolases are the primary changes in sucrose nephrosis, these droplet alterations could also occur as a consequence of other cytologic disturbances. One may ask: "Do intracellular disturbances of another nature, e.g., mitochondrial damage, occur prior to changes in the droplets?" The question may be answered in part by the fact that in early stages of sucrose nephrosis there were few alterations in the histochemical activity of the mitochondrial enzymes investigated.

Since the droplets are damaged when isolated in hypotonic media [32] and many believe that osmotic disturbances with an increase of cellular water account for the sucrose tubular lesions, the possibility that osmotic changes precede the droplet alterations must be considered. Wilmer believed that sucrose diffused into the tubular epithelium from the lumen and created an osmotic disturbance with a subsequent entry of water.[8] Allen proposed that the high concentration of sucrose in the tubule lumen produced an osmotic effect whereby water might enter the tubular epithelium from peritubular capillaries.[9] Since in the rat the maximum diuresis occurred 1 to 2 hours after sucrose injection,[42] it might be assumed that the greatest quantity of sucrose was present in the glomerular filtrate during that period. If the presence of sucrose in the tubule lumen produced the lesions by virtue of an osmotic effect, the cell changes would be expected to develop during or shortly after this period. In the present study no typical lesions were found in the kidneys of animals sacrificed 3 to 6 hours after injection. Hamburger also believed that the tubular changes in osmotic nephrosis were a result of cellular hyperhydration because there was a fall in the concentration of sodium in the extracellular fluid after osmotic diuresis.[11] In view of the decrease in osmolarity in this compartment, it was postulated that water entered the cell by virtue of the osmotic gradient created. If the renal lesions developed on the basis of such a gradient, it would appear to be selective since in the present experiment similar changes were not seen in other organs although Morard [13] and Hamburger [11] found swelling of liver cells in glucose nephrosis.

While the possibility that intracellular osmotic disturbances precede droplet changes cannot be definitely excluded, certain observations in this study suggest that another mechanism may alter the droplets. The ability of renal epithelium to incorporate macromolecular substances is well known,[45] and recent demonstrations of this phenomenon with the electron microscope have been reported by Trump [46] and Farquhar and Palade.[47] The phenomenon has been related to pinocytosis or athrocytosis, and with some proteins has been associated with the

activity of phagosomes[19,25] and dense cytoplasmic bodies.[47] In occasional instances the apparent transport of injected particles, i.e., trypan blue and ferritin, sometimes within pinocytotic vesicles,[47] can be traced from the cell membrane to a juxtanuclear zone in the renal epithelium near the Golgi apparatus; here they are incorporated into cytoplasmic bodies.[46,47] The incorporation of injected foreign protein by renal epithelial phagosomes is occasionally accompanied by perinuclear aggregation of the latter elements.[25] In most instances this intracellular association of foreign material, often within pinocytotic vesicles, with phagosomes or dense cytoplasmic particles has been related to the role of these bodies in intracellular phagocytosis or digestion because of their complement of hydrolases.[18,19,22,25,26,28,29,47]

After the injection of sucrose in the mouse, the apical vesicles of proximal tubules increase in size and numbers and, as the time after injection increases, appear to descend to, or form *de novo* in the mid and basal zones of the cells.[15] In the present study, this phenomenon was observed, and was accompanied by perinuclear aggregation, swelling and disruption of acid phosphatase droplets. Thus by analogy, these findings suggest that sucrose is incorporated into the tubular epithelium through pinocytosis and is taken up by the phagosomes. The subsequent swelling of the bodies appears to account for the vesicle formation in tubular epithelium.

Vacuole Formation

The vacuoles formed in the renal tubular epithelium after injections of sucrose and glucose are believed by some to be derived from mitochondria,[10,12,13] or from a confluence of distended intracytoplasmic membranes.[14] Yolac, however, did not find evidence for either in sucrose nephrosis in the mouse.[15] In the present study the large vacuoles appeared to originate from a confluence of vesicles. The histochemical demonstration of acid phosphatase activity within the vacuoles would seem to support the suggestion that the vesicles were derived from acid phosphatase droplets. Once formed, the vacuoles continued to enlarge. At this point the increase in size might have been due to an actual increase in intracellular water, as many believe. If this is true, another mechanism might be conjectured.

It is now generally conceded that the osmolarity of the intracellular and extracellular fluids is similar[48] and that the swelling and increased water content of liver or kidney slices, incubated in "isotonic" media, is due to an increase in intracellular osmolarity as a result of autolysis. Conway has shown that even if rat kidney is maintained at 0° C. for 60 minutes, there is a breakdown of intracellular substances, with a

large increase in the concentration of nonprotein nitrogen constituents. The production of these extra molecules accounts for a pronounced increase in the intracellular osmolarity.[49] In a biochemical study of mouse liver necrosis and autolysis, Berenbom, Chang, Betz and Stowell found an increase in acid-soluble nitrogen and free amino acids from disintegrating protein, and also a rise of acid-soluble phosphorus, indicating breakdown of nucleic acids by their hydrolases.[16] In sucrose nephrosis an increase of cellular water might occur after the droplets are altered and hydrolases released. The access of intracellular substrates to these released enzymes would be expected to lead to an increase in intracellular organic and nonorganic constituents and therefore to an increase in intracellular osmolarity. The entry of water either from the tubule lumen or peritubular capillaries could be explained by this osmolar change.

Summary

Various histochemical staining techniques were applied to rat kidneys after intraperitoneal injections of a hypertonic sucrose solution. Early morphologic changes consisted of diffuse cytoplasmic swelling in the proximal convoluted tubules followed by the appearance of multiple small cytoplasmic vesicles. The vesicles increased in size toward the basal portions of the cells, becoming confluent to form large vacuoles.

Characteristic changes in the acid phosphatase droplets of proximal tubular cells were observed. With initial cell swelling, juxtanuclear aggregation of droplets occurred. Later, coinciding with vesicle formation, these were transformed into large irregular masses. Adjacent nuclei and cytoplasm were diffusely stained, and tubular casts were found to have acid phosphatase activity. There was also an increase of urinary acid phosphatase excretion. In vacuolated tubular epithelium, little acid phosphatase activity remained although it was sometimes observed around and within vacuoles. Only after the alteration of the acid phosphatase droplets and after the cell changes were established were decreases in the histochemical reactivity of succinic dehydrogenase, cytochrome oxidase and diphosphopyridine nucleotide reductase observed.

The results indicate that tubular epithelial changes in sucrose nephrosis are preceded and accompanied by topographic and structural alterations of tubular acid phosphatase droplets. Correlation of the morphologic and histochemical studies suggest that sucrose enters the tubular epithelium by a process akin to pinocytosis and is incorporated into these droplets. Their subsequent enlargement and fusion to form vacuoles appear to provide the cytologic basis of sucrose nephrosis.

The possible significance of the apparent release of acid phosphatase

from the damaged droplets, and their relationship to the phagosomes of Straus are discussed.

References

1. Cameron, G. R. Pathology of the Cell. Oliver & Boyd, Edinburgh, 1951, pp. 304–316.
2. Manuelides, E. E. Pathological Swelling and Vacuolization of Cells. In: Frontiers in Cytology. Palay, S. (ed.). Yale Univ. Press, New Haven, 1958, pp. 417–446.
3. Helmholz, H. F. Renal changes in the rabbit resulting from intravenous injection of hypertonic solution of sucrose. *J. Pediat.*, 1933, **3**, 144–157.
4. Cutler, H. H. Effects of sucrose on the kidney. *Proc. Staff Meet. Mayo Clin.*, 1939, **14**, 318–320.
5. Anderson, W. A. D., and Bethea, W. R., Jr. Renal lesions following administration of hypertonic solutions of sucrose; report of six cases. *J.A.M.A.*, 1940, **114**, 1983–1987.
6. Anderson, W. A. D. Sucrose nephrosis and other types of renal tubular injuries. *South. M.J.*, 1941, **34**, 257–263.
7. Rigdon, R. H., and Cardwell, E. S. Renal lesions following the intravenous injection of hypertonic solution of sucrose; a clinical and experimental study. *Arch. Int. Med.*, 1942, **69**, 670–690.
8. Wilmer, H. A. The mechanism of sucrose damage of the kidney tubules. *Am. J. Physiol.*, 1944, **141**, 431–438.
9. Allen, A. C. The Kidney. Medical and Surgical Diseases. Grune & Stratton, New York, 1951, pp. 207–214.
10. Zingg, W. Über experimentelle Rohrzuckerspeicherung in den Mitochondrien der Nierentubuli. *Schweiz. Ztschr. allg. Path.*, 1951, **14**, 1–16.
11. Hamburger, J.; Halpern, B., and Funck-Brentano, J. L. Une variété d'anurie provoquée par l'hydratation excessive des cellules rénales. *Presse méd.*, 1954, **62**, 972–976.
12. Lanz, R., and Zollinger, H. U. Ein Fall von postoperativer Anurie bei hydropischer Degeneration der Nierentubuli durch Zuckerspeicherung; Kasuistische Mitteilung. *Schweiz. med. Wchnschr.*, 1955, **85**, 1078–1080.
13. Morard, J.-C. Contribution expérimentale à l'étude des néphroses osmotiques; surcharge glucosée-surcharge hydrique-hyponatrémie aiguë. *Helvet. med. acta*, 1956, **23**, 215–239.
14. Rouiller, C., and Modjtabai, A. La néphrose expérimentale du lapin; comparaison entre la microscopie optique et électronique. I. Les modifications des cellules à bordure striée. *Ann. anat. path.*, 1958, **3**, 223–250.
15. Yolac, A. B. Elektronenmikroskopische Untersuchungen zur Morphologie der Hauptstückepithelien der Mäuseniere nach Injektion von hypertoner Saccharoselösung. *Verhandl. deutsch. Ges. Path.*, 1959, **43**, 235–240.
16. Berenbom, M.; Chang, P. I.; Betz, H. E., and Stowell, R. E. Chemical and enzymatic changes associated with mouse liver necrosis *in vitro*. *Cancer Res.*, 1955, **15**, 1–5.
17. De Duve, C.; Pressman, B. C.; Gianetto, R.; Wattiaux, R., and Appelmans, F. Tissue fractionation studies. 6. Intracellular distribution patterns of enzymes in rat liver tissue. *Biochem. J.*, 1955, **60**, 604–617.
18. Straus, W. Segregation of an intravenously injected protein by "droplets"

of the cells of the rat kidneys. *J. Biophys. & Biochem. Cytol.*, 1957, **3**, 1037–1040.

19. STRAUS, W. Colorimetric analysis with N,N-dimethyl-p-phenylenediamine of the uptake of intravenously injected horseradish peroxidase by various tissues of the rat. *J. Biophys. & Biochem. Cytol.*, 1958, **4**, 541–550.
20. BEAUFAY, H.; VAN CAMPENHOUT, E., and DE DUVE, C. Tissue fractionation studies. 11. Influence of various hepatotoxic treatments on the state of some bound enzymes in rat liver. *Biochem. J.*, 1959, **73**, 617–623.
21. DE DUVE, C., and BEAUFAY, H. Tissue fractionation studies. 10. Influence of ischaemia on the state of some bound enzymes in the rat liver. *Biochem. J.*, 1959, **73**, 610–616.
22. DE DUVE, C. The function of intracellular hydrolases. *Exper. Cell Res.*, 1959, Suppl. 7, 169–182.
23. VAN LANCKER, J. L., and HOLTZER, R. L. The release of acid phosphatase and beta-glucuronidase from cytoplasmic granules in the early course of autolysis. *Am. J. Path.*, 1959, **35**, 563–573.
24. NOVIKOFF, A. B. The proximal tubule cell in experimental hydronephrosis. *J. Biophys. & Biochem. Cytol.*, 1959, **6**, 136–138.
25. STRAUS, W. Rapid cytochemical identification of phagosomes in various tissues of the rat and their differentiation from mitochondria by the peroxidase method. *J. Biophys. & Biochem. Cytol.*, 1959, **5**, 193–204.
26. ESSNER, E. An electron microscopic study of erythrophagocytosis. *J. Biophys. & Biochem. Cytol.*, 1960, **7**, 329–334.
27. TAFT, E. B. Quantitative histochemical observations of postmortem autolysis in rat liver. *Lab. Invest.*, 1960, **9**, 169–173.
28. NOVIKOFF, A. B., and ESSNER, E. The liver cell. Some new approaches to its study. *Am. J. Med.*, 1960, **29**, 102–131.
29. DE DUVE, C. Lysosomes, a New Group of Cytoplasmic Particles. In: Subcellular Particles. HAYASHI, T. (ed.). Ronald Press Co., New York, 1959, pp. 128–159.
30. STRAUS, W. Isolation and biochemical properties of droplets from the cells of rat kidney. *J. Biol. Chem.*, 1954, **207**, 745–755.
31. STRAUS, W. Concentration of acid phosphatase, ribonuclease, desoxyribonuclease, β-glucuronidase, and cathepsin in "droplets" isolated from the kidney cells of normal rats. *J. Biophys. & Biochem. Cytol.*, 1956, **2**, 513–521.
32. STRAUS, W. Changes in "droplet" fractions from rat kidney cells after intraperitoneal injection of egg white. *J. Biophys. & Biochem. Cytol.*, 1957, **3**, 933–947.
33. BAKER, J. R. The histochemical recognition of lipine. *Quart. J. Micr. Sc.*, 1946, **87**, 441–470.
34. FEDER, N., and SIDMAN, R. L. Methods and principles of fixation by freeze-substitution. *J. Biophys. & Biochem. Cytol.*, 1958, **4**, 593–600.
35. MOWRY, R. W., and MILLICAN, R. C. A histochemical study of the distribution and fate of dextran in tissues of the mouse. *Am. J. Path.*, 1953, **29**, 523–545.
36. GOMORI, G. Microscopic Histochemistry: Principles and Practice. University of Chicago Press, Chicago, 1952, 273 pp.
37. HOLT, S. J. Factors governing the validity of staining methods for enzymes, and their bearing upon the Gomori acid phosphatase technique. *Exper. Cell Res.*, 1959, Suppl. 7, 1–27.

38. BURSTONE, M. S. Histochemical demonstration of cytochrome oxidase with new amine reagents. *J. Histochem.*, 1960, **8**, 63–70.

39. SCARPELLI, D. G.; HESS, R., and PEARSE, A. G. E. The cytochemical localization of oxidative enzymes. I. Diphosphopyridine nucleotide diaphorase and triphosphopyridine nucleotide diaphorase. *J. Biophys. & Biochem. Cytol.*, 1958, **4**, 747–752.

40. NACHLAS, M. M.; TSOU, K.-C.; DE SOUZA, E.; CHENG, C.-S., and SELIGMAN, A. M. Cytochemical demonstration of succinic dehydrogenase by the use of a new p-nitrophenyl substituted ditetrazole. *J. Histochem.*, 1957, **5**, 420–436.

41. NOVIKOFF, A. B. The Intracellular Localization of Chemical Constituents. In: Analytical Cytology; Methods for Studying Cellular Form and Function. MELLORS, R. C. (ed.). McGraw-Hill Book Co., Inc., New York, 1959, ed. 2, pp. 127–130.

42. TRUMP, B. F.; JANIGAN, D. T., and SANTAMARIA, A. Unpublished observations.

43. HOLT, S. J. A new approach to the cytochemical localization of enzymes. *Proc. Roy. Soc. London, s.B*, 1954, **142**, 160–169.

44. PEARSE, A. G. E. Histochemistry, Theoretical and Applied. J. & A. Churchill Ltd., London, 1959, ed. 2, 998, pp.

45. SMETANA, H., and JOHNSON, F. R. The origin of colloid and lipoid droplets in the epithelial cells of the renal tubules. *Am. J. Path.*, 1942, **18**, 1029–1049.

46. TRUMP, B. F. Electron microscopic study of the uptake of trypan blue by the cells of the rat nephron. (Abstract) *Anat. Rec.*, 1960, **136**, 293.

47. FARQUHAR, M. G., and PALADE, G. E. Segregation of ferritin in glomerular protein absorption droplets. *J. Biophys. & Biochem. Cytol.*, 1960, **7**, 297–304.

48. ROBINSON, J. R. Metabolism of intracellular water. *Physiol. Rev.*, 1960, **40**, 112–149.

49. CONWAY, E. J.; GEOGHEGAN, H., and MCCORMACK, J. I. Autolytic changes at zero centigrade in ground mammalian tissues. *J. Physiol.*, 1955, **130**, 427–437.

[*Illustrations follow*]

Legends for Figures

Fig. 1. Control rat. Proximal convoluted tubules. A few faintly staining PAS-positive intracytoplasmic bodies are evident. Freeze-substituted; methanol-periodic acid-Schiff (PAS) stain. × 960.

Fig. 2. Control rat. Acid phosphatase droplets are manifest in cells of the proximal convoluted tubules. Nuclei and cytoplasm are unstained. Gomori stain. × 960.

Fig. 3. Control rat. Small aggregates of 2 to 3 acid phosphatase droplets appear in some proximal tubular cells. Gomori stain. × 960. Inset shows details of one aggregate of 3 droplets. × 1160.

Fig. 4. Rat, sucrose injection. Multiple small cytoplasmic vesicles are manifest in cells of the proximal convoluted tubules. Vesicles close to the basement membrane are larger than those at the cell apexes. A portion of a distal tubule is shown in the lower right. Freeze-substituted; methanol-PAS stain. × 960.

Fig. 5. Rat, sucrose injection. Proximal convoluted tubules exhibit advanced aggregation and apparent fusion of acid phosphatase droplets accompanying vesicular swelling. Outlines of some enlarged droplets are present in the margins of the large masses. Gomori stain. × 960.

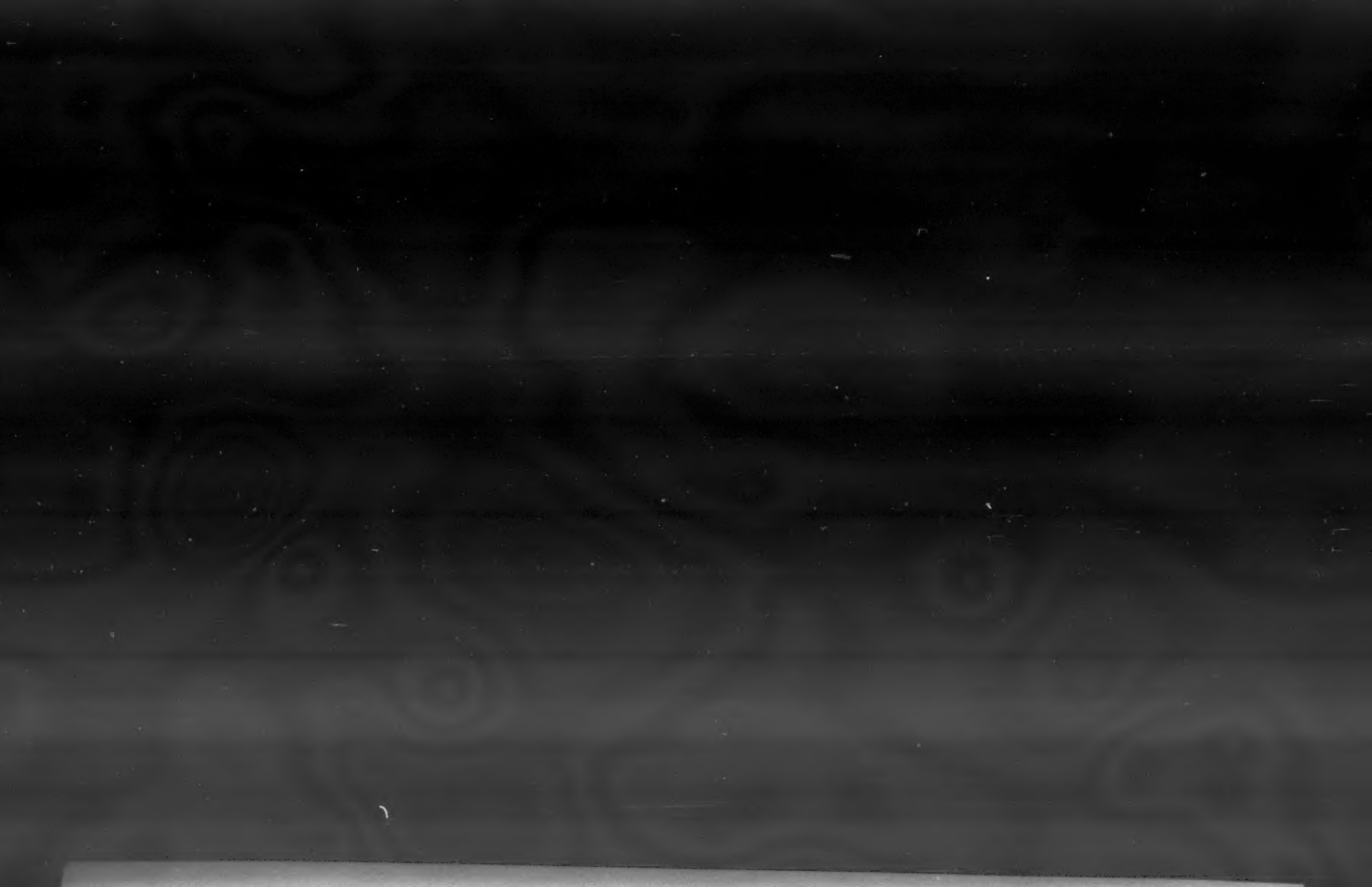

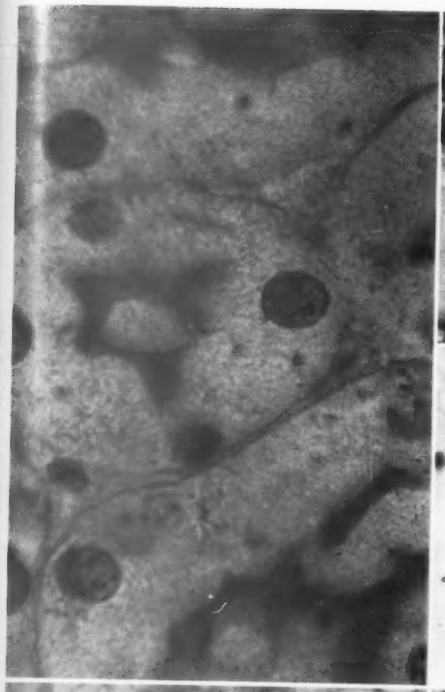

1

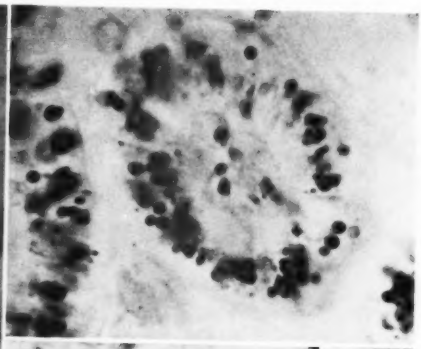

2

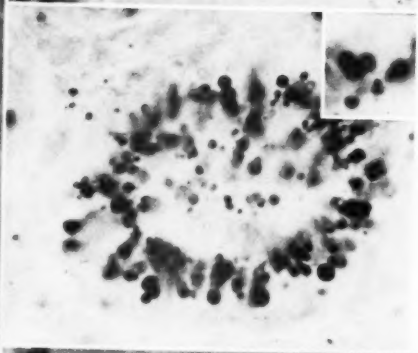

3

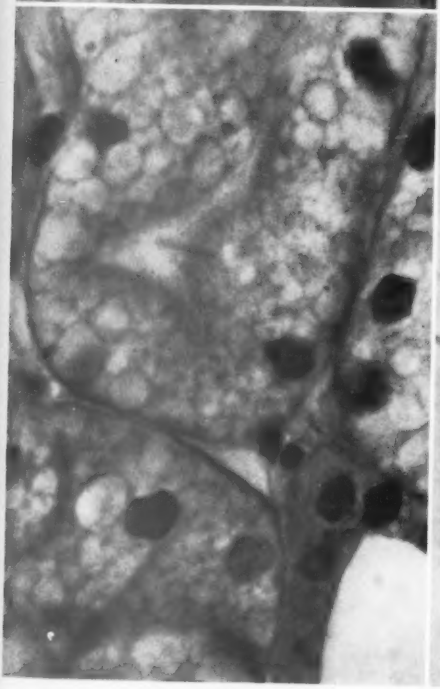

4

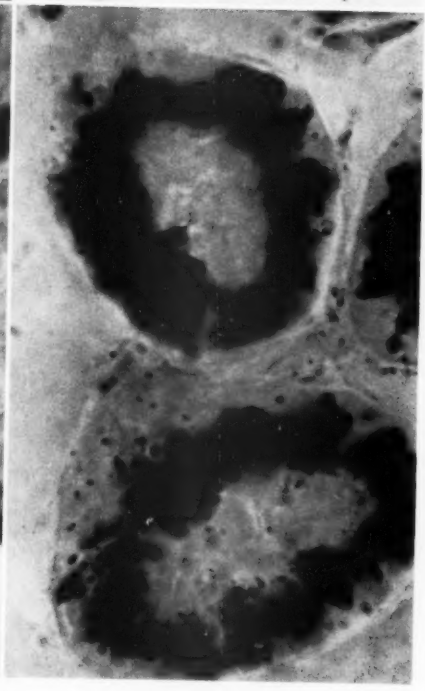

5

FIG. 6. Rat, sucrose injection. Diffuse and focally dense acid phosphatase reactivity appears in tubular epithelium with vesicular swelling. Only a few discrete droplets remain, and the nuclei are stained. Gomori stain. × 960.

FIG. 7. Rat, sucrose injection. Vacuoles form through rupture and confluence of enlarging vesicles near the basement membrane. A remnant of a ruptured membrane is seen in the vacuole at the right center. Freeze-substituted; methanol-PAS stain. × 960.

Figures 8 to 11 are from rats injected with sucrose, showing segments of proximal tubules, stained by Gomori's method. × 960. For orientation, the marker "m" indicates the position of the basement membrane.

FIG. 8. A vacuolated cell at the left is surrounded by droplets and contains a stained nucleus. The vacuole on the right contains faintly staining remnants of vesicle membranes (arrows).

FIG. 9. A vacuolated cell at the left contains large acid phosphatase active particles. A greatly enlarged droplet (arrow) and an acid phosphatase mass, extruded into the tubular lumen, are situated to the lower right of the vacuole.

FIG. 10. Vacuolated cells are surrounded by a thick rim of acid phosphatase-reactive cytoplasm. There is reactive particulate material within the vacuole on the left (arrow).

FIG. 11. A large vacuole contains acid phosphatase-active debris. The heavily stained nucleus is displaced toward the tubule lumen.

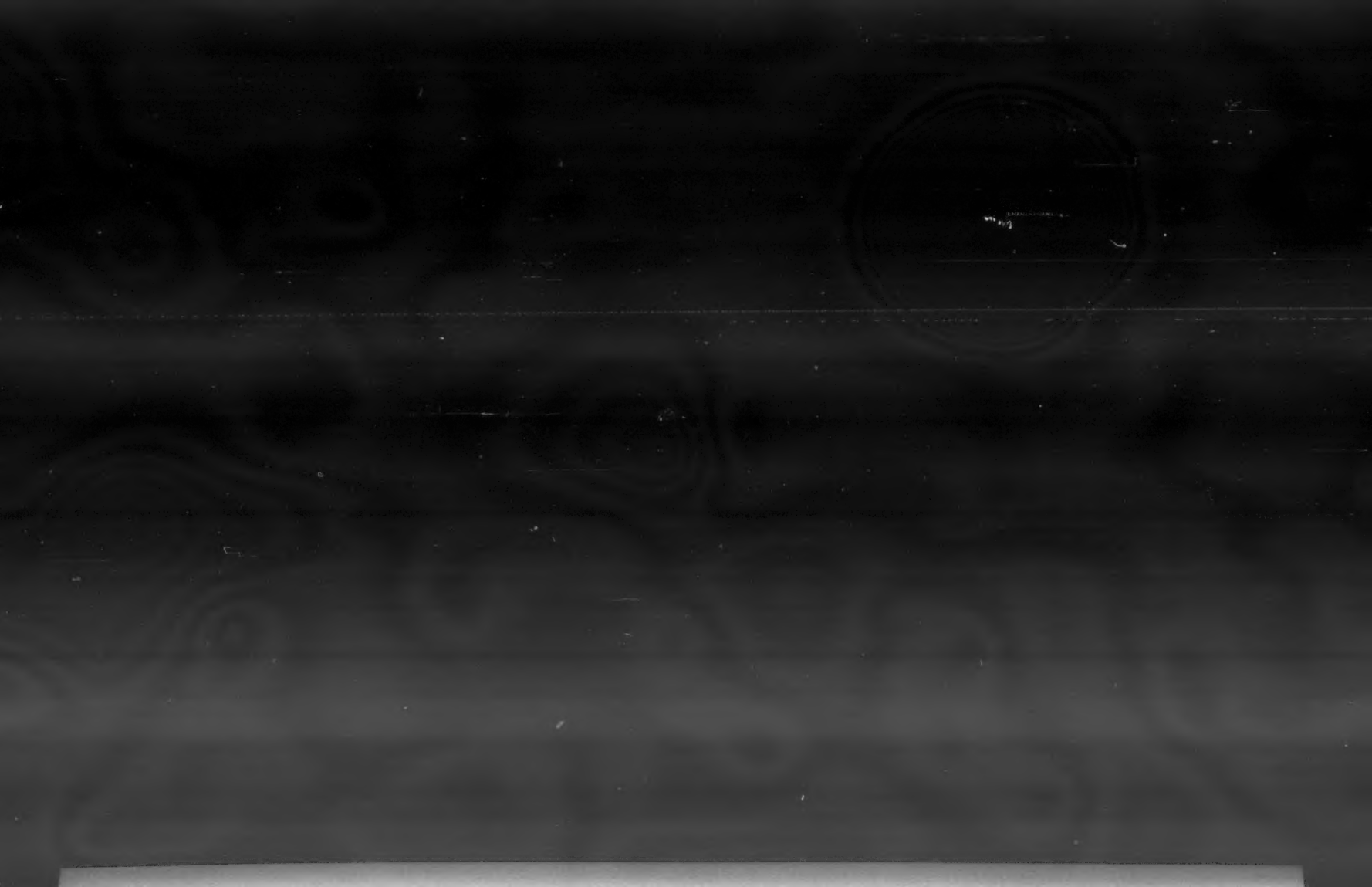

6

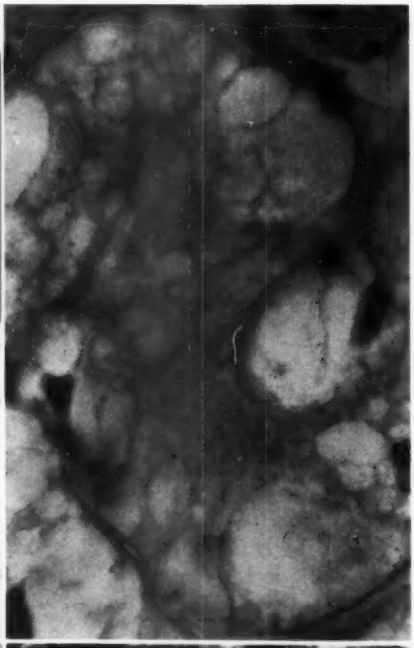

7

8

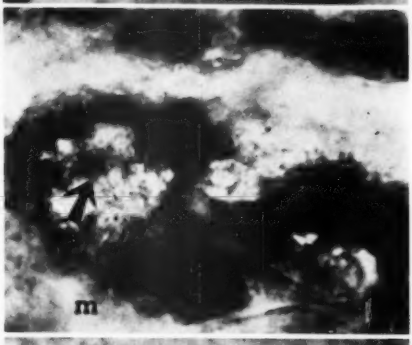

10

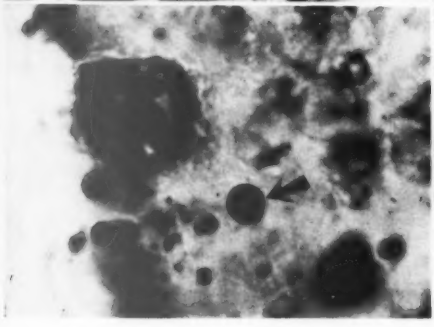

9

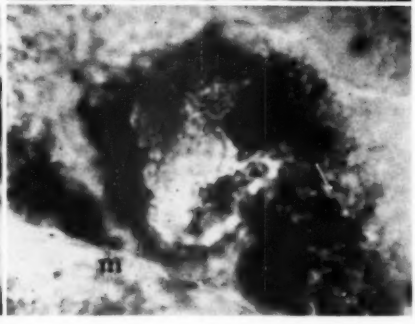

11

FIG. 12. Control rat. A cryostat section of a kidney incubated for cytochrome oxidase activity shows sites of reaction in the proximal convoluted tubules. × 960.

FIG. 13. Rat, sucrose injection. Discrete sites of cytochrome oxidase activity are still present in vacuolated proximal tubular cells. × 960.

FIG. 14. Control rat. A cryostat section of a kidney, showing succinic dehydrogenase activity in the proximal tubules. × 340.

FIG. 15. Rat, sucrose injection. Succinic dehydrogenase activity in vacuolated proximal tubular cells shows a slight over-all decrease of reactivity. × 340.

FIG. 16. Rat, sucrose injection. Acid phosphatase casts are evident in terminal proximal and collecting tubules. There is diffuse staining of tubular epithelium and stroma. Gomori stain. × 425.

FIG. 17. A rat kidney incubated for acid phosphatase activity 45 minutes after ligation of the renal vein. There is aggregation of droplets and the formation of large masses, similar to those occurring in sucrose nephrosis. Gomori stain. × 425.

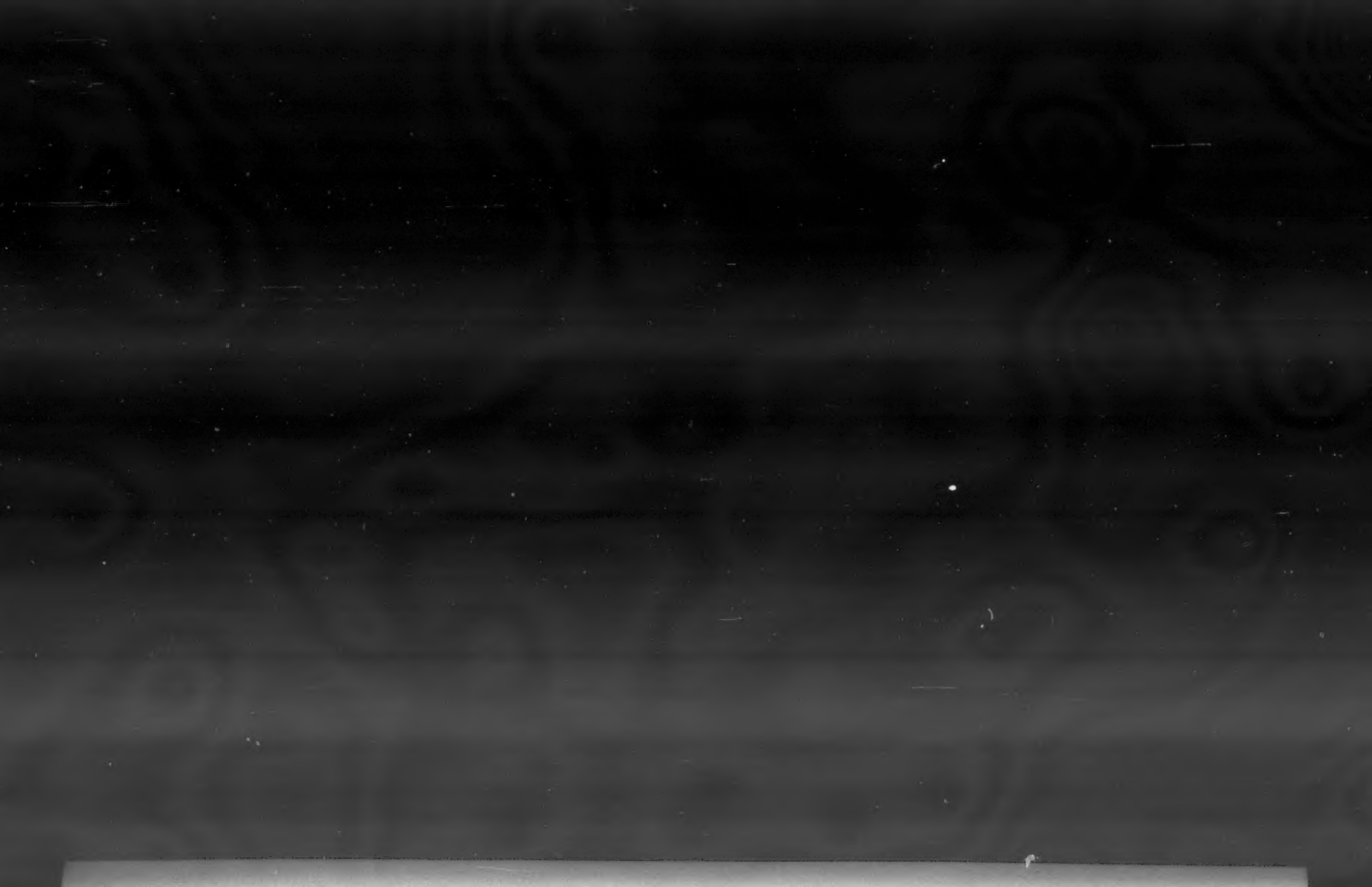

12

14

15

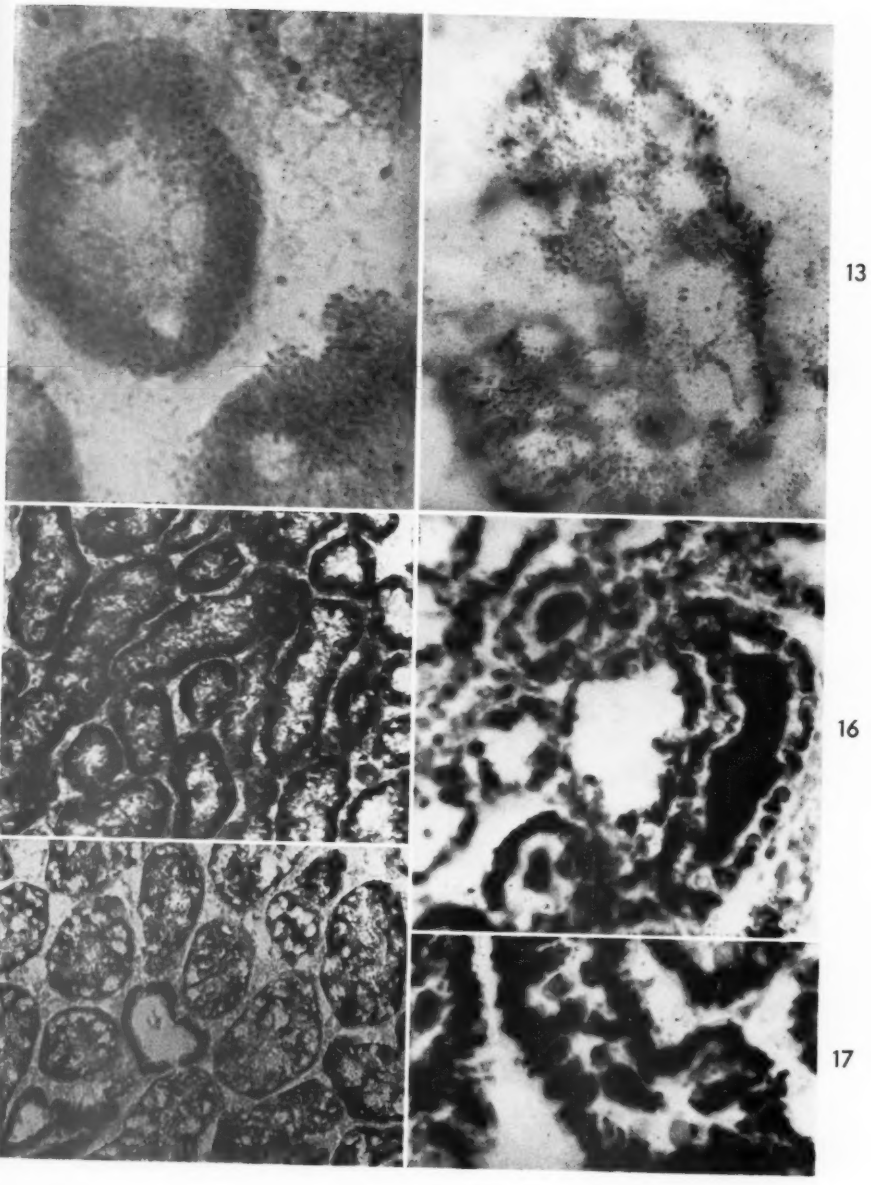

12

13

14

16

15

17

THE ULTRASTRUCTURE OF THE KIDNEY IN LEAD INTOXICATION WITH PARTICULAR REFERENCE TO INTRANUCLEAR INCLUSIONS

DAVID L. BEAVER, M.D.*

From the Department of Anatomy, Washington University School of Medicine, St. Louis, Mo.

Although the toxic properties of lead have been recognized since the time of Hippocrates,[1] plumbism continues to be a present-day medical problem. It is no wonder then that from 1616 to 1938 the medical and scientific literature contained more than 10,000 references on the subject.[2] In subsequent years the number of publications has increased progressively; and as far as the kidney is concerned, lead at one time or another has been incriminated as an etiologic factor in the production of practically all of the pathologic states involving that organ, running the gamut from hypertensive vascular disease and nephritis[3–5] to neoplasia.[6]

The one constant feature of the kidney in this disorder, however, is the presence of intranuclear inclusions in the convoluted tubules. These bodies, which appear in Pejić's photomicrographs,[3] but which were not described until several years later by Blackman,[7] are so characteristic of lead poisoning that some authors consider their presence as almost pathognomonic.[8,9] The inclusions are particularly significant in that they occur as a direct toxic effect of lead. Since they are Feulgen-positive[10] and may or may not contain deoxyribonucleic acid (DNA),[11] they must inevitably, in the final analysis, be differentiated from inclusions of viral etiology. It was felt, therefore, that the ultrastructure of a purely metabolically induced inclusion might be of comparative as well as possibly diagnostic interest.

MATERIAL AND METHODS

Twenty albino weanling rats were divided into groups and given drinking water containing basic lead acetate in concentrations of 0.05 per cent, 0.1 per cent, and, for a limited time, 1 per cent. The solutions were supplied *ad libitum*, as was Purina Laboratory Chow. Of 5 control rats, 1 was killed initially; the remainder were kept on the above diet and plain water for the duration of the experiment. The experimental animals were killed at 1 to 2 month intervals; and the experiment was ter-

This work was supported in part by United States Public Health Service grants RG 3784 and 2G-240.

Accepted for publication, March 24, 1961.

* On leave of absence from the Department of Pathology, Vanderbilt University School of Medicine, Nashville, Tenn. This project was carried out during the tenure of a United States Public Health Service Senior Research Fellowship GSF-448-S.

minated at the end of 7 months. In an effort to produce acute lead poisoning, rats which had been on 1 per cent basic lead acetate for 2 months or longer were given an additional 10 gm. per cent of this same substance mixed with their food, the food pellets having been weighed dry, moistened, made into a mash, mixed with lead subacetate, reformed into pellets and allowed to dry. After 6 weeks of receiving lead in both their food and drinking water, the animals were killed.

Rats were sacrificed by decapitation following ether anesthesia. Specimens were taken from both the renal cortex and renal medulla. For electron microscopy, tissue was routinely fixed for one hour at room temperature in Dalton's fluid.[12] Tissue from several animals was also fixed for one hour with 10 per cent formalin in White's balanced salt solution [13] without added $Fe(NO_3)3.9\ H_2O$ (pH 7.6); in 10 per cent formol-saline; in 10 per cent formol-saline saturated with H_2S, in an attempt to demonstrate lead [14,15]; and in Richardson's potassium permanganate solution without prefixation.[16] In addition, the ferric ferricyanide reduction test [17] was carried out on small bits of tissue following one hour fixation in formol-saline. As a control, similar specimens of formalin-fixed tissue were treated for 15 minutes with concentrated hydrogen peroxide in order to oxidize sulfhydryl groups prior to immersion in the ferricyanide reagent.[17] Following the various fixation procedures and reactions, the tissues were carried through graded alcohols and toluene, and embedded in a 6 to 1 mixture of butyl and methyl methacrylate. Sections were cut with a glass knife in a Porter-Blum microtome, mounted on collodion-coated grids and examined unstained in an RCA EMU 2D, 2E or 3B electron microscope. Tissue for light microscopy was fixed in 10 per cent formalin, embedded in paraffin and stained with hematoxylin and eosin.

Results

Intranuclear inclusions occurred in the kidneys of rats receiving 0.1 per cent or more basic lead acetate. Fully formed inclusions were present at the time of the first examination at the end of one month, and subsequently increased only slightly in number and size, although a few inclusions in early stages of development could usually be found in any given kidney. Inclusion-bearing cells occurred focally and in groups but were apparently limited to the proximal convoluted tubules, as determined by the presence of a brush border, or by the type of mitochondria and basal infolding if a brush border were lacking,[18,19] and by the absence of similar changes in other definitely identifiable segments of the nephron.[20]

The inclusion appeared first as a small electron-dense zone midway between the nucleolus and the nuclear membrane (Fig. 1). Except for one or two larger particles (see below), it was composed of densely packed granules considerably smaller than those comprising the nucleolus or those found in the surrounding nucleoplasm. Frequently two distinct sites of inclusion formation were present within a single nucleus (Fig. 2).

As the inclusion increased in size, radiating, intertwining, beaded filaments appeared in the periphery, so that the mass was now composed of a compact central core surrounded by a granular, mycelia-like en-

velope (Fig. 3). The distinct separation of inner and outer zones, which was readily apparent at this stage, tended to become somewhat obscured when inclusions developing in different sites fused. Because of this fusion, the mature inclusion was, more often than not, irregular in shape, rather than spherical. The nucleolus, on the other hand, instead of being similarly incorporated into the expanding masses, was displaced peripherally, so that the fully developed inclusion occupied a central position within the nucleus (Fig. 4). Although nuclei apparently increased in volume with inclusion growth, distinct margination of chromatin was not observed.

Randomly distributed throughout many of the inclusions were irregular electron-dense granules of varying size, ranging up to approximately 300 mμ in their greatest diameters (Fig. 5). These particles were present during all stages of inclusion development (Figs. 2 to 4), and seemed to increase in number with maturation. Although they tended to be slightly more concentrated within the central compact area, they also extended into, and sometimes beyond, the outer filamentous zone. The granules were not present after formalin (Fig. 6) or permanganate fixation (Fig. 7) and were not precipitated by fixation in H_2S saturated formol-saline.

The ferric ferricyanide reduction test, with and without prior peroxide oxidation, resulted primarily in increased electron density of the chromatin. The inclusions in both cases were considerably less dense and somewhat granular in appearance (Fig. 8). The larger irregular particles were absent.

The mitochondria of some inclusion-bearing cells appeared swollen and rounded, when compared to those of adjacent cells (Fig. 4), and at times mitochondrial swelling was marked. Scattered among recognizable mitochondria were ovoid bodies composed of dense osmiophilic material which lacked the irregular crystalloid appearance of the inclusion granules (Fig. 9). These dense bodies were absent following H_2S and formalin fixation and, since they seemed to give rise to myelin figures (Fig. 10), were interpreted as probably representing degenerating mitochondria.

Although by light microscopy the inclusion-bearing cells were the primary site of significant tubular abnormality, by electron microscopy other cells of the proximal convoluted tubules also exhibited rather marked morphologic alterations, even in areas where inclusions were apparently absent. There was a loss of brush border and dilatation of the subvillous spaces and basal labyrinth, which frequently progressed to a rather remarkable "vacuolar degeneration" (Fig. 11). Many of the distended vacuoles contained precipitated material, presumably protein.

Actual cellular necrosis was uncommon, but sloughed cells were sometimes present within the tubular lumens. Other segments of the nephron for the most part showed only fatty degeneration and mitochondrial swelling. In no instances were changes noted in the glomeruli or basement membranes.

None of the animals developed overt symptoms of lead intoxication, and none died spontaneously. Even rats receiving the extremely high doses of lead exhibited only pallor and severe emaciation. No inclusion bodies were present in the kidneys of control rats.

Discussion

It was first thought that the electron-dense granules, which were present in inclusions of chrome-osmium-fixed tissue, represented either aggregated crystals of an inorganic lead salt such as lead dichromate, or actual particles of metallic lead—similar to the silver deposits described by Dempsey and Wislocki in argyria.[21] However, the failure of the granules to be precipitated by hydrogen sulfide, carbon dioxide (present in White's balanced salt solution[13]), peroxide or ferricyanide should rule out the former possibility, while their absence from permanganate and formalin-fixed, alcohol-dehydrated tissue should exclude the latter. A nonprecipitable organic form of lead associated with a lipid or lipoprotein fraction cannot, of course, be eliminated by any of these methods. However, such a compound is not known to exist within the body,[22] and the reported presence of histochemically demonstrable lead in the inclusion[23] has never been confirmed by other investigators.[11,24,25] Nonetheless, it is difficult to accept these irregular, apparently osmiophilic or chromated particles as being primarily lipid in composition. The peculiar nature of some proteins in regard to fixation[26,27] and alcohol extraction[28] is known, as is the *in vitro* affinity of heavy metals,[29] including lead,[30,31] for protein-reactive groups. Whether the same affinity exists *in vivo* is another matter, but does pose an interesting problem. In thin sections, lipid *per se* is ordinarily visualized as rounded cytoplasmic droplets which, because of shrinkage, are occasionally slightly retracted and somewhat stellate in configuration (Fig. 11). In contrast, the granules of the lead inclusion occur within the nucleus and exhibit a clumped, almost faceted irregularity which is much more characteristic of a particulate structure. However, since the majority of the granules are beyond the limits of resolution by light microscopy, electron or x-ray diffraction may offer the only solution.

In regard to the remainder of the inclusion, it is presumably the loose, granular, filamentous outer zone which accounts for the peripheral stippled basophilia on light microscopy and which, by virtue of its position, could mask to some extent reactions of the inner core. It is known,

for example, that a hematoxylin counterstain with the Ziehl-Neelsen method results in a purple hue,[24] and even in Wachstein's original colored photomicrographs the intensity of the acid-fast reaction of the lead inclusion was quite weak in comparison to that shown for the bismuth-induced inclusions, which lacked a basophilic rim.

If it is true that the core and the envelope, which are morphologically distinct, are also histochemically different, then some of the apparent discrepancies in staining reactions [10,11,24,25,32] might be resolved.

As far as the presence of sulfhydryl is concerned, the ferric ferricyanide reaction probably resulted only in a nonspecific iron staining of tissue protein.[29,33] However, even if large numbers of sulfhydryl groups were present, it is still doubtful that such groups should be incriminated as the cause of acid fastness.[25] The nucleolus, which is also said to contain sulfhydryl groups and which has been suggested as a possible donor,[25] is not acid fast.[24] Moreover, the inclusion is never, even initially, closely associated or identical with the nucleolus, as it sometimes appears by light microscopy.[34]

In any event, the lead-induced inclusion bears no resemblance ultrastructurally to those intranuclear inclusions of viral origin thus far described. In practically all cases, virus particles have been identified within the nucleus, if not within the inclusion itself.[35–41] Measles, to be sure, is an exception, but even in this disease the intranuclear inclusion contains doubly arrayed fibrillar material which may be related in some way to viral replication.[42]

As has been previously shown,[2,43] the rat appears to be remarkably resistant to the toxic effects of lead. In spite of tubular lesions, no dysfunction as measured by the TMPAH has been demonstrated,[44] although there is an apparent insensitivity to vasopressin and nicotine.[45] It is not known if the rat exhibits aminoaciduria [46] and glycosuria,[47] but in man amino acids and glucose normally are reabsorbed by the proximal convoluted tubule [48] and probably are in rats as well.[49] Certainly their loss could explain in part at least the severe emaciation of animals on high doses of lead. That lead interferes with protein metabolism has already been shown.[50]

On the other hand, as would be expected from the histologic structure, glomerular filtration is not affected in lead poisoning.[44] The electron microscopic alterations in basement membranes and foot processes of glomeruli which have been reported [51] were not observed.

SUMMARY

The specific effect of inorganic lead upon the rat kidney was apparently limited to the cells of the proximal convoluted tubules, where its major pathologic manifestations were the production of intranuclear

inclusions and degenerative changes in the cytoplasm. With chrome-osmium fixation, the inclusion ultrastructurally consisted of 3 portions, viz.: a compact core; a looser, beaded, filamentous periphery; and scattered electron-dense particles. Metallic or ionic lead could not be demonstrated, and the inclusion developed independently of the nucleolus. Electron microscopically, the inclusion produced by lead was quite different from intranuclear inclusions of viral origin, which usually are associated with infective particles.

References

1. Goodman, L., and Gilman, A. The Pharmacological Basis of Therapeutics; a Textbook of Pharmacology and Therapeutics for Physicians and Medical Students. The MacMillan Co., New York, 1941, 1383 pp.
2. Calvery, H. O. Chronic effects of ingested lead and arsenic; a review and correlation. *J.A.M.A.*, 1938, **111**, 1722–1729.
3. Pejic, S. The nature of the primary renal lesion produced by lead. *Ann. Int. Med.*, 1928, **1**, 577–604.
4. Eger, W. Experimentelle Bleischrumpfnieren. *Virchows Arch. path. Anat.*, 1937, **299**, 654–666.
5. Diaz-Rivera, R. S., and Horn, R. C., Jr. Postmortem studies on hypertensive rats, chronically intoxicated with lead acetate. *Proc. Soc. Exper. Biol. & Med.*, 1945, **59**, 161–163.
6. Zollinger, H. U. Durch chronische Bleivergiftung erzeugte Nierenadenome und -carcinome bei Ratten und ihre Beziehungen zu den entsprechenden Neubildung des Menschen. *Virchows Arch. path. Anat.*, 1953, **323**, 694–710.
7. Blackman, S. S., Jr. Intranuclear inclusion bodies in the kidney and liver caused by lead poisoning. *Bull. Johns Hopkins Hosp.*, 1936, **58**, 384–403.
8. Zak, F. G., and Finklestein, W. E. Plumbism in children. *J. Mt. Sinai Hosp.*, 1952, **19**, 352–358.
9. Wachstein, M. Lead poisoning diagnosed by the presence of nuclear acid-fast inclusion bodies in kidney and liver. *Arch. Path.*, 1949, **48**, 442–446.
10. Wolman, M. On the absence of desoxyribonucleic acid from some chemically-induced cytoplasmic and intranuclear inclusions, with reference to a special type of false positive staining by Feulgen's nuclear technique. *J. Path. & Bact.*, 1954, **68**, 159–164.
11. Bracken, E. C.; Beaver, D. L., and Randall, C. C. Histochemical studies of viral and lead-induced intranuclear bodies. *J. Path. & Bact.*, 1958, **75**, 253–256.
12. Dalton, A. J. A chrome-osmium fixative for electron microscopy. (Abstract) *Anat. Rec.*, 1955, **121**, 281.
13. White, P. R. The Cultivation of Animal and Plant Cells. The Ronald Press Co., New York, 1954, 239 pp.
14. Sieber, E. Histochemischer Bleinachweis im Knochen. *Arch. exper. Path. u. Pharmakol.*, 1936, **181**, 273–280.
15. Pearse, A. G. E. Histochemistry; Theoretical and Applied. Little, Brown & Co., Boston, 1959, ed. 2, 998 pp.
16. Richardson, K. C. Personal communication.
17. Lillie, R. D. Histopathologic Technic and Practical Histochemistry. The Blakiston Co., New York, 1954, 501 pp.

18. PEASE, D. C. Electron microscopy of the tubular cells of the kidney cortex. *Anat. Rec.*, 1955, **121**, 723–743.

19. RUSKA, H.; MOORE, D. H., and WEINSTOCK, J. The base of the proximal convoluted tubule cells of rat kidney. *J. Biophys. & Biochem. Cytol.*, 1957, **3**, 249–254.

20. PEASE, D. C. Fine structures of the kidney seen by electron microscopy. *J. Histochem.*, 1955, **3**, 295–308.

21. DEMPSEY, E. W., and WISLOCKI, G. B. An electron microscopic study of the blood-brain barrier in the rat, employing silver nitrate as a vital stain. *J. Biophys. & Biochem. Cytol.*, 1955, **1**, 245–256.

22. ORESTANO, G. Sulla formazione di composti tra piombo e lipoidi nell'organismo. Comportamento degli acidi grassi del fegato nell'avvelenamento saturnino. II. *Arch. internat. pharmacodyn.*, 1930, **39**, 285–293.

23. FINNER, L. L., and CALVERY, H. O. Pathologic changes in rats and in dogs fed diets containing lead and arsenic compounds. Compounds used: lead arsenate, arsenic trioxide, calcium arsenate and lead acetate. *Arch. Path.*, 1939, **27**, 433–446.

24. WACHSTEIN, M. Studies on inclusion bodies. I. Acid-fastness of nuclear inclusion bodies that are induced by ingestion of lead and bismuth. *Am. J. Clin. Path.*, 1949, **19**, 608–614.

25. LANDING, B. H., and NAKAI, H. Histochemical properties of renal lead-inclusions and their demonstration in urinary sediment. *Am. J. Clin. Path.*, 1959, **31**, 499–503.

26. LILLIE, R. D. Symposium: Problems of fixation in histochemistry. Opening remarks. *J. Histochem.*, 1958, **6**, 301–302.

27. BARRNETT, R. J., and ROTH, W. D. Effects of fixation on protein histochemistry. *J. Histochem.*, 1958, **6**, 406–415.

28. BEAVER, D. L. Der Einfluss verschiedener Fixierungsmittel auf das Strukturbild der Präputialdrüsen der Ratte. *Ztschr. Zellforsch.*, 1959, **51**, 88–96.

29. WIGGLESWORTH, V. B. The role of iron in histological staining. *Quart. J. Micr. Sc.*, 1952, **93**, 105–118.

30. WATSON, M. L. Staining of tissue sections for electron microscopy with heavy metals. II. Application of solutions containing lead and barium. *J. Biophys. & Biochem. Cytol.*, 1958, **4**, 727–730.

31. DALTON, A. J., and ZEIGEL, R. F. A simplified method of staining thin sections of biological material with lead hydroxide for electron microscopy. *J. Biophys. & Biochem. Cytol.*, 1960, **7**, 409–410.

32. MARSDEN, H. B., and WILSON, V. K. Lead-poisoning in children; correlation of clinical and pathological findings. *Brit. M. J.*, 1955, **1**, 324–326.

33. BEAVER, D. L. A re-evaluation of the rat preputial gland as a "dicrine" organ from the standpoint of its morphology, histochemistry and physiology. *J. Exper. Zool.*, 1960, **143**, 153–173.

34. TÖNZ, O. Nierenveränderungen bei experimenteller chronischer Bleivergiftung (Ratten). *Ztschr. ges. exper. Med.*, 1957, **128**, 361–377.

35. REISSIG, M., and MELNICK, J. L. The cellular changes produced in tissue cultures by herpes B virus correlated with the concurrent multiplication of the virus. *J. Exper. Med.*, 1955, **101**, 341–352.

36. FAWCETT, D. W. Electron microscope observations on intracellular virus-like particles associated with the cells of the Lucké renal adenocarcinoma. *J. Biophys. & Biochem. Cytol.*, 1956, **2**, 725–742.

37. BRACKEN, E. C., and NORRIS, J. L. Electron microscopy of equine abortion virus. *Proc. Soc. Exper. Biol. & Med.*, 1958, **98**, 747–750.

38. LUSE, S. A., and SMITH, M. G. Electron microscopy of salivary gland viruses. *J. Exper. Med.*, 1958, **107**, 623–632.

39. LUSE, S. A., and SMITH, M. G. Electron microscope studies of cells infected with the salivary gland viruses. *Ann. New York Acad. Sc.*, 1959, **81**, 133–144.

40. MORGAN, C.; ROSE, H. M.; HOLDEN, M., and JONES, E. P. Electron microscopic observations on the development of herpes simplex virus. *J. Exper. Med.*, 1959, **110**, 643–656.

41. MORGAN, C.; GODMAN, G. C.; BREITENFELD, P. M., and ROSE, H. M. A correlative study by electron and light microscopy of the development of type 5 adenovirus. I. Electron microscopy. *J. Exper. Med.*, 1960, **112**, 373–382.

42. KALLMAN, F.; ADAMS, J. M.; WILLIAMS, R. C., and IMAGAWA, D. T. Fine structure of cellular inclusions in measles virus infections. *J. Biophys. & Biochem. Cytol.*, 1959, **6**, 379–382.

43. FAIRHALL, L. T., and MILLER, J. W. A study of the relative toxicity of the molecular components of lead arsenate. *Pub. Health Rep.*, 1941, **56**, 1610–1625.

44. PARDOÉ, A. U. Renal function in lead poisoning. *Brit. J. Pharmacol.*, 1952, **7**, 349–357.

45. PARDOÉ, A. U., and WEATHERALL, M. The uptake and excretion of water in rats poisoned with lead. *Brit. J. Pharmacol.*, 1952, **7**, 358–369.

46. WILSON, V. K.; THOMSON, M. L., and DENT, C. E. Amino-aciduria in lead poisoning; a case in childhood. *Lancet*, 1953, **2**, 66–68.

47. MILLICHAP, J. G.; LLEWELLIN, K. R., and ROXBURGH, R. C. Lead paint; a hazard to children. *Lancet*, 1952, **2**, 360–362.

48. WORTHEN, H. G. Growth failure due to diseases of the proximal tubule. *J. Pediat.*, 1960, **57**, 14–22.

49. HARRISON, H. E., and HARRISON, H. C. Experimental production of renal glycosuria, phosphaturia and aminoaciduria by injection of maleic acid. *Science*, 1954, **120**, 606–608.

50. CHIODI, H., and CARDEZA, A. F. Hepatic lesions produced by lead in rats fed a high fat diet. *Arch. Path.*, 1949, **48**, 395–404.

51. COHEN, S.; SWEET, A. Y.; MAUTNER, W.; CHURG, J., and GRISHMAN, E. Light and electron microscopy of lead nephropathy. (Abstract) *Am. J. Dis. Child.*, 1960, **100**, 559–560.

LEGENDS FOR FIGURES

Except where indicated, micrographs were prepared from sections of tissue fixed in buffered chrome-osmium (Dalton's fluid).

FIG. 1. A lead-induced intranuclear inclusion (arrow) in an early stage of development. The nucleolus (N) appears below and to the right of the inclusion. Small dark granules in a mitochondrion (M) are a normal finding and are unrelated to lead intoxication. A portion of the brush border (BB) is seen in the lower right. × 15,000.

FIG. 2. Intranuclear inclusions (arrows) in early stages of development. Note the larger electron-dense granules in the upper inclusion. A nucleolus (N) is on the left; the nuclear membrane appears on the right. × 45,000.

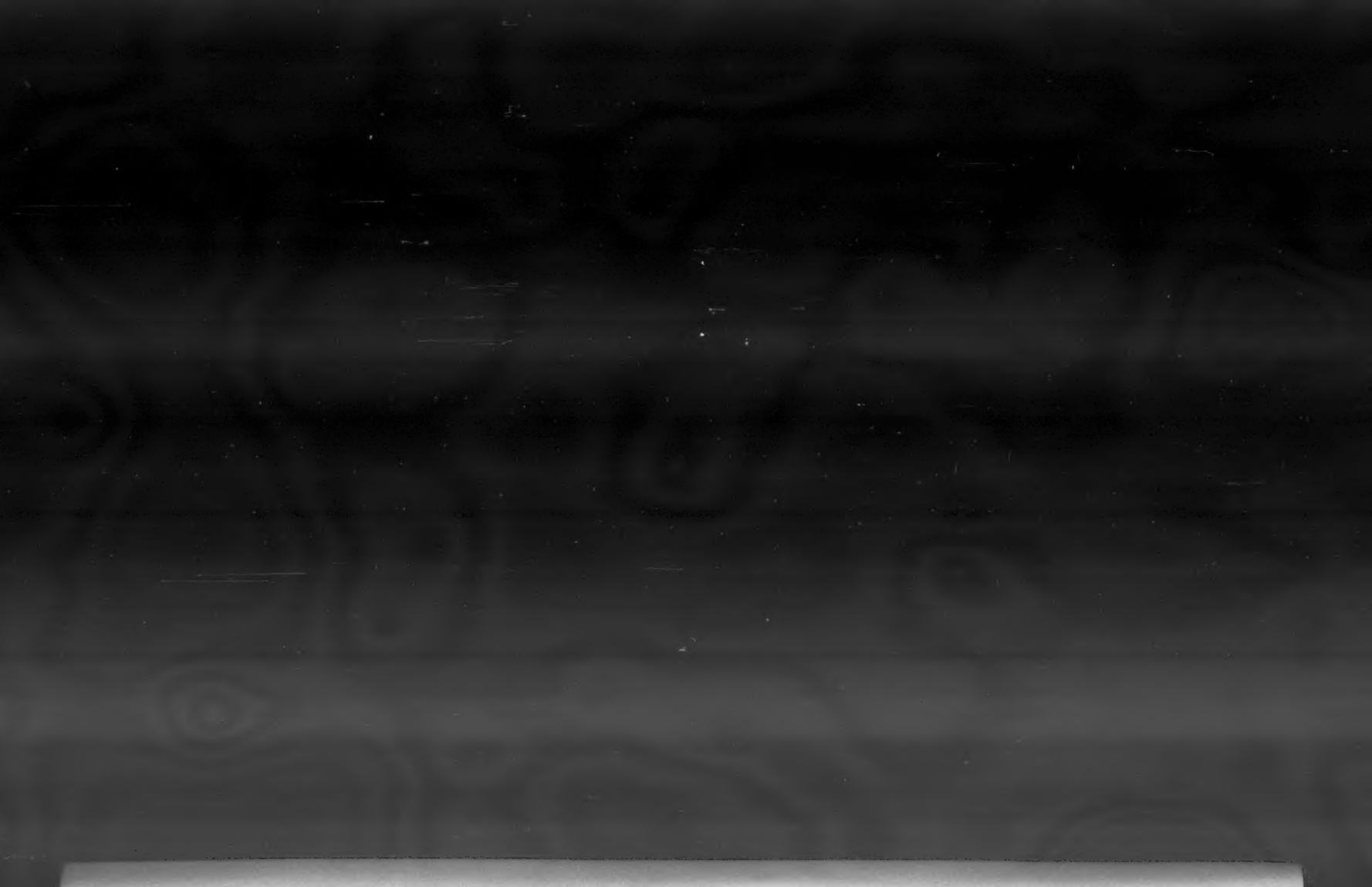

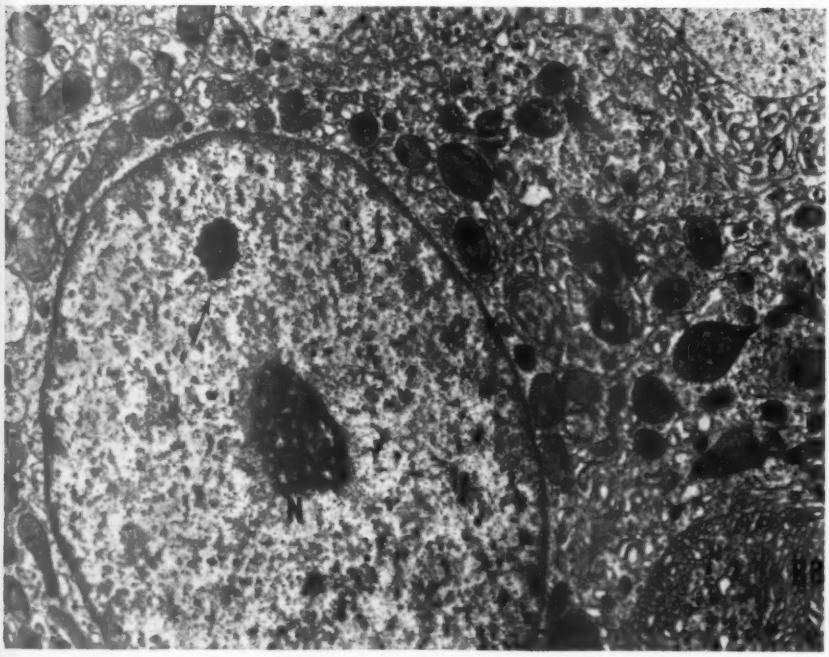

1

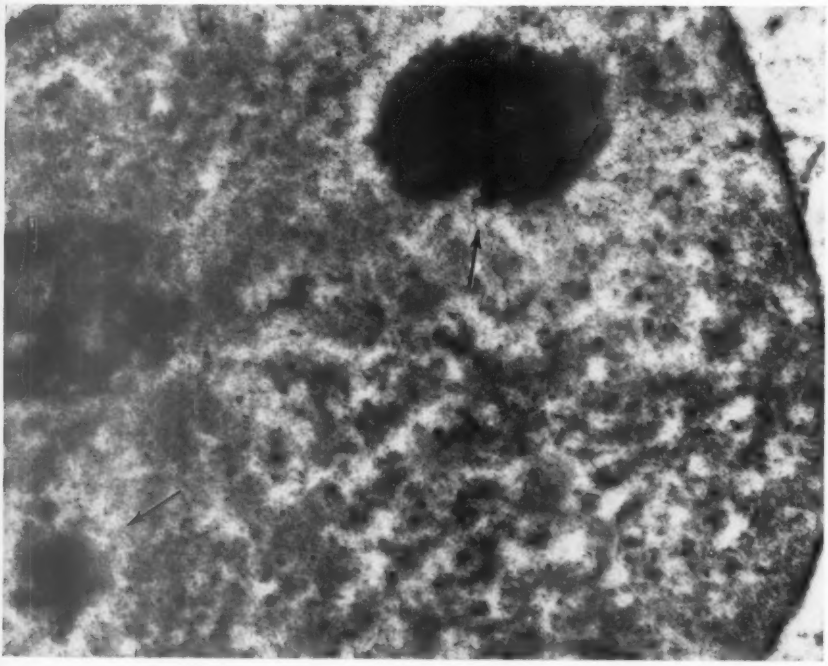

2

3

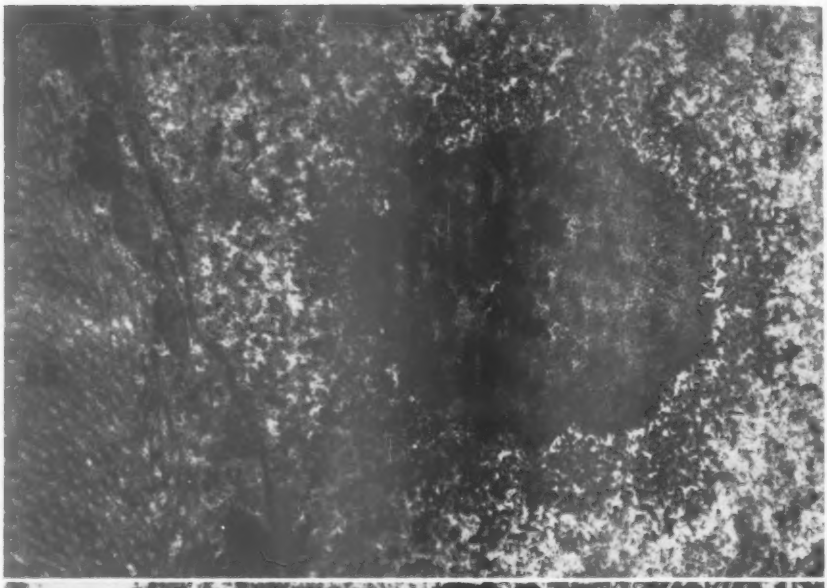

4

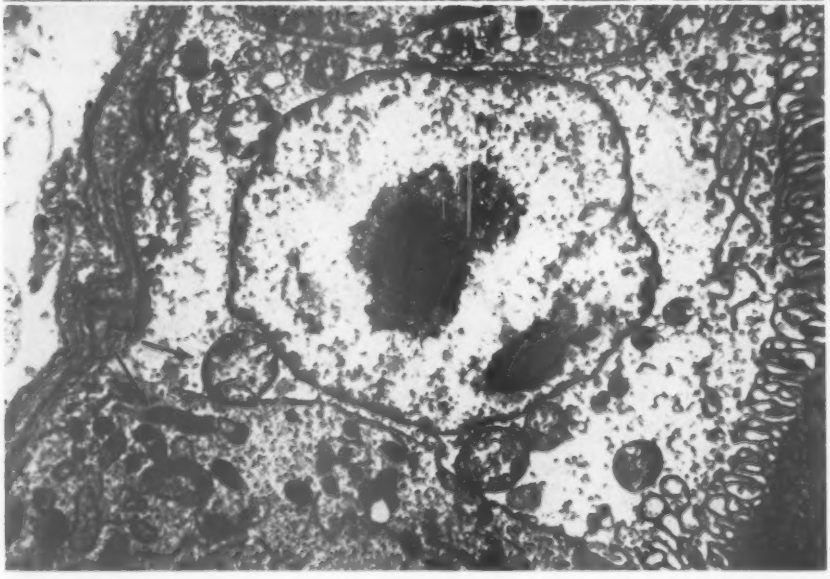

FIG. 3. A spherical inclusion in a later stage of development. Note the beaded filamentous periphery and compact core containing irregular dense particles. The nuclear membrane, mitochondria and brush border (BB) are on the left. × 25,000.

FIG. 4. A fully developed inclusion is apparent in the center of the nucleus. The nucleolus (N) is displaced peripherally. Compare the mitochondria (M) of the inclusion-bearing cell (upper arrow) to those of a cell below (lower arrow). Portion of a nucleus (NUC) of an adjacent cell may be seen above. The basement membrane and interstitial space are shown to the left; the brush border (BB) on the right. × 8,000.

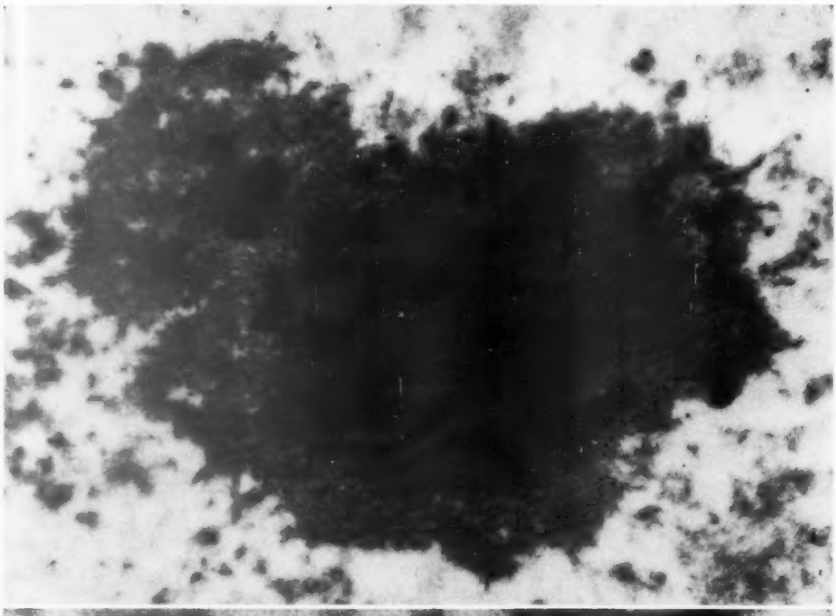

5

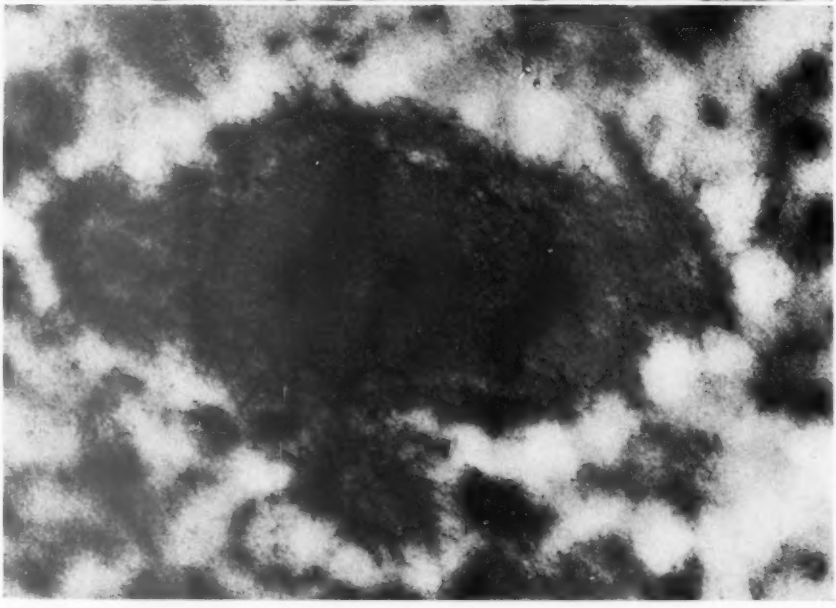

6

FIG. 5. An inclusion contains numerous electron-dense irregular granules. Note also the typical two-zonal architecture of the inclusion proper. This is the same inclusion shown in Figure 4. × 50,000.

FIG. 6. The bizonal architecture of the inclusion is still apparent, but electron-dense granules are completely absent. Fixation with 10 per cent formalin in White's balanced salt solution without added iron at pH 7.6. × 35,000.

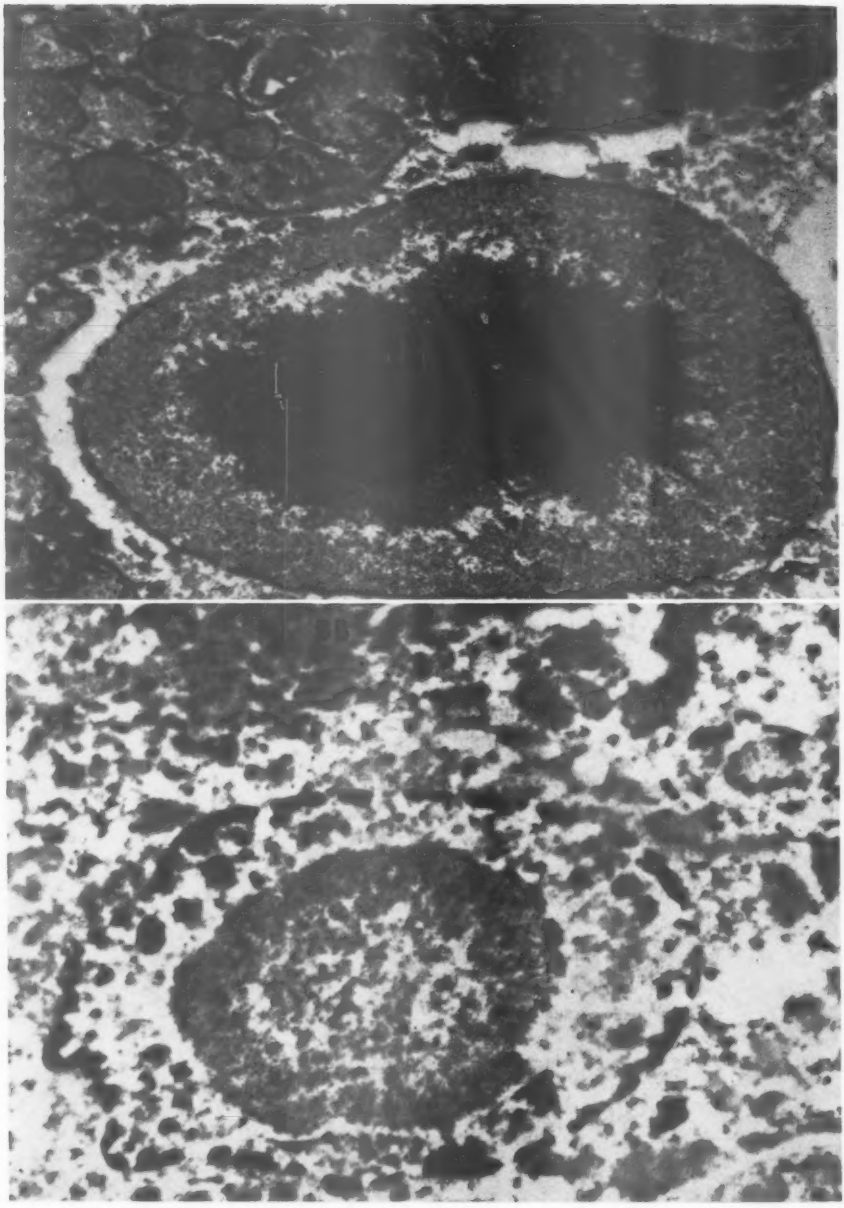

FIG. 7. The fusion of inclusions developing at different sites. Granules are absent. Note also the degenerating mitochondria above and compare these with the osmiophilic ovoid forms seen with Dalton's fixation in Figures 9 and 10. Permanganate fixation. × 16,000.

FIG. 8. Nuclear chromatin is extremely dense. The inclusion is considerably less dense and somewhat granular. Distorted gray profiles in the cytoplasm (M) are mitochondria. A barely identifiable brush border (BB) may be seen above. Effect of ferric ferricyanide reagent. Fixation in 10 per cent formol-saline. × 12,000.

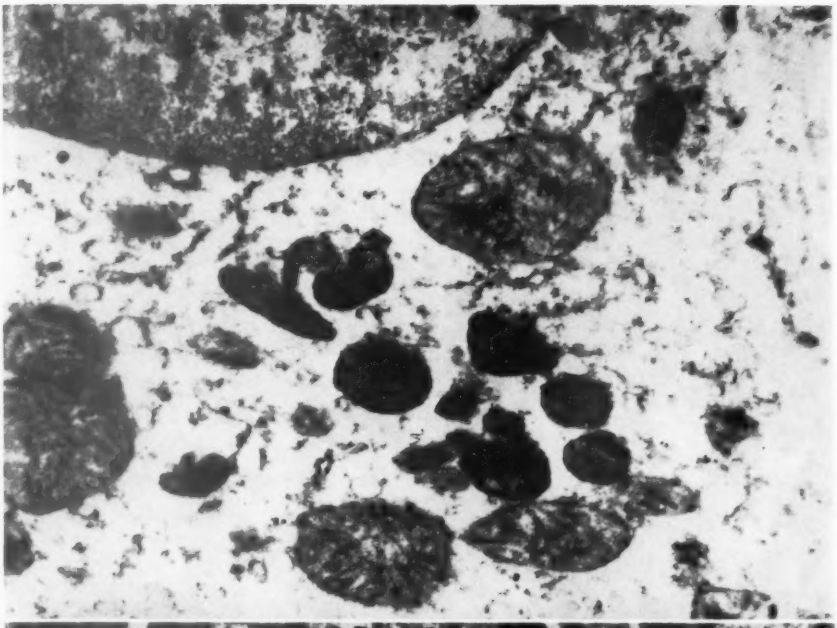

9

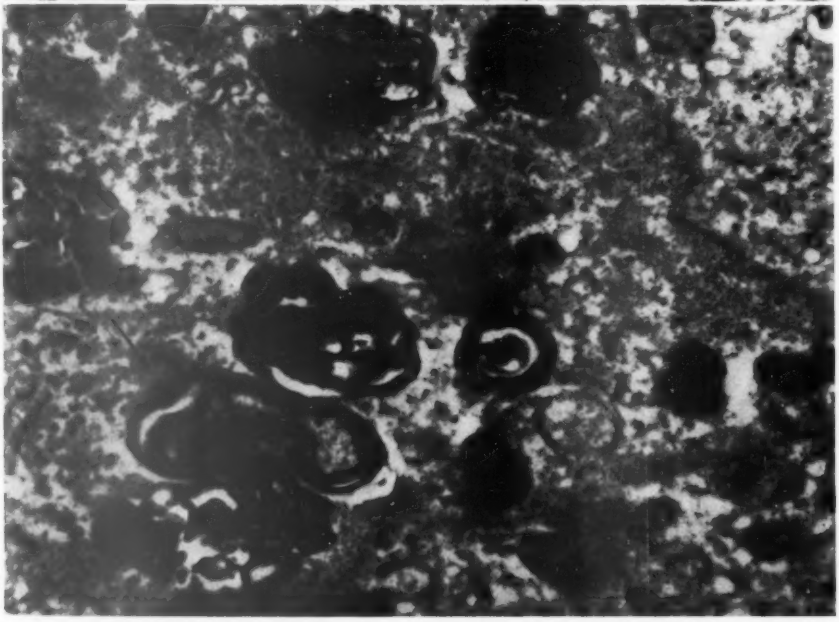

10

FIG. 9. Ovoid osmiophilic bodies are scattered among mitochondria (M). Compare these with the degenerating mitochondria shown in Figure 7. A nucleus (NUC) appears above. × 30,000.

FIG. 10. Cytoplasmic formation of myelin figures (arrow). Note the apparent breakdown of ovoid osmiophilic profiles. × 18,000.

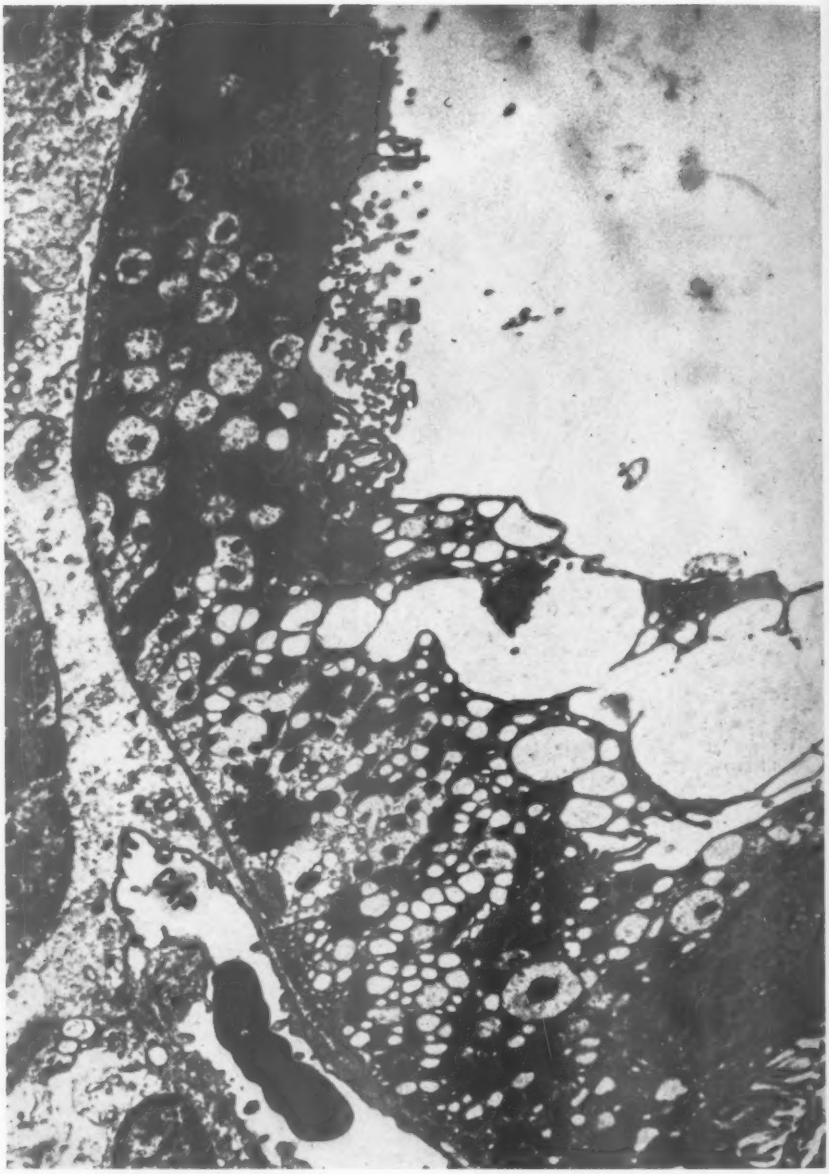

FIG. 11. A proximal convoluted tubule in an area without inclusions. Nuclei (NUC) are shown above and below. There is marked cellular vacuolation, some vacuoles containing precipitated material. Remnants of a brush border (BB) appear above and in the lower right hand corner. A lipid droplet (L) is evident and an interstitial capillary (CAP) with a red cell is shown in the lower left. × 11,000.

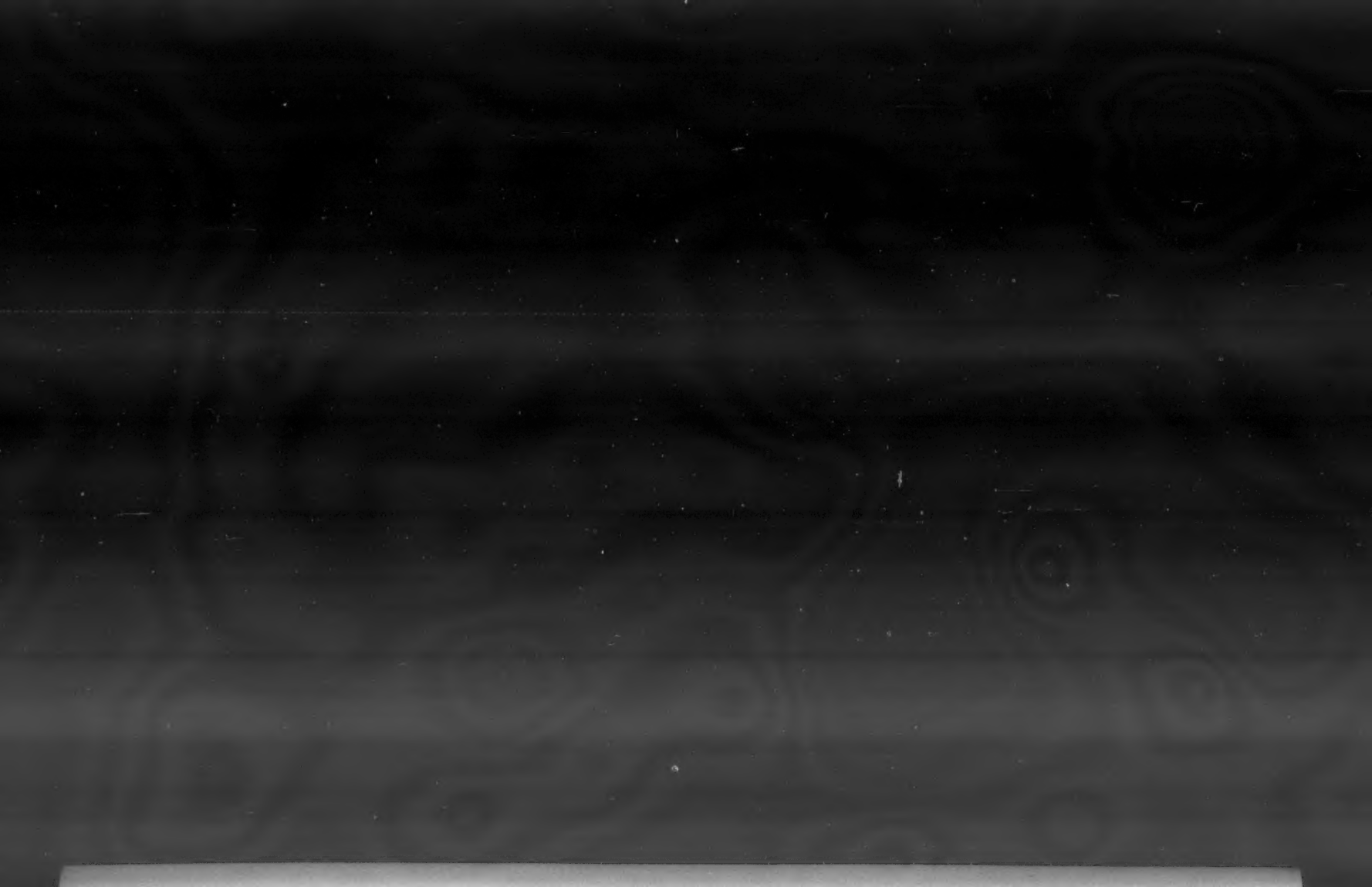

EXPERIMENTAL CARCINOMA OF THE LIVER

"Regeneration" of Liver Cells in Premalignant Stages

Richard A. MacDonald, M.D.

From the Department of Pathology, Harvard Medical School, and the Mallory Institute of Pathology, Boston City Hospital, Boston, Mass.

In the United States primary hepatic carcinoma occurs with greater frequency in livers with than in those without cirrhosis. One theory to explain this relationship is that in cirrhosis there is an unusually great regeneration which may give rise, possibly by way of chromosomal aberrations in the course of repeated cell divisions, to malignant neoplastic cells. In the present study, experimental carcinoma of the liver was produced in rats by feeding a butter yellow derivative, 3′-methyl-4-dimethylaminoazobenzene (3′-Me-4-DAB). Deoxyribonucleic acid (DNA) synthesis as an index of cellular proliferation was quantitated in stages preceding the occurrence of tumors, and preneoplastic cytologic alterations were correlated with DNA synthesis. Tritiated thymidine (H^3-thymidine) was injected into rats prior to sacrifice; cell nuclei that utilized labeled thymidine for DNA synthesis were identified and quantitated in autoradiographs.

Review

Experimental liver tumors in rats have been investigated since 1924, when Schmidt noted hepatic neoplasms after feeding scarlet red dye to mice. Earlier, in 1906, Fischer had produced epithelial tumors at injection sites by introducing the dye into the ears of rabbits. Since that time there have been many studies with this and other carcinogens, fully reviewed elsewhere.[1]

Opie and others observed that degeneration of liver cells occurred when butter yellow was fed to rats, before proliferative alterations appeared.[2-6] The earliest premalignant change recognized was an increased basophilia in the cytoplasm of groups of liver cells[2-9]; Opie showed this to be due to an increase in the ribonucleic acid (RNA) particles associated with mitochondria. Nuclear alterations and mitotic activity followed cytoplasmic changes. The possible significance of increased regeneration in the precancerous stages of hepatic tumors was empha-

Aided by grants C-4119 and C-4666 from the United States Public Health Service, and in part by Contract DA-49-007-MD-863, Office of the Surgeon General, Department of the Army.

Accepted for publication, March 13, 1961.

sized by the work of Griffin, Nye, Noda and Luck; these authors quantitated hepatic DNA in rats being fed an azo dye with a synthetic diet.[10] They found that as the dye was fed, the DNA content of the liver increased progressively until it approached that of tumor tissue. Glinos, Bucher and Aub reported that the occurrence of tumors was accelerated by regeneration induced by partial hepatectomy in rats fed butter yellow.[11] However, this was not found by others, using a different carcinogenic dye.[12]

The use of a carcinogen in conjunction with a synthetic diet, high in carbohydrate and low in protein, was noted by Opie and others to result in a greater and more rapid production of tumors than when the carcinogen was fed with a normal diet. As a result, nearly all investigators have since used a synthetic diet in their studies. In the present work, the effect of a synthetic diet on DNA synthesis was investigated.

Material and Methods

One hundred and sixty-eight male rats of the Sprague-Dawley strain, 85 days old, of average weight—320 gm.—were housed in individual cages in an air-conditioned room. Litter mates were separated into 4 groups. Laboratory meal (Purina Laboratory Meal) and tap water *ad libitum* were administered to 32 rats; 32 received laboratory meal containing 0.06 per cent 3′-Me-4-DAB; 52 rats received a synthetic diet alone; 52 rats received the synthetic diet containing 0.06 per cent 3′-Me-4-DAB. The composition of the synthetic diet was: vitamin-free casein, 16 per cent; corn oil, 5 per cent; sucrose, 75 per cent; salt mixture W (Nutritional Biochemicals Corp., Cleveland, Ohio), 4 per cent. Vitamins were added, in mg. per thousand gm. of diet: thiamine, 10; riboflavin, 3.75; pyridoxine, 10; nicotinic acid, 37.5; calcium pantothenate, 26; folic acid, 1; vitamin B_{12}, 0.1; biotin, 0.2; choline, 3,000. Cod liver oil was added at the rate of 1 drop per rat per week.

The food consumption and body weight of each animal were recorded weekly, and at the time of sacrifice. Eight rats, 2 from each of the 4 groups, were killed each week for 5 weeks, then at approximately 2-week intervals up to 218 days. With the exception of 15 rats which died before the conclusion of the study, all rats received injections of H^3-thymidine (specific activity, 1.9 curies per mM) in a dose of 1 μc. per gm. of body weight, via a femoral vein 4 hours prior to sacrifice. Rats died, usually of weakness and pulmonary infection, after approximately 20 weeks; all but one that died had been fed the carcinogen, either with laboratory meal or the synthetic diet.

Animals were sacrificed by etherization and decapitation. Tissues were fixed in 10 per cent neutral buffered formalin. Sections were stained with hematoxylin and eosin and occasionally with selected special stains. Sections used for autoradiographs were stained with hematoxylin alone. Autoradiographs were prepared as described elsewhere [13]; exposure time of the films was 4 weeks. H^3-thymidine-labeled hepatic cells were counted in 100 consecutive high power (400 ×) fields containing hepatic parenchyma.

Results

Although the primary purpose was to study premalignant stages of tumor formation, 17 rats were fed carcinogen until tumors appeared.

When sacrificed, 10 of the 17 had neoplasms. In 9 of the 10 the tumors were of both liver cell and bile duct origin, usually with additional areas of undifferentiated carcinoma (Figs. 1 to 3).

"Regeneration"

Rats fed laboratory meal alone showed a progressive reduction in the number of hepatic cells synthesizing DNA; this was attributable to decreasing growth with aging (Text-fig. 1). Rats fed the carcinogen with laboratory meal showed a slightly greater number of hepatic cells in DNA synthesis, and the same changes with age; the differences were not of statistical significance by the *t* test. Rats fed the synthetic diet

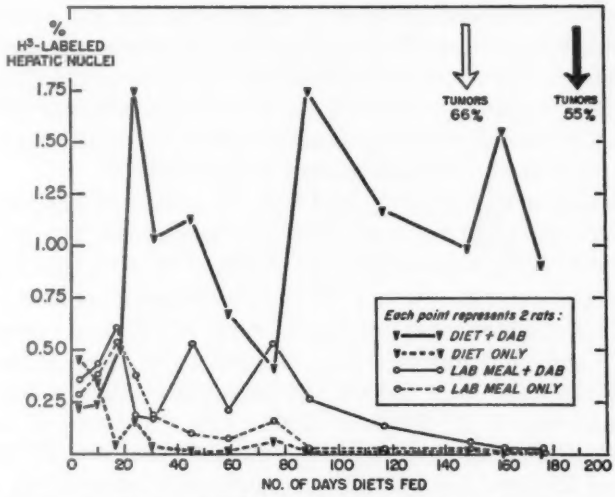

TEXT-FIGURE 1. Uptake of tritiated thymidine by rat liver cells preceding occurrence of hepatic carcinomas produced by feeding 3'-Me-4-DAB.

alone showed nearly the same number of cells with DNA synthesis as those fed laboratory meal alone; a decrease with age was also observed. By contrast, rats fed the carcinogen in a synthetic diet showed significantly more liver cells with DNA synthesis after the third week. There appeared to have been cyclic changes, and there was no decrease with age. The increased DNA synthesis in this group was not related to the development of tumors, however, as neoplasms appeared in a slightly lower proportion, and later (at 190 days) in this group than in rats fed the carcinogen with laboratory meal (at 148 days).

Regeneration or increased DNA synthesis was not of importance in the premalignant stages of hepatic tumors as evidenced by an earlier

and greater number of tumors in livers without increased DNA synthesis. Moreover, rats with the greater degree of hepatic cell proliferation (synthetic diet plus carcinogen) did not develop more tumors. In fact, slightly fewer developed, and these appeared later than in rats with nearly normal DNA synthesis. It was also noteworthy that in livers with premalignant changes and tumors, adjacent normal parenchyma did not show increased DNA synthesis, indicating that there were not diffuse proliferative changes (Fig. 4).

Stages in the Development of Neoplasms

Before tumors developed in liver or bile duct cells, degenerative alterations of liver cells occurred. This was seen after 10 days of carcinogen feeding with either laboratory meal or synthetic diet, and consisted of a homogeneous eosinophilic staining of the cytoplasm, predominantly in periportal areas, with no histologic or DNA changes in the nuclei. Later, the cytoplasm formed oval masses or "hyaline bodies" (Fig. 5). This hyalin was different from so-called "alcoholic" hyalin observed in human subjects with alcoholic or nutritional cirrhosis.[14]

Beginning at approximately 120 days, the earliest histologically recognized premalignant cytologic alteration was observed. This was characterized by increased basophilia and density of the cytoplasm in groups of 10 to 30 liver cells, or 2 to 5 bile duct cells; hepatic cells were often located about a blood vessel such as a central vein or near a portal area (Figs. 6 and 7). These cells were of normal size; their nuclei occasionally showed a slight but variable enlargement. At this time there was no increase in H^3-thymidine uptake (Fig. 8). Later, at the next observed time of 148 days, foci of preneoplastic cells showed increased uptake of H^3-thymidine, while the surrounding liver showed only normal liver cells with scattered DNA synthesis. Nuclear chromatin was now present in larger, more abundant clumps; nucleoli were also larger and more frequent, and there were increased numbers of mitotic figures. Kupffer cells were enlarged, and an increased number manifested DNA synthesis. Concurrent with the appearance of neoplasms in bile duct and hepatic parenchymal cells, Kupffer cells showed alterations in nuclear chromatin and in nucleoli similar to those of liver cells, and may have been the cells of origin of areas of undifferentiated carcinoma. In neoplastic lesions, fibroblastic proliferation occasionally formed a connective tissue stroma; more often, however, there was only minimal supporting tissue, and infarction was a feature. Livers containing tumors invariably showed additional foci with all stages of degeneration and preneoplastic change.

Fibrosis and Cirrhosis

In addition to bile duct alteration giving rise to neoplasm, a type of small bile duct proliferation occurred. This did not appear to be associated with the development of malignant neoplasm, and occasionally gave rise to a pattern resembling cirrhosis (well-defined cirrhosis was present in only one rat). Sprouting of these small bile ducts eventually resulted in the connection of adjacent portal areas; this was accompanied by slight fibroblastic proliferation. Despite their prominence, the nuclei

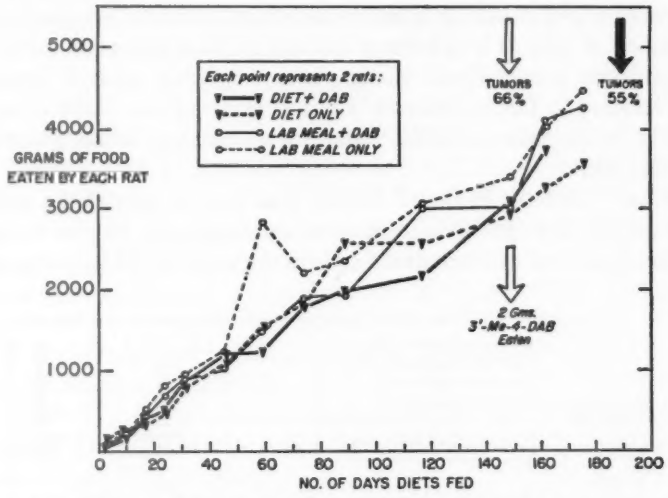

TEXT-FIGURE 2. Food consumption of rats fed hepatic carcinogen 3'-Me-4-DAB.

of these cells did not always exhibit uptake of H^3-thymidine, indicating that DNA synthesis and proliferation were intermittent. The extension of small ducts and their interconnection with adjacent portal areas gave an impression of hepatic "nodularity" in a few instances. These apparent nodules were not composed of proliferated liver cells, however, since at no time was there an increased uptake of H^3-thymidine in hepatic nuclei in these areas (Fig. 9).

Miscellaneous Features

Total food and carcinogen consumption was essentially the same in all 4 groups of rats (Text-fig. 2). Rats fed the synthetic diet and carcinogen failed to gain normally; rats in the other 3 groups showed normal weight gain, with minor variations (Text-fig. 3). DNA synthesis in liver cells was greater in those rats that failed to gain in weight. This

group, fed the synthetic diet with carcinogen, had a food consumption approximately the same as in the other 3 groups.

The synthetic diet alone produced a slight but variable degree of fatty infiltration of liver cells, usually periportal in location. There were no parenchymal alterations in rats fed the carcinogen with laboratory meal or with the synthetic diet, other than those ascribable to the effects of the synthetic diet alone.

Comment

It is apparent that the formation of hepatic tumors in rats fed the carcinogen 3′-Me-4-DAB is not preceded by a diffuse increase in proliferation of cells. It is of interest that cytoplasmic alteration is the first recognizable preneoplastic change, preceding both nuclear alteration and increase in DNA synthesis. There is evidence that RNA is important in the formation of DNA,[15] and this may be true in malignant neoplastic cells.

Potter[16] and the Millers[17] believe that loss of a catabolic enzyme or a protein is responsible in azo dye carcinogenesis for the transformation of normal into neoplastic cells in the rat liver. This is supported

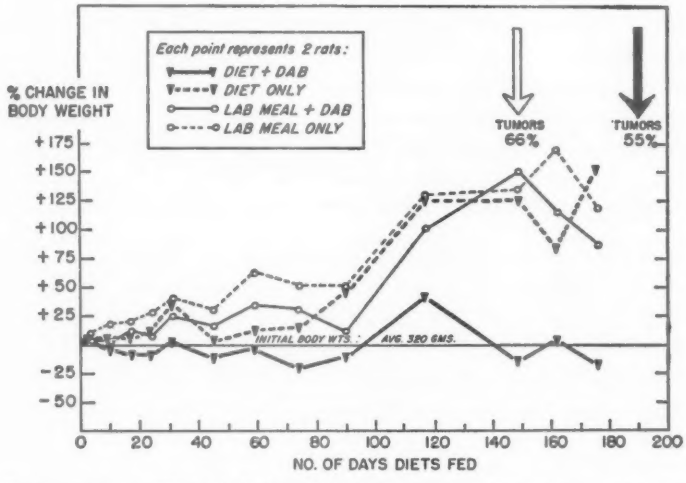

Text-figure 3. Change in body weight of rats fed hepatic carcinogen 3′-Me-4-DAB.

by the observation that there is a loss of dye-binding protein in the liver at the time that tumors develop. The significance of the cytoplasmic hyaline alteration in hepatic cells is not known; this has been thought to represent binding of the azo dye by proteins of the cytoplasm.

The synthetic diet used in this study did not result in accelerated tumor genesis or in a greater number of neoplasms. However, the synthetic diet and the carcinogen appeared to interact in some way to result in increased DNA synthesis by liver cells, a change which was not apparently related to tumor development. Many histochemical and biochemical studies have been made of preneoplastic cellular changes in azo dye carcinogenesis in the rat liver, using a synthetic diet. Unless such work includes studies of dietary effects with and without added carcinogen, and comparable studies using a normal diet, the results obtained may not be relevant to preneoplastic cellular changes. Indeed, alterations of this nature may be obscured by interactions between the synthetic diet and the carcinogen.

Summary

Rats were fed a derivative of butter yellow, 3′-methyl-4-dimethylaminoazobenzene, to produce tumors of the liver. Histologic alterations in hepatic, bile duct, and Kupffer cells preceding tumor formation were correlated with an autoradiographic study of the utilization of H^3-thymidine for DNA synthesis.

Degenerative changes, particularly of the cytoplasm of liver cells, with the formation of "hyaline bodies," was the first histologic alteration in the livers of rats fed the carcinogen. This was followed by alterations in staining and density of cytoplasm. Predominantly characterized by increased basophilia, this constituted the earliest recognizable preneoplastic change. The cells later showed histologic nuclear alterations and increased DNA synthesis.

A diffuse increase in hepatic cell synthesis of DNA did not precede the development of tumors in rats fed the carcinogen with laboratory meal. Those fed the carcinogen with a synthetic diet exhibited an increased cellular proliferation prior to the appearance of tumors. However, this did not accelerate carcinogenesis or cause an increase in the number of tumors. It is concluded that increased cellular proliferation is not of importance in the development of hepatic tumors in this form of azo dye carcinogenesis.

References

1. Miller, J. A., and Miller, E. C. The Carcinogenic Aminoazo Dyes. In: Advances in Cancer Research. Greenstein, J. P., and Haddow, A. (eds.). Academic Press, Inc., New York, 1953, Vol. 1, pp. 339–396.
2. Opie, E. L. The influence of diet on the production of tumors of the liver by butter yellow. *J. Exper. Med.*, 1944, **80**, 219–230.
3. Opie, E. L. The pathogenesis of tumors of the liver produced by butter yellow. *J. Exper. Med.*, 1944, **80**, 231–246.

4. Opie, E. L. Mobilization of basophile substance (ribonucleic acid) in the cytoplasm of liver cells with the production of tumors by butter yellow. *J. Exper. Med.*, 1946, **84**, 91–106.

5. Opie, E. L. Normal structure and degenerative changes of the cytoplasm of liver cells and of tumor cells derived from them. *J. Exper. Med.*, 1947, **85**, 339–346.

6. Opie, E. L. Cytochondria of normal cells, of tumor cells, and of cells with various injuries. *J. Exper. Med.*, 1947, **86**, 45–54.

7. Price, J. M.; Harman, J. W.; Miller, E. C., and Miller, J. A. Progressive microscopic alterations in the livers of rats fed the hepatic carcinogens 3′-methyl-4-dimethylaminoazobenzene and 4′-fluoro-4-dimethylaminoazobenzene. *Cancer Res.*, 1952, **12**, 192–200.

8. Farber, E. Similarities in the sequence of early histological changes induced in the liver of the rat by ethionine, 2-acetylaminofluorene, and 3′-methyl-4-dimethylaminoazobenzene. *Cancer Res.*, 1956, **16**, 142–148.

9. Firminger, H. I. Histopathology of carcinogenesis and tumors of the liver in rats. *J. Nat. Cancer Inst.*, 1955, **15** (2), 1427–1441.

10. Griffin, A. C.; Nye, W. N.; Noda, L., and Luck, J. M. Tissue proteins and carcinogenesis. I. The effect of carcinogenic azo dyes on liver proteins. *J. Biol. Chem.*, 1948, **176**, 1225–1235.

11. Glinos, A. D.; Bucher, N. L. R., and Aub, J. C. The effect of liver regeneration on tumor formation in rats fed 4-dimethylaminoazobenzene. *J. Exper. Med.*, 1951, **93**, 313–324.

12. Skoryna, S. C., and Webster, D. R. Production of cirrhosis and liver tumors in male rats using high dosages of 2-acetylaminofluorene. *Proc. Soc. Exper. Biol. & Med.*, 1951, **78**, 62–67.

13. MacDonald, R. A., and Mallory, G. K. Autoradiography using tritiated thymidine; detection of a new cell formation in rat tissues. *Lab. Invest.*, 1959, **8**, 1547–1562.

14. Norkin, S. A.; Weitzel, R.; Campagna-Pinto, D. C.; MacDonald, R. A., and Mallory, G. K. "Alcoholic" hyalin in human cirrhosis; histochemical studies. *Am. J. Path.*, 1960, **37**, 49–61.

15. Kit, S. Nucleic acid synthesis in the neoplastic cell and impact of nuclear changes on the biochemistry of tumor tissue: a review. *Cancer Res.*, 1960, **20**, 1121–1148.

16. Potter, V. R. The present status of the deletion hypothesis. *Univ. Michigan M. Bull.*, 1957, **23**, 401–412.

17. Miller, E. C., and Miller, J. A. *In vivo* combinations between carcinogens and tissue constituents and their possible role in carcinogenesis. *Cancer Res.*, 1952, **12**, 547–556.

Legends for Figures

Unless otherwise indicated, photographs were prepared from sections stained with hematoxylin and eosin.

Fig. 1. Left: A large hepatic tumor. Center: Multiple hepatic tumors. Right: An essentially normal liver in a rat fed a synthetic diet for 190 days.

Fig. 2. An experimentally induced hepatoma. × 400.

Fig. 3. Hepatic tumor with features of adenocarcinoma. × 400.

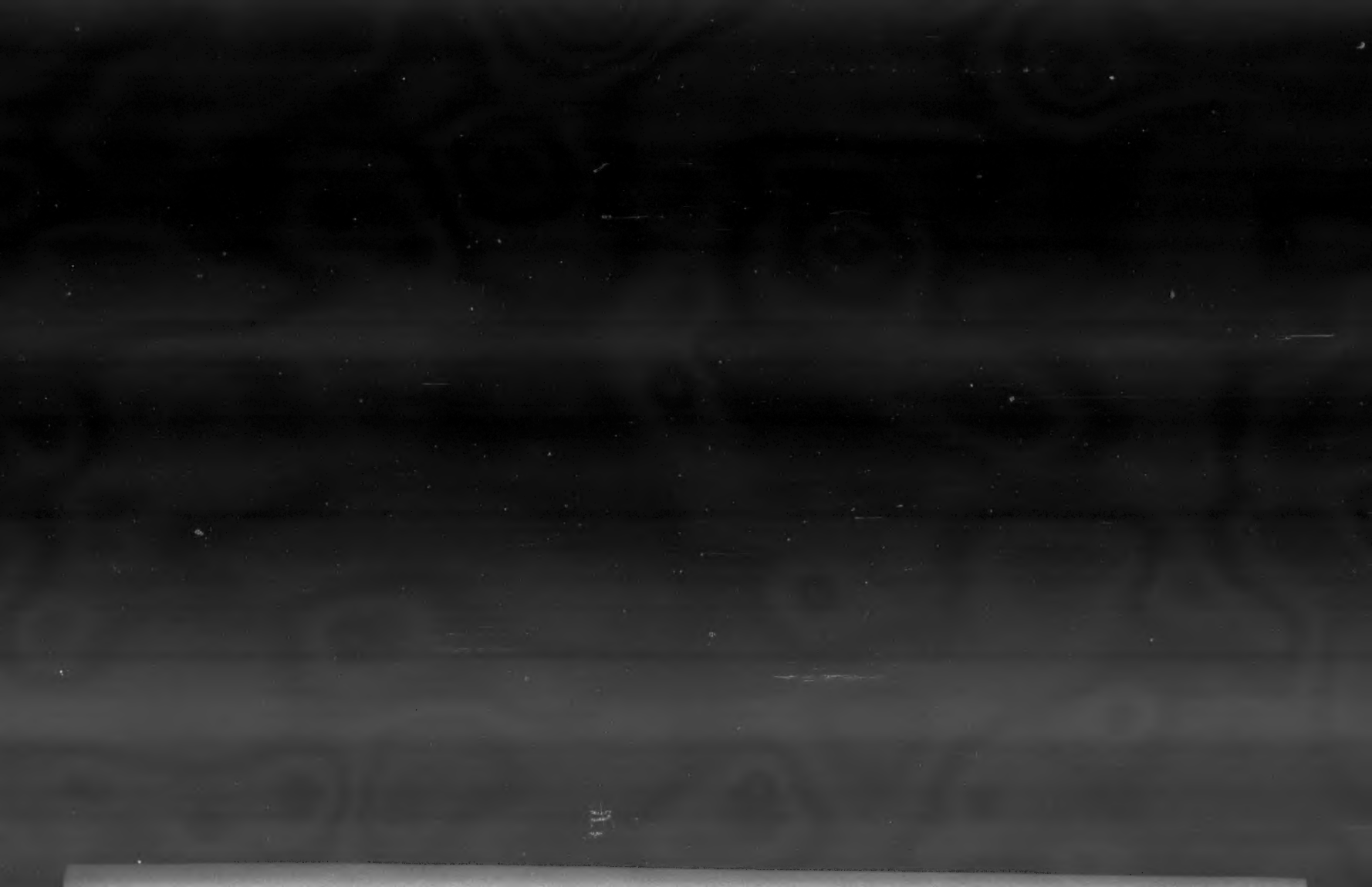

1

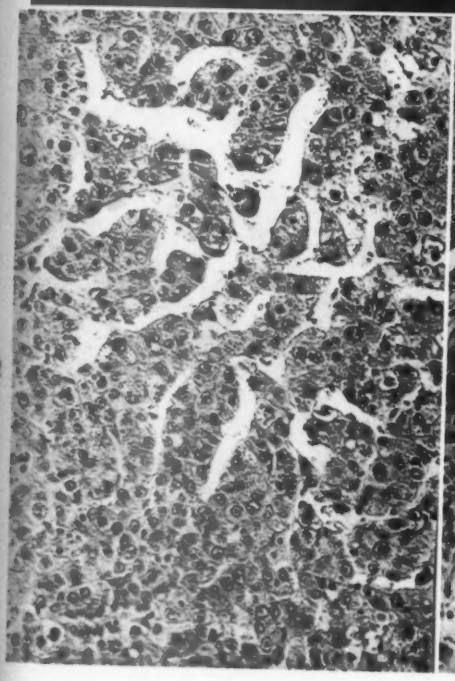

2

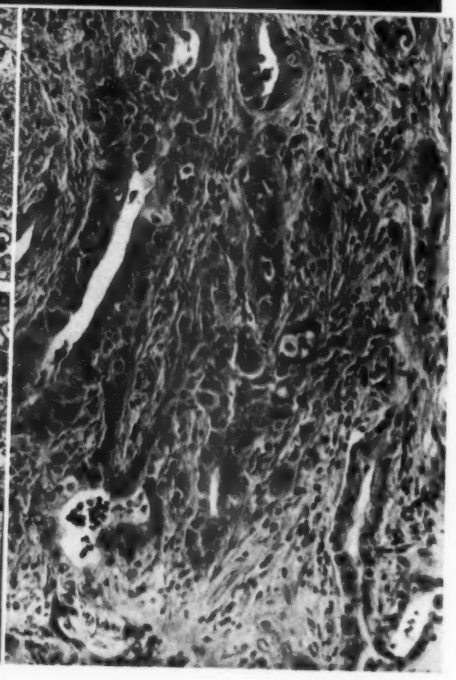

3

4

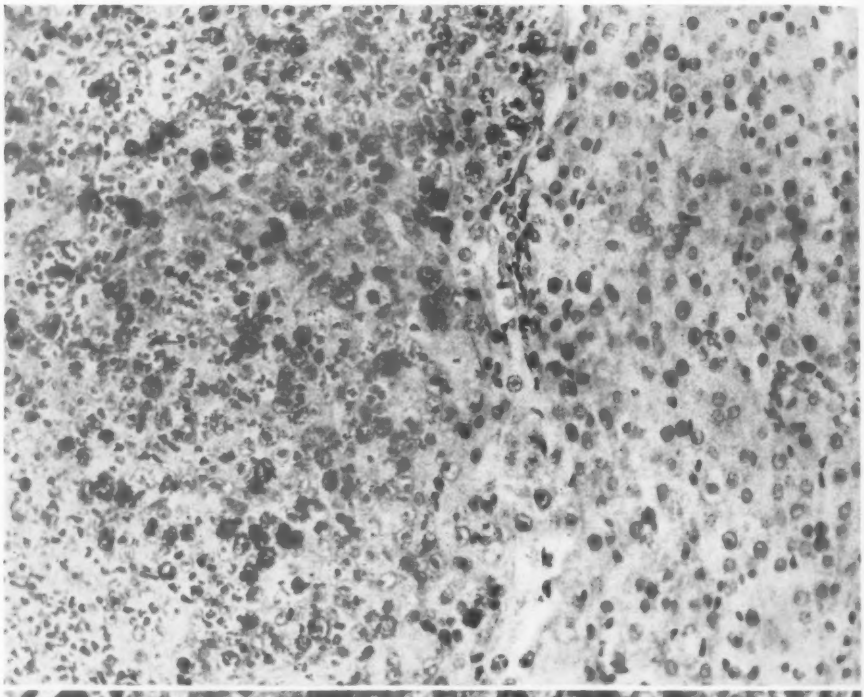

5

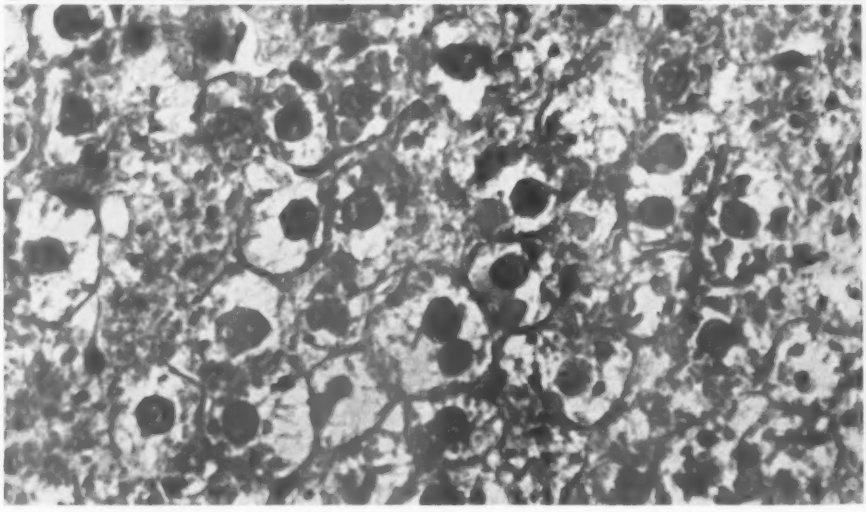

FIG. 4. An autoradiograph showing hepatoma on the left side of the illustration and normal liver on the right. There is abundant H^3-thymidine labeling of tumor nuclei and only 3 labeled nuclei of Kupffer cells in the adjacent normal liver. Hematoxylin stain. × 400.

FIG. 5. Hyaline degeneration in the cytoplasm of liver cells forming "hyaline bodies" in a rat fed the carcinogen with synthetic diet. × 800.

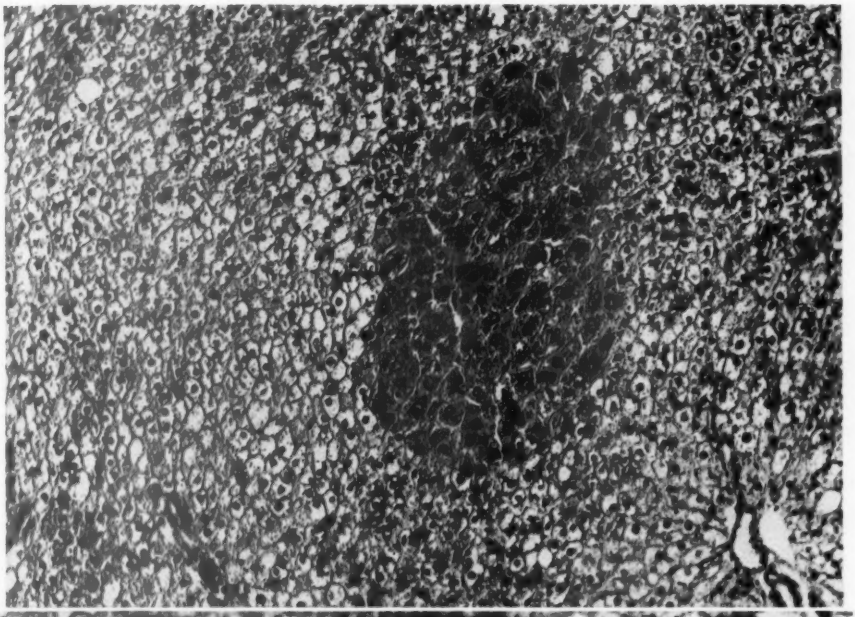

6

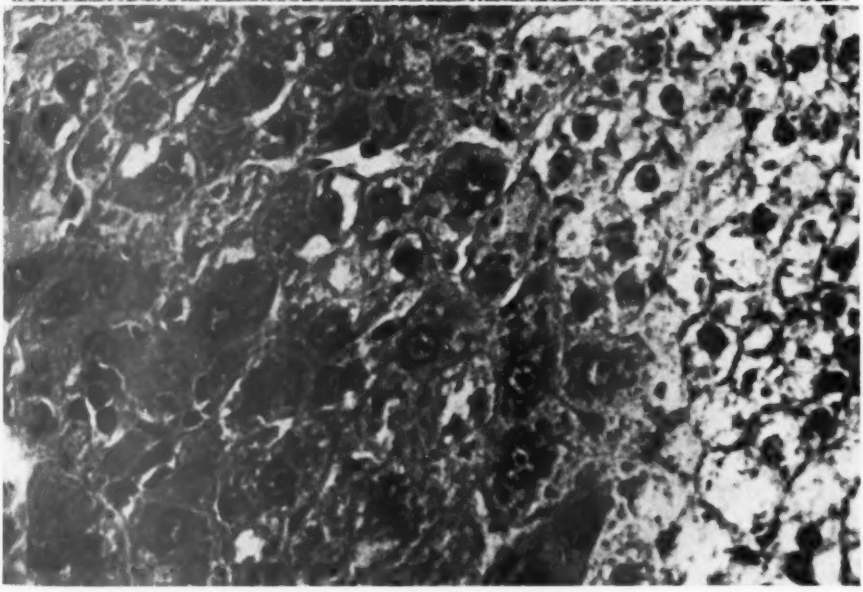

7

FIG. 6. A focus of liver cells illustrates preneoplastic alterations. There is increased density and basophilia of the cytoplasm. This rat was fed carcinogen with a synthetic diet for 190 days and had tumor elsewhere in the liver. × 400.

FIG. 7. Portion of the same group of liver cells shown in Figure 6. Normal liver cells appear in the right half of the illustration. × 800.

8

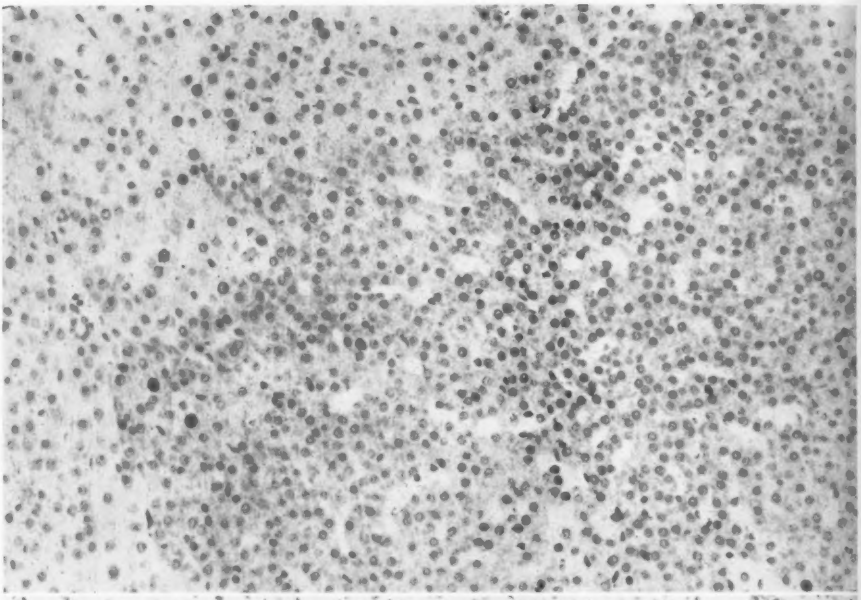

9

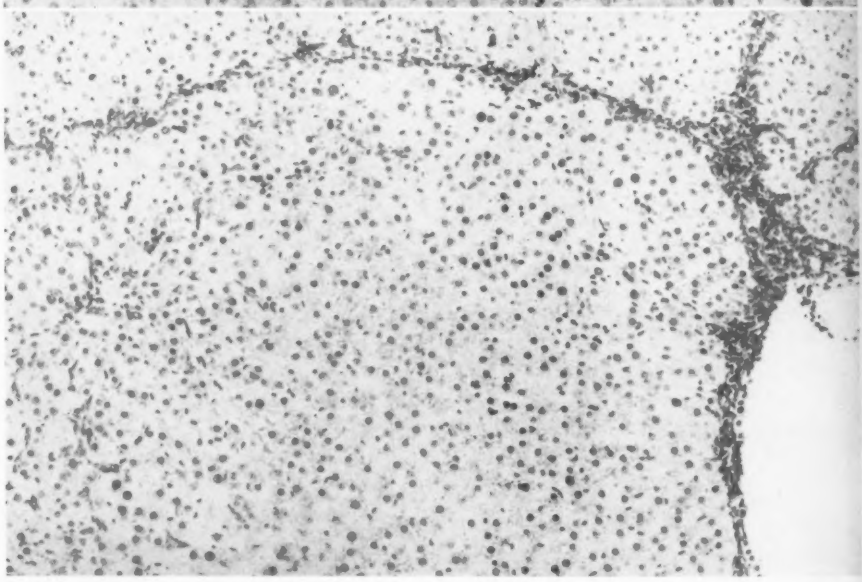

FIG. 8. An autoradiograph showing a preneoplastic focus of liver cells filling nearly the entire field. There are only 3 H^3-thymidine labeled hepatic nuclei in the left lower portion, illustrating that cytoplasmic changes precede nuclear synthesis of DNA. Hematoxylin stain. × 400.

FIG. 9. An autoradiograph of small proliferated bile ducts beginning to enclose an area of hepatic parenchyma to form a "nodule." There is no H^3-thymidine labeling of hepatic nuclei. Hematoxylin stain. × 400.

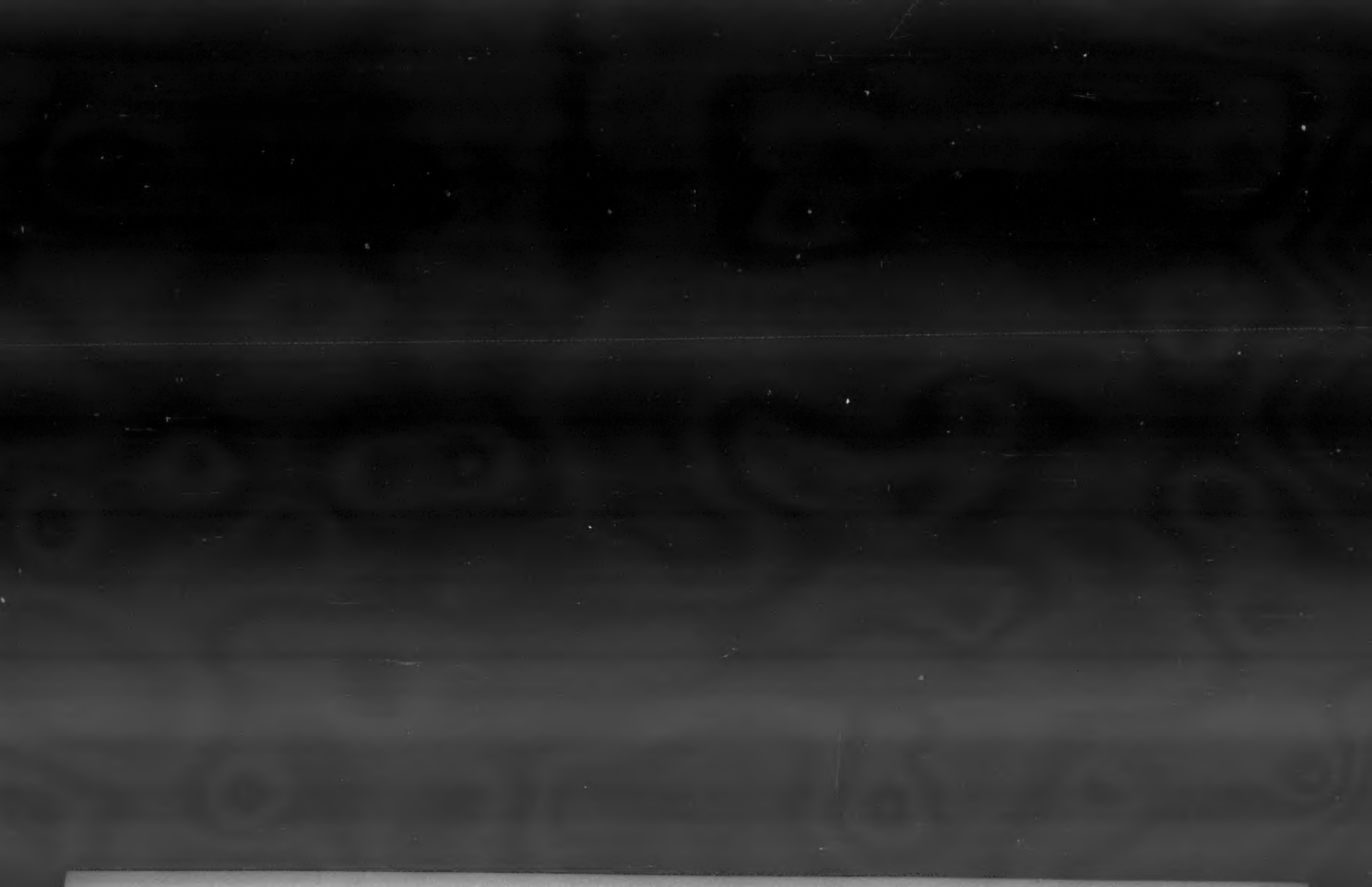

THE EFFECT OF CIRRHOSIS ON IRON STORAGE

B. A. Bradlow, M.B.; J. A. Dunn, B.A., and John Higginson, M.B.*

From the Department of Pathology and Microbiology (Division of Chemical Pathology), Witwatersrand University Medical School, and the South African Institute for Medical Research, Johannesburg, South Africa

Apart from the etiologic background, the pathologic distinction between the various iron storage diseases has been based largely on morphologic differences in the pattern of iron deposition. Since the pathologic patterns overlap in many instances, the belief that idiopathic hemochromatosis is a distinct entity has been challenged.[1]

In the Bantu Negro population of South Africa, excessive iron deposits are present in approximately 80 per cent of the adult population.[2–4] In the milder forms, hemosiderin deposits predominate in the reticuloendothelial tissues throughout the body, although iron is also present in the parenchymal cells of the liver. Iron deposits are prominent in the spleen, bone marrow, jejunal mucosa, and lymph nodes. They are generally absent or scanty in the parenchymal cells of the pancreas, myocardium, gastric mucosa, thyroid, salivary gland and choroid plexus, although iron-laden macrophages may be present. Periportal fibrosis is common, but cirrhosis is relatively infrequent.[2–5] In idiopathic hemochromatosis,[6,7] the hemosiderin deposits are believed to affect the parenchymal cells throughout the body, even at an early stage. When, however, Bantu siderosis is more severe, parenchymal pigment increases, and the pattern approximates that in idiopathic hemochromatosis, although jejunal and spleen hemosiderin deposits are still prominent.[2] In idiopathic hemochromatosis, the spleen, bone marow, and lymph nodes show relatively little hemosiderin, the jejunum usually is not pigmented, and cirrhosis of the liver and fibrosis of the pancreas are almost constant findings.

Although most cases of transfusional siderosis resemble Bantu siderosis from a pathologic viewpoint, in some instances the pattern simulates idiopathic hemochromatosis.[8–13] The presence of cirrhosis is, however, variable and not directly related to iron concentration in the liver.[11]

The etiology of Bantu siderosis is still uncertain.[14] All authors are

The work was supported in part by a grant from the National Cancer Association of South Africa.

Accepted for publication, April 1, 1961.

* Present address: Department of Pathology, University of Kansas Medical Center, Kansas City, Kans.

agreed that the high dietary iron intake, partly from native drink and partly from food, is a major factor. There is disagreement, however, on the possible role of dietary inadequacy as a predisposing factor in man, although inadequate diets have been shown to potentiate iron absorption in experimental animals.[15–17]

Cirrhosis as distinct from periportal fibrosis is not a typical feature of Bantu siderosis. On the other hand, we have observed a number of cases at necropsy in which the two conditions were associated. In these, the iron storage differed from the usual pattern and resembled that of idiopathic hemochromatosis. This observation suggested the possibility that cirrhosis *per se* might modify the distribution of iron pigment. A comparison of the iron-storage pattern in Bantu siderosis with cirrhosis, with that of siderosis without cirrhosis constitutes the essence of this study.

Material and Methods

A group of 34 necropsies on Bantu patients seen at Baragwanath Hospital were investigated. These showed varying degrees of siderosis, hepatic fibrosis and cirrhosis, and were classified as follows:

Group 1. Nineteen cases in which there were both cirrhosis and siderosis. The diagnosis of cirrhosis was based on the presence of fibrous scarring, nodular regeneration and architectural distortion (Fig. 1). The cases representing those fulfilling these criteria were collected during a 2½-year period.

Group 2. There were 10 cases with normal hepatic architecture or with slight to moderate periportal fibrosis (Fig. 2).

Group 3. In 5 cases, the liver showed marked periportal fibrosis and early linkage of portal areas, but with retention of the normal architecture and without nodular regeneration.

Groups 2 and 3 were selected at random from recognized cases of siderosis in which sufficient tissue was available for chemical analysis. Tissues were fixed in 10 per cent neutral formalin, and all sections were stained with hematoxylin and eosin. Hemosiderin was demonstrated by the method of Dry [18]; these sections were counterstained with either safranine or basic fuchsin.

In all cases, the iron concentration in the liver, spleen, pancreas and heart was determined by the thioglycolic acid method, as previously described.[2] Results were expressed in gm. per cent dry weight. In 3 cases, either the pancreas or heart were not available for estimation.

Where tissues were available, sections were also made of the stomach, jejunum, thyroid, adrenal and kidney. In addition to the chemical analysis, all histologic sections were graded 0 to +++ on the basis of visible hemosiderin deposits, without knowledge of the iron content (Table I). Correlation with the chemical findings was good at the lower concentrations, but when the iron content of the liver was above 2 per cent dry weight and the spleen 3 per cent dry weight, correlation became unsatisfactory.

Classification According to Degree of Siderosis. It is clearly necessary to compare cases having similar degrees of iron overload. Unfortunately, it was not possible to estimate the total body iron content, but Sheldon [6] has shown that the largest quantity of iron in idiopathic hemochromatosis is in the liver. This is also true in Bantu siderosis [2–4] and in experimental iron overload in rats.[19] It thus seemed reasonable to use the concentration of hepatic iron as an index for the comparison of cases. In

Bantu siderosis large quantities of iron are also present in the spleen, but this organ is usually small and the concentration correlates well with that in the liver.[14]

Previous studies [2] indicated that when the concentration of hepatic iron was of the order of 3 gm. per cent dry weight, parenchymal deposits in the pancreas and other organs tended to rise rapidly. Accordingly, cases were classified as to whether the concentration of liver iron was between 1 and 3 gm. per cent dry weight, or above 4 gm. per cent dry weight.

Parenchymal Iron. The concentration of iron in the pancreas and heart was utilized as an index of parenchymal iron storage, since these organs contain relatively little

TABLE I

HISTOLOGIC GRADING OF HEMOSIDERIN CORRELATED WITH IRON CONTENT AS DEMONSTRATED BY CHEMICAL ANALYSIS

Histologic grading	Iron content expressed as gm. per 100 gm. dry wt.			
	Liver	Spleen	Pancreas	Heart
0	< 0.1	< 0.1	< 0.05	< 0.1
Slight (+)	0.1 — 0.5	0.1 — 1.0	0.05 — 0.15	0.10 — 0.15
Moderate (++)	0.5 — 2.0	1.0 — 3.0	0.15 — 0.60	0.15 — 0.20
Severe (+++)	> 2.0	> 3.0	> 0.6	> 0.2

interstitial tissue and since parenchymal storage is observed early in idiopathic hemochromatosis. Histologic examination of the thyroid, adrenal, choroid plexus and gastric mucosa indicated that the concentration of chemical iron in these organs was a reasonably satisfactory index of parenchymal iron in other organs. For the purpose of discussion, differences in the concentration and distribution of iron between hepatic parenchymal and Kupffer cells have been ignored. Further, the term "parenchymal iron" refers only to the distribution of hemosiderin in organs other than the liver.

Cause of Death. In the cases without cirrhosis (groups 2 and 3), death was due to a variety of causes not related to hepatic disorder or siderosis. Of the 19 cases in the group with cirrhosis (group 1), the cause of death was directly related to the cirrhosis in 10 cases, including 3 instances of hepatocellular carcinoma. In 3 patients with cirrhosis, diabetes mellitus was present.

RESULTS

Age and Sex Distribution

The sex ratios were similar in the 3 groups and showed a preponderance of male cases (ratio, 2.2 to 1). The mean age in group 2 was slightly lower (52 years) than that in group 1 (60 years), but in view of the wide scatter, this difference is probably not significant. In group 3, the average age was lower than that in group 2 (45 years).

Liver Weight

The mean weight of livers without cirrhosis was 1,730 gm. (range 1,370 to 2,210 gm.). For those with cirrhosis the mean was 1,893 gm. (range 1,050 to 4,100 gm.). The corresponding mean weights for the cases with an iron concentration between 1 and 3 gm. were 1,760 gm. and 1,680 gm. respectively, if a case with a large primary carcinoma (4,100 gm.) is excluded from the group with cirrhosis. The corresponding fig-

ures for the spleen were 204 gm. for the group without cirrhosis and 269 gm. for cases with cirrhosis.

Chemical Findings

In the scatter diagrams (Text-figs. 1 and 2) the concentration of iron in the pancreas and heart are shown for the various concentrations of hepatic iron in each group. The concentrations in the heart and pancreas

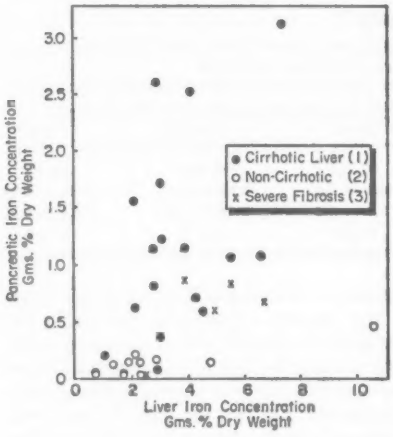

TEXT-FIGURE 1. Scattergram illustrating the correlation between the concentrations of liver and pancreatic iron in cases with cirrhosis (group 1), without cirrhosis (group 2), and with severe hepatic fibrosis (group 3).

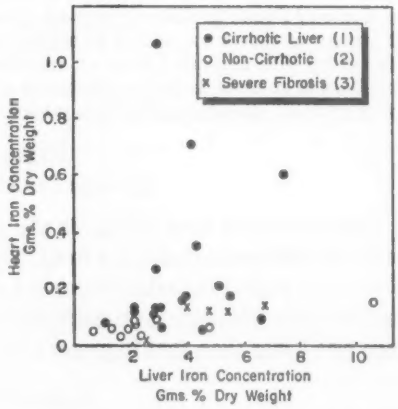

TEXT-FIGURE 2. Scattergram illustrating the correlation between the concentrations of liver and cardiac iron in cases with cirrhosis (group 1), without cirrhosis (group 2), and with severe hepatic fibrosis (group 3).

tended to be much higher in the group with cirrhosis than in those without cirrhosis, especially in the less severe cases. Also, in both series, the concentration of iron in these organs increased with the severity of hepatic siderosis. In a single instance of cirrhosis with hepatic iron concentration of 0.7 per cent, the iron distribution resembled that observed in the group without cirrhosis.

In Tables II and III, the data have been arranged for livers with a concentration of iron of 1 and 3 per cent dry weight, and for those with iron concentrations of over 4 gm. In the former category (Table II) only cases from group 2 were included in the group without cirrhosis. The mean liver iron content was slightly higher in the groups with cirrhosis than in those without, but the differences were not significant. The concentrations of both cardiac and pancreatic iron were, however, significantly higher and the differences were clearly visible on microscopic examination. The concentration of splenic iron was lower in the group with cirrhosis.

TABLE II

MEAN IRON CONCENTRATION IN SPLEEN, PANCREAS, AND HEART; LIVER IRON CONCENTRATION BETWEEN 1 AND 3 GM.*

Group	Liver	Spleen	Pancreas	Heart
With cirrhosis				
Group 1 (7)				
Mean †	2.24	2.90	0.698	0.171
95% confidence limits	1.58 — 3.17	1.63 — 5.18	0.276 — 1.77	0.101 — 0.472
Without cirrhosis				
Group 2 (7)				
Mean †	2.09	5.25	0.107	0.060
95% confidence limits	1.63 — 2.51	3.20 — 8.61	0.050 — 0.228	0.041 — 0.088
Difference between means				
P value	< 0.5	< 0.1	< 0.001	< 0.01
Group 1				
Arithmetic mean	2.35	3.78	1.01	0.32
Group 2				
Arithmetic mean	2.05	6.90	0.13	0.068

* Expressed as gm. per cent dry weight.

† To reduce the variance and to use a more suitable scale for calculation, the geometric mean has been used.

The analysis of cases with liver iron concentration greater than 4 gm. per cent are shown in Table III. Since only one case in group 2 showed this concentration, groups 2 and 3 have been combined. Although the trends observed at the lower concentrations were still present, they were less prominent, and considerable quantities of iron were present in the heart and pancreas in both groups. The differences in the concentration of pancreatic iron were barely significant ($P < 0.05$).

Histologic Observations

The histologic features essentially confirmed the chemical analysis. The hemosiderin content in the 10 pancreases available in group 2 was graded as nil or slight. In cases with cirrhosis, the iron content was graded as severe in 15 and as moderate in 2.

Of the 15 pancreases examined in groups 2 and 3, only one showed moderate fibrosis, but in 8 of the 19 cases with cirrhosis in group 1 there was moderate to severe pancreatic fibrosis.

The mean concentration of pancreatic iron in pancreases with moderate or severe fibrosis was 1.46 gm. per cent dry weight. This was in contrast to 0.97 per cent dry weight in the group without pancreatic

TABLE III

MEAN IRON CONCENTRATION IN SPLEEN, PANCREAS, AND HEART; LIVER IRON CONCENTRATION GREATER THAN 4 GM.*

Group	Liver	Spleen	Pancreas	Heart
With cirrhosis				
Group 1 (7)				
Mean †	5.26	5.51	1.331	0.234
95% confidence limits	4.27 — 6.50	3.02 — 10.02	0.750 — 2.360	0.104 — 0.525
Without cirrhosis				
Groups 2 and 3 (5)				
Mean †	6.19	7.66	0.466	0.120
95% confidence limits	4.08 — 9.40	5.13 — 11.42	0.203 — 1.07	0.087 — 0.167
Difference between means P value	>0.3	>0.2	<0.05	<0.1
Group 1				
Arithmetic mean	5.35	6.61	1.57	0.32
Groups 2 and 3				
Arithmetic mean	6.49	8.11	0.54	0.12
Idiopathic hemochromatosis				
Mean after Sheldon[6]	3.6	0.5	2.0	0.5

* Expressed as gm. per cent dry weight.

† To reduce the variance and to use a more suitable scale for calculation, the geometric mean has been used.

fibrosis. The mean concentrations of iron in the pancreases from cases with diabetes were 1.14, 3.17 and 2.52 gm. per cent dry weight respectively. The distribution of hemosiderin pigment in the liver and Kupffer cells and in the portal tracts showed no constant pattern. However, deposits in the portal areas tended to be very prominent in livers with periportal fibrosis (Fig. 2).

In the stomach, only slight hemosiderin deposit was demonstrated in 2 cases in group 2, whereas all stomachs in the group with cirrhosis contained demonstrable hemosiderin which was graded as moderate or severe in 9 cases. One of the 4 stomachs examined in group 3 showed slight hemosiderin deposit and one contained a moderate amount. Hemosiderin, when present, was observed in both interstitial and mucosal cells. Siderosis was prominent in the substantia propria of the jejunal villi in both series. Although the differences between the groups with and with-

out cirrhosis were not clear-cut, the results suggested a tendency to more severe jejunal siderosis in the noncirrhotic group.

In the thyroid and adrenal, siderosis of the acinar cells was more prominent in association with cirrhosis, but the differences were most distinct when the liver iron concentration was less than 3 gm. per cent.

Type of Cirrhosis

The distinction between cirrhotic and noncirrhotic livers was based on criteria previously utilized by us.[5] A clear distinction was made between periportal fibrosis, a lesion frequently observed among Bantu Negroes, and a true cirrhosis with complete architectural distortion (Figs. 1 and 2). The livers in group 3 showed more damage than those in group 2, but the degree of architectural distortion and nodular regeneration was insufficient to merit the term "cirrhosis."

Cirrhotic livers among the Bantu can be divded into a fine monolobular cirrhosis which is believed to be partly the result of iron deposition, and a coarse nodular cirrhosis, possibly of postviral infectious origin, in which hemosiderin deposition appears incidental.[5] The hepatic iron concentrations in the two groups were similar, and no significant differences could be demonstrated in the related pancreatic and cardiac iron concentration. In the spleen, the iron concentration was lower in the group with coarse nodular cirrhosis. This may be due to an increased size of the spleen with fibrosis in these cases.

Degree of Siderosis

In Table IV, the correlation coefficients between the iron content of the various organs in cases with and without cirrhosis are shown. It will

TABLE IV

CORRELATION COEFFICIENTS; IRON CONTENT OF VARIOUS ORGANS IN CASES WITH AND WITHOUT CIRRHOSIS

	Group 1 (cirrhosis)			Group 2 (no cirrhosis)		
	R	$\frac{1}{\sqrt{n-1}}$		R	$\frac{1}{\sqrt{n-1}}$	
Liver and spleen	0.565	0.236	S	0.75	0.316	S
Liver and pancreas	0.695	0.243	S	0.74	0.355	S
Liver and heart	0.32	0.243	NS	0.72	0.33	S

S = Significant, i.e., $R > 2 \times \frac{1}{\sqrt{n-1}}$

NS = Not significant, i.e., $R < 2 \times \frac{1}{\sqrt{n-1}}$

be observed that in general there is a significant correlation between the concentration of liver iron and that in the spleen, pancreas, and heart,

with the possible exception of the liver and heart in the group with cirrhosis.

Discussion

The results show that there is a significant difference in the pattern of hemosiderin distribution among cases of Bantu siderosis with and without cirrhosis. On chemical estimation, the group with cirrhosis shows a much higher concentration of iron in the pancreas and heart than the group without cirrhosis, and the histologic features suggest that this is also true for the stomach, thyroid, and adrenal. Lower concentrations are present in the spleen. These different patterns are most obvious when cases with liver iron concentrations between 1 and 3 gm. are considered. However, even when the concentration of hepatic iron is greater than 4 gm. per cent, differences are still present between the groups, although less marked. It should be noted, however, that the majority of livers with this degree of iron concentration were placed in group 3, in which there was considerable liver damage. The type of cirrhosis did not appear to affect the distribution of iron.

For comparative purposes, only the present series of cases has been considered, but a review of previous studies from this region[2,4,20] indicates a similar pattern (Table V). Unfortunately, data for individual

Table V

Iron storage disease with and without cirrhosis; concentrations of hepatic iron between 1 and 3 gm. per cent dry weight

		Concentration of iron (gm. per 100 gm. dry weight)				
	Cirrhosis	Liver	Spleen	Pancreas	Heart	Reference
Bantu siderosis	Absent	1.23	2.63	0.09	0.05	Higginson *et al.*[3] (cases 19 to 23)
		1.19	3.73	0.07	0.09	
		1.55	5.16	0.08	0.07	
		2.34	5.75		0.05	
		2.45	3.50	0.15	0.07	
	Present	1.30	0.90	2.20	0.80	Seftel *et al.*[20] (case 4)
	See note *	2.80	2.95	0.17	0.033	Wainwright[4] (average all cases)
Idiopathic hemochromatosis	Present	2.95	2.66	2.65		Bernouilli †
		2.12	0.13	2.14	0.283	Ramage and Sheldon †
		2.44		2.30	0.550	
		2.15	0.37	0.871	0.212	
		2.56	0.39	0.71	0.51	Higginson *et al.*[3] (case 26)

* Not stated, but probably the majority without cirrhosis.
† Abstracted from Sheldon.[6]

cases in Wainwright's study [4] are not available. A review of the cases in which the liver iron concentration was greater than 3 gm. per cent also would indicate that in extrahepatic areas, parenchymal storage tends to be more marked when cirrhosis is present.[2,20] However, the number of examples of Bantu siderosis reported within this range is small.

It appears unlikely that the different patterns of distribution are dependent on differences in degree of iron overload. Moreover, there is no manifest correlation between iron distribution and any disease process apart from cirrhosis. Thus, the results suggest that the presence of cirrhosis *per se* may modify the pattern of iron distribution and also the degree of siderosis.

It is clear that when cases of Bantu siderosis show both cirrhosis and parenchymal iron deposits, they exhibit a morphologic pattern very similar to that seen in idiopathic hemochromatosis. Moreover, diabetes mellitus was manifest in 3 of the present cases. MacDonald and Mallory [1] have pointed out that idiopathic hemochromatosis is recognized usually at necropsy by the presence of cirrhosis associated with excessive parenchymal iron deposition. In the majority of reported cases, the iron concentration has been greater than 3 gm. per cent. Nonetheless, if only the reported cases of idiopathic hemochromatosis in which the iron deposition has been between 1 and 3 gm. per cent dry weight are considered, the pancreatic and cardiac iron concentrations are high, corresponding to the group with cirrhosis in the present study. If the examples of Bantu siderosis in the present series with hepatic iron concentration greater than 4 gm. per cent are considered, the mean concentration of pancreatic and cardiac iron in the cases without cirrhosis is considerably less than the average for hemochromatosis as given by Sheldon [6] (Table III). Even in the cases with cirrhosis, the concentration of splenic and jejunal iron is much higher than is usually seen in hemochromatosis. The possibility that some cases in our cirrhotic group may represent instances of idiopathic familial hemochromatosis cannot be excluded with certainty without genetic and biochemical studies on iron absorption and transport. However, the available evidence weighs against this view. It would seem more likely that the cirrhotic group represents cases of Bantu siderosis, complicated by cirrhosis. This is also the view of Seftel, Isaacson and Bothwell in 4 similar cases.[20]

If the relationship of cirrhosis to parenchymal iron deposition is reviewed in relation to other iron-storage diseases, especially transfusional hemosiderosis, the position is difficult to clarify. While both Bantu siderosis and idiopathic hemochromatosis would appear to be diseases of long duration, in transfusional siderosis the time factor varies as does the degree of iron overload. Further, the distinction between periportal

fibrosis and cirrhosis has not always been made.[11] In some cases, as in the series of Cappell, Hutchinson and Jowett,[11] the degree of iron overload was very severe, and parenchymal deposits were prominent in the absence of cirrhosis. On the other hand, a high parenchymal iron concentration was found by these authors in their case 2, although the liver concentration was 1.15 gm. per cent and cirrhosis was absent. The largest series in which chemical estimations were made are those of Wyatt.[18,21] Among 7 cases of transfusional siderosis without cirrhosis, with iron concentrations between 1 and 3 gm., only one (case 4) showed markedly increased pancreatic and cardiac iron. In two cases of "nutritional siderosis" with cirrhosis (cases 1 and 4) and hepatic iron concentrations within this range, the pattern tended toward that of hemochromatosis. In one case without cirrhosis (case 2) the pancreatic and cardiac iron were low, but the splenic iron was also markedly reduced.[21] In general, however, it appears that in the majority of cases of transfusional siderosis with high concentrations of liver iron, parenchymal distribution is prominent whether cirrhosis is present or not.

The relationship of cirrhosis to the hepatic iron deposits has not been clarified. In idiopathic hemochromatosis, it has been claimed that iron deposits preceded the development of cirrhosis.[6,22] Others,[23,24] however, have indicated the reverse to be the case. Bothwell, Cohen, Abrahams and Perold[25] recently described extensive hemosiderin deposits in noncirrhotic livers in asymptomatic relatives of 6 patients with idiopathic hemochromatosis. Similar results were obtained by Brick[26] who, after reviewing the literature, regarded the disease as definitely genetic in nature. The claim that iron storage due to excessive blood transfusions could result in cirrhosis[27–29] has been disputed.[9,11,12,30] No common denominator to explain the hemochromatotic pattern in such patients has as yet been demonstrated. In Bantu siderosis, it appears probable on morphologic grounds that periportal fibrosis can result from iron deposition. This may occasionally develop into a true cirrhosis[2,3] although it is believed that the fibrosis is not attributable to iron pigment alone but to an additional factor.[2,31]

Experimentally, cirrhosis has not been induced by iron overload alone in rats,[15,16,32–34] rabbits,[35,36] or dogs.[37] Recently, however, Golberg and Smith[17] have shown that heavy deposits of iron in the rat liver cause the organ to be more susceptible to damage by ethionine or low-protein diet. These authors also postulated that a substance "haptosiderin," synthesized in excess in the damaged liver, increased the affinity of the cells for iron. MacDonald[38] has attempted to produce hemochromatosis by the administration of iron salts in rats on a choline-deficient diet. Although the pattern in the liver resembled that of hemochromatosis, parenchymal

iron deposits were not present in the pancreas or other organs. In another study of iron distribution in rats, we gave saccharated iron oxide intramuscularly after cirrhosis had been produced by carbon tetrachloride. We were unable to detect any difference either by chemical or histologic estimation between the normal rat and the animal with cirrhosis, in relation to the degree of parenchymal siderosis. However, the dosage of iron was very large and might well have been excessive.

It should be noted that in Bantu siderosis, in addition to iron there is an increase in other elements in the liver.[39]

It appears that in Bantu siderosis, parenchymal iron deposition is dependent partly on the presence of cirrhosis and partly on the degree of iron overload. These results support MacDonald and Mallory's view[1] that distinctions between hemosiderosis and hemochromatosis based only on histologic studies are not reliable. Even though hemosiderosis may eventually mimic hemochromatosis morphologically, however, this would not necessarily imply a common etiology. The demonstration of excessive iron pigment deposit in siblings of patients with idiopathic hemochromatosis[25,26] would support the concept of an inborn metabolic error.[6] Moreover, excessive iron absorption has been observed in many cases diagnosed during the early stages; in these instances this is probably secondary to increased requirements. In 4 of 5 cases of Bantu siderosis, Bothwell, van Doorn-Wittkampf, du Preez and Alper demonstrated that iron absorption was normal.[40] In the fifth case, increased iron absorption was found, but the patient also had cirrhosis and diabetes mellitus. Moreover, if hemochromatosis merely represents a late stage of hemosiderosis, it is surprising that the basic morphologic pattern still differs from that seen in Bantu siderosis in relation to the spleen and jejunum, even when cirrhosis is present, although in both disorders the iron presumably is absorbed from the intestine. It is possible that differences in splenic iron concentration are of little significance since the alterations may result from cirrhosis causing fibrosis and enlargement of this organ with secondary reduction in the iron concentration.

Accepting the effect of cirrhosis in increasing the severity of extrahepatic parenchymal iron deposits, our views on the nature of this mechanism are speculative. The suggestion by Golberg and Smith[17] that liver damage results in an increased cellular affinity for iron, because of the formation of a hypothetical "haptosiderin," is attractive. Schwartz[27] suggested that extrahepatic parenchymal deposits of iron only occurred after the development of cirrhosis in hemochromatosis, although there is no evidence that the effects of the defect leading to increased iron absorption is limited to the liver. He also suggested that saturation of the total serum iron-binding capacity as found in idiopathic

hemochromatosis was an important factor in parenchymal deposition. In the majority of cases of Bantu siderosis, although the serum iron levels were increased,[4,41] the total iron-binding capacity (TIBC) was far from saturated. This was in contrast to idiopathic hemochromatosis and transfusional siderosis. In Durban, Wainwright[4] reported on the serum iron levels in Bantu siderosis with and without cirrhosis. In only 4 of 17 cases without cirrhosis was the TIBC saturation level greater than 50 per cent, but in 13 cases with cirrhosis the TIBC was 62 to 97 per cent saturated. He suggested that serum iron levels in the Bantu might be due to a balance between cirrhosis and siderosis. Rath and Finch[42] also found a reduction of the total iron-binding protein in non-pigmented cirrhosis. Unfortunately, we have no data on the TIBC in the present cases. If the findings of Wainwright and of Rath and Finch are accepted, however, it would appear probable that in the presence of cirrhosis, the degree of saturation of the TIBC was increased, with a resulting deposition of iron in the parenchyma of various organs, as suggested by Schwartz. The varying results observed in transfusional hemosiderosis could be explained by the fact that saturation occurred rapidly and in an early stage. Indeed, it might vary over prolonged periods and be unrelated to cirrhosis.

Summary

The pattern of body iron distribution has been compared in 18 cases of Bantu siderosis with cirrhosis and 16 cases without cirrhosis. In the cirrhosis group, the distribution of iron resembled that found in idiopathic hemochromatosis in that extrahepatic parenchymal deposits were prominent. In cases without cirrhosis, parenchymal deposits were scanty or absent. The difference between the two groups was most obvious when cases with concentrations of liver iron between 1 and 3 gm. were compared.

It is suggested that the pattern of iron deposition in Bantu siderosis is dependent on the presence or absence of cirrhosis and on the total concentration of body iron as well. It is believed that the different patterns are dependent on the degree of saturation of the total serum iron-binding capacity.

The significance of these results in relation to other iron storage diseases is briefly discussed. It is suggested that in idiopathic hemochromatosis, cirrhosis may be a factor in the parenchymal deposition of iron. The mechanism in transfusional siderosis is not clear-cut because saturation of the total serum iron-binding capacity occurs early, and iron overload is often rapid.

References

1. MacDonald, R. A., and Mallory, G. K. Hemochromatosis and hemosiderosis; study of 211 autopsied cases. *Arch. Int. Med.*, 1960, **105**, 686–700.
2. Higginson, J.; Gerritsen, T., and Walker, A. R. P. Siderosis in the Bantu of Southern Africa. *Am. J. Path.*, 1953, **29**, 779–815.
3. Gillman, J., and Gillman, T. Perspectives in Human Malnutrition; a Contribution to the Biology of Disease from a Clinical and Pathological Study of Chronic Malnutrition and Pellagra in the African. Grune & Stratton, New York, 1951, 584 pp.
4. Wainwright, J. Siderosis in the African. *South African J. Lab. Clin. Med.*, 1957, **1**, 1–28.
5. Higginson, J.; Grobbelaar, B. G., and Walker, A. R. P. Hepatic fibrosis and cirrhosis in man in relation to malnutrition. *Am. J. Path.*, 1957, **33**, 29–53.
6. Sheldon, J. H. Haemochromatosis. Oxford University Press, London, 1935, 382 pp.
7. Golberg, L. Hemosiderosis and hemochromatosis: the question of pathogenesis. *Postgrad. Med.*, 1957, **22**, 382–388.
8. Schwartz, S. O., and Blumenthal, S. A. Exogenous hemochromatosis resulting from blood transfusions. *Blood*, 1948, **3**, 617–640.
9. Dubin, I. N. Idiopathic hemochromatosis and transfusion siderosis: a review. *Am. J. Clin. Path.*, 1955, **25**, 514–542.
10. Kleckner, M. S., Jr.; Baggenstoss, A. H., and Weir, J. F. Iron-storage diseases. *Am. J. Clin. Path.*, 1955, **25**, 915–931.
11. Cappell, D. F.; Hutchinson, H. E., and Jowett, M. Transfusional siderosis: the effects of excessive iron deposits on the tissues. *J. Path. & Bact.*, 1957, **74**, 245–264.
12. Rather, L. J. Hemochromatosis and hemosiderosis. Does iron overload cause diffuse fibrosis of the liver? *Am. J. Med.*, 1956, **21**, 857–866.
13. Wyatt, J. P. Patterns of pathological iron storage. I. The nature and significance of transfusional siderosis and its relationship to idiopathic hemochromatosis and allied conditions. *Arch. Path.*, 1956, **61**, 42–55.
14. Bothwell, T. H., and Bradlow, B. A. Siderosis in the Bantu; a combined histopathological and chemical study. *Arch. Path.*, 1960, **70**, 279–292.
15. Kinney, T. D.; Hegsted, D. M., and Finch, C. A. The influence of diet on iron absorption. I. The pathology of iron excess. *J. Exper. Med.*, 1949, **90**, 137–146.
16. Gillman, T.; Hathorn, M., and Canham, P. A. S. Experimental dietary siderosis. *Am. J. Path.*, 1959, **35**, 349–367.
17. Golberg, L., and Smith, J. P. Iron overloading and hepatic vulnerability. *Am. J. Path.*, 1960, **36**, 125–149.
18. Dry, D. S. Improved methods for the demonstration of mitochondria, glycogen, fat and iron in animal cells. *South African J. Sc.*, 1945, **41**, 298–301.
19. Finch, C. A.; Hegsted, M.; Kinney, T. D.; Thomas, E. D.; Rath, C. E.; Hoskins, D.; Finch, S., and Fluharty, R. G. Iron metabolism: the pathophysiology of iron storage. *Blood*, 1950, **5**, 983–1008.
20. Seftel, H. C.; Isaacson, C., and Bothwell, T. H. The relationship between siderosis and diabetes in the Bantu. *South African J. M. Sc.*, 1960, **25**, 89–98.

21. WYATT, J. P. Patterns of pathological iron storage. II. Exogenic siderosis in chronic anemia due to prolonged oral iron medication. *Arch. Path.*, 1956, **61**, 56–61.

22. HARVIER, P.; DI MATTÉO, J., and BESCOL-LIVERSAC, J. Ponction-biopsie du foie et cirrhose pigmentaire. *Presse méd.*, 1953, **61**, 423–426.

23. MUIR, R. Text Book of Pathology. Revised by CAPPELL, D. F. E. Arnold & Co., London, 1951, ed. 6, 1090 pp.

24. MUIR, R., and DUNN, J. S. The iron content of the organs in bronzed diabetes (haemochromatosis). *J. Path. & Bact.*, 1914–1915, **19**, 226–238.

25. BOTHWELL, T. H.; COHEN, I.; ABRAHAMS, O. L., and PEROLD, S. M. A familial study of idiopathic hemochromatosis. *Am. J. Med.*, 1959, **27**, 730–738.

26. BRICK, I. B. Liver histology in six asymptomatic siblings in a family with hemochromatosis; genetic implications. *Gastroenterol.*, 1961, **40**, 210–214.

27. SCHWARTZ, S. O. Exogenous haemochromatosis; concept and general description. *Am. J. Clin. Path.*, 1956, **26**, 744–749.

28. PENGELLY, C. D. R., and JONES, P. Acquired haemochromatosis following multiple blood-transfusions for hypoplastic anaemia. *Lancet*, 1956, **2**, 445–446.

29. HUGHES, J. T., and TRUELOVE, L. H. Transfusional haemosiderosis simulating haemochromatosis. *J. Clin. Path.*, 1958, **11**, 128–132.

30. AUFDERHEIDE, A. C.; HORNS, H. L., and GOLDISH, R. J. Secondary hemochromatosis; transfusion (exogenous) hemochromatosis. *Blood*, 1953, **8**, 824–836.

31. LUONGO, M. A., and BJORNSON, S. S. The liver in ferrous sulphate poisoning; a report of three fatal cases in children and an experimental study. *New England J. Med.*, 1954, **251**, 995–999.

32. POLSON, C. The failure of prolonged administration of iron to cause haemochromatosis. *Brit. J. Exper. Path.*, 1933, **14**, 73–76.

33. CAPPELL, D. F. The late results of intravenous injection of colloidal iron. *J. Path. & Bact.*, 1930, **33**, 175–196.

34. NISSIM, J. A. Experimental siderosis: a study of the distribution, delayed effects and metabolism of massive amounts of various iron preparations. *J. Path. & Bact.*, 1953, **66**, 185–204.

35. ROUS, P., and OLIVER, J. Experimental haemochromatosis. *J. Exper. Med.*, 1918, **28**, 629–644.

36. POLSON, C. J. The storage of iron following its oral and subcutaneous administration. *Quart J. Med.*, 1929, **23**, 77–84.

37. BROWN, E. B.; MOORE, C. V.; REYNAFARJE, C., and SMITH, D. E. Intravenously administered saccharated iron oxide in the treatment of hypochromic anaemia; therapeutic results, potential dangers and indications. *J.A.M.A.*, 1950, **144**, 1084–1089.

38. MACDONALD, R. A. Experimental pigment cirrhosis. Its production in rats by feeding a choline-deficient diet with excess iron. *Am. J. Path.*, 1960, **36**, 499–519.

39. BUTT, E. M., and HIGGINSON, J. Trace element pattern in liver disease and liver carcinoma. *Acta Unio internat. contra cancrum*, 1957, **13**, 599–601.

40. BOTHWELL, T. H.; VAN DOORN-WITTKAMPF, H. V.; DU PREEZ, M. L., and ALPER, T. The absorption of iron; radioiron studies in idiopathic hemochromatosis; malnutritional cytosiderosis and transfusional hemosiderosis. *J. Lab. & Clin. Med.*, 1953, **41**, 836–848.

41. GERRITSEN, T., and WALKER, A. R. P. Serum iron and iron-binding capacity in the South African Bantu. *Nature, London*, 1953, **171**, 699.

42. RATH, C. E., and FINCH, C. A. Chemical, clinical and immunological studies on the products of human plasma fractionation. 38. Measurement of iron binding capacity of serum in man. *J. Clin. Invest.*, 1949, **28**, 79–85.

[*Illustrations follow*]

Legends for Figures

Fig. 1. Liver in group 1, showing cirrhosis and moderate siderosis. Marked distortion of architecture is evident. Hematoxylin and eosin stain. × 57.

Fig. 2. Liver in group 2, showing periportal fibrosis and moderate siderosis. Note the retention of architecture and the heavy deposits of intra- and extracellular hemosiderin in the portal areas. Hematoxylin and eosin stain. × 50.

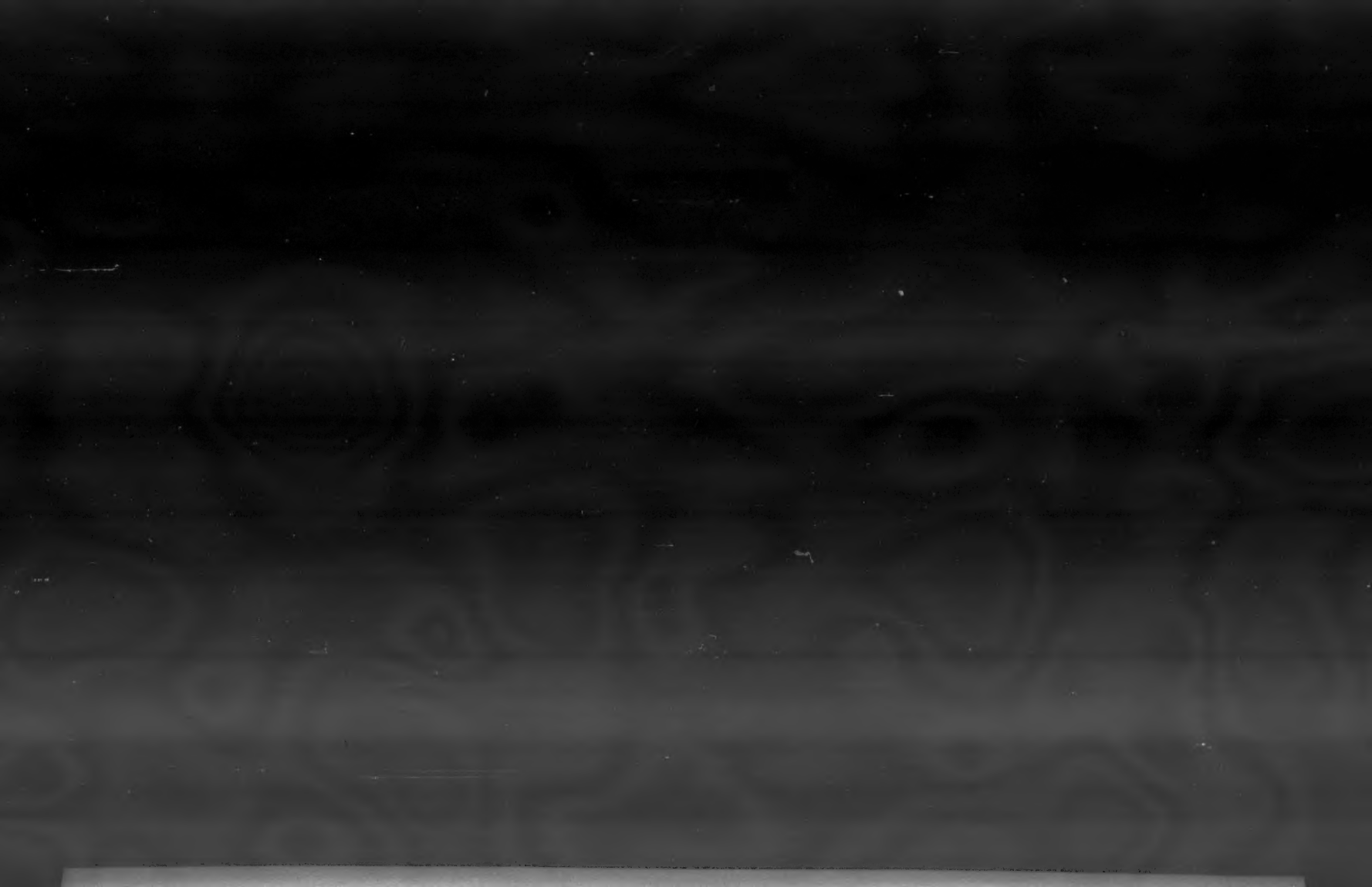

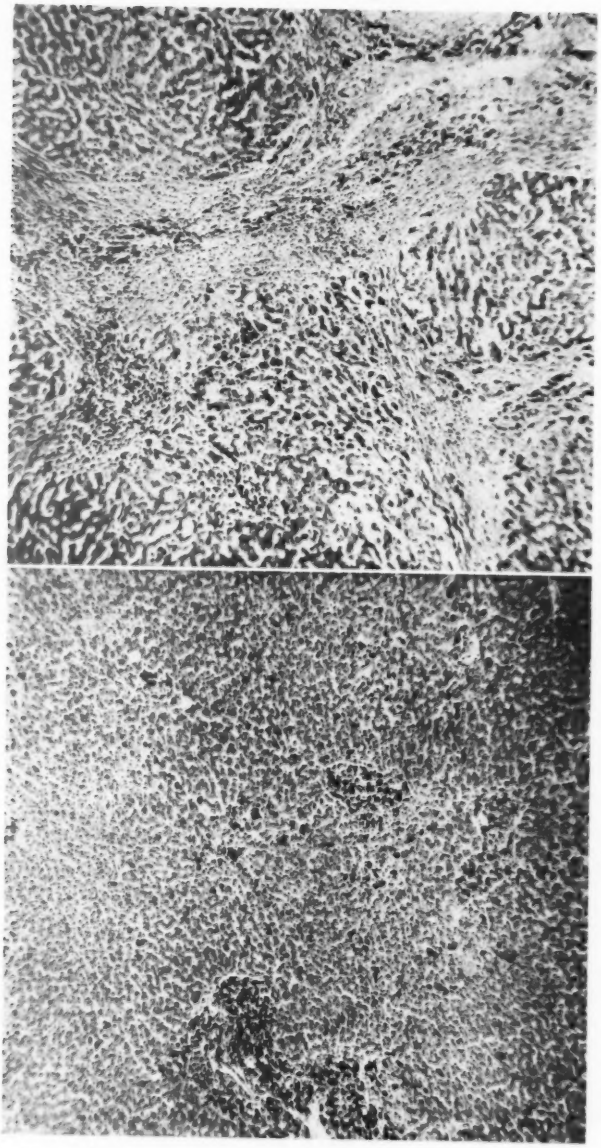

1

2

ELECTRON MICROSCOPY OF LEUKOCYTIC MARGINATION AND EMIGRATION IN ACUTE INFLAMMATION IN DOG PANCREAS

JOSEPH R. WILLIAMSON, M.D.,* AND JOE W. GRISHAM, M.D.†

From the Department of Pathology, Washington University School of Medicine, St. Louis, Mo.

Emigration of white blood cells through vessels in acute inflammation has been studied extensively by light microscopy, and the basic sequence of events is well known.[1-3] However, the mechanisms involved and the precise manner in which leukocytes pass through the vessel wall are still not fully understood. An investigation of the fine structural alterations in inflammation has been made in dogs. We have observed changes in small vessels which further elucidate the processes involved in the localization and emigration of leukocytes. Our preliminary observations have already appeared in brief [4] and differ somewhat from the results in similar studies by Marchesi and Florey.[5]

MATERIAL AND METHODS

Material for this study consisted of pancreas from 5 dogs in which acute inflammation was produced by ligation of pancreatic lobules. Tissue adjacent to ligatures was removed from the side with intact circulation after intervals of 1, 2, 3 and 4 hours. Blocks of tissue approximately one cu. mm. in size were fixed in Dalton's "chrome-osmium" fixative [6] for 1 to 1½ hours. They were then dehydrated rapidly in a series of graded ethanol solutions, infiltrated in a mixture of uncatalyzed methacrylate (7 parts butyl methacrylate to 1 part methyl methacrylate) followed by infiltration in the same mixture catalyzed with benzoyl peroxide. Embedding was carried out in a partially polymerized methacrylate mixture in gelatin capsules. Polymerization was completed at 60° C. overnight. Tissue was also placed in Zenker-formol fixative for light microscopy.

Sections for both phase and electron microscopy were cut with a Servall Porter-Blum microtome. Sections were examined in an RCA EMU 2B or 2E electron microscope at original magnifications of 1,000 to 10,000 times; further enlargements were made photographically. Thick sections from tissue embedded in methacrylate were stained by a periodic acid-Schiff (PAS)-methylene blue technique [7] and viewed with the light microscope.

OBSERVATIONS

Normal

The fine structure of the normal capillary has been described by Palade,[8] Moore and Ruska,[9] and Bennett, Luft and Hampton.[10] The

Supported by the United States Public Health Service, Grants No. A-1226 and No. CRT-5017.

Accepted for publication, April 10, 1961.

* National Cancer Institute Trainee.

† Life Insurance Medical Research Fund Fellow.

inflammatory changes to be related occurred in vessels in the acinar portion of the pancreas. The endothelium of these vessels contained scattered mitochondria, ergastoplasm and Golgi material, and the cytoplasm itself was often very thin (Fig. 1). Nuclei were flattened but protruded somewhat into the vessel lumen. Small vesicles about 200 to 300 Å in diameter were most conspicuous just beneath plasma membranes; the latter were generally smooth, except for indentations where vesicles opened on the surface and for small cytoplasmic projections at points of contact with adjoining cells. At such points the plasma membranes were often focally thickened to form terminal bars. A thin, irregular layer of amorphous substance on the luminal margin of endothelial cells (Fig. 1) probably represented intercellular cement substance.[11] A rather prominent, homogeneous basement membrane surrounded the entire vessel. Varying numbers of cells, usually fibroblasts or macrophages, were located in the perivascular space.

Changes Associated with Inflammation

Examination of hematoxylin and eosin-stained sections revealed the characteristic appearances of acute inflammation (Fig. 3). Although the dimensions of the processes to be described were within the limits of resolution of the light microscope, we were unable to identify them with absolute certainty in conventionally stained paraffin sections.

Inflammatory alterations observed by electron microscopy occurred primarily in small, thin-walled vessels which lacked a muscular coat. Development of intraluminal cytoplasmic processes and large intracytoplasmic vesicles were the first clearly defined changes in the endothelium (Fig. 2). These vesicles were much larger (1 μ in diameter) than those seen in normal capillaries; however, they appeared to arise in an analogous manner and to be formed of infolded plasma membranes. In most instances the cytoplasmic projections were thought to represent finger-like processes since many of them were round or oval in cross section. They were quite long (up to 8 μ) and thin (not more than 1μ) and were often irregular in configuration and thickness and formed odd-shaped hooks or loops. They contained many small vacuoles but few cytoplasmic organelles. In some areas the endothelial processes were so numerous and extensive as to form a network in the vessel lumen (Fig. 4). These were best seen in tangential sections.

Leukocytes appeared to become enmeshed in these processes and were then gradually enveloped and surrounded by endothelial cytoplasm (Figs. 4 to 6). Some appeared to be contained within the cytoplasm of single cells; on the other hand, many obviously lay between endothelial cells (Figs. 8 and 11). When numerous white cells were enmeshed and

enveloped in this manner (Fig. 4), the appearance in adjacent sections examined by light microscopy was that of margination.

Occasional leukocytes were adherent to the surface of endothelial cells without any evidence of endothelial spikes or enveloping processes in the plane of section (Fig. 7). In such cases, roughening and interdigitation of cytoplasm of both leukocytes and endothelium occurred in the area of contact.

Subsequent to margination, white cells emerged from the anti-luminal margin of endothelial cells. At points of exit, endothelial cytoplasm

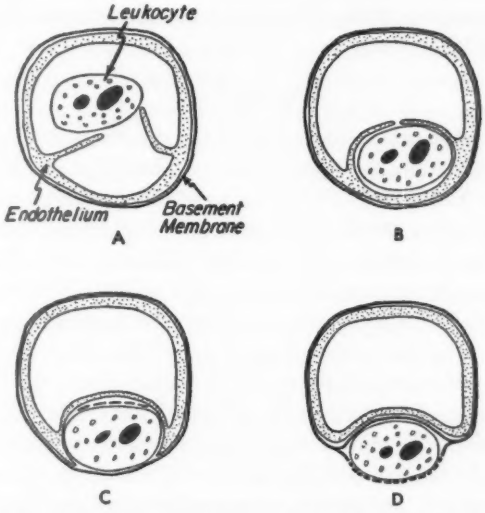

TEXT-FIGURE 1. Schematic representation of leukocytic emigration in acute inflammation. A. Development of long finger-like endothelial processes in which leukocytes become enmeshed. B. Envelopment of an enmeshed leukocyte by endothelial cytoplasm. C and D. Formation of a new basement membrane (dotted line) between the leukocyte and endothelium as the leukocyte emerges from the extraluminal margin and separates from the endothelium. The new basement membrane is continuous with the pre-existing perivascular membrane. The perivascular basement membrane separating the leukocyte from the extravascular space ultimately undergoes fragmentation and dissolution, releasing the leukocyte into the extravascular space.

became markedly attenuated and eventually separated (Figs. 6 and 9 to 11). Leukocytes were then separated from the extravascular space only by the basement membrane. Alterations in the latter structure during emigration of white cells were complex. When the leukocyte was completely surrounded by endothelial cytoplasm, a space of about 100 Å was discernible between the plasma membranes of the two cells. After the antiluminal border of the endothelial cell was breached and the two cells had separated by as much as 200 to 300 Å, new basement mem-

brane, continuous with the original one, formed between them (Figs. 10 to 12). Concomitant with the formation of the new basement membrane, the outermost membrane separating leukocytes from the extravascular space became frayed and smudged and ultimately disintegrated (Fig. 12). Dissolution of this portion of the basement membrane released the white cells into the extravascular space. This sequence of events is depicted diagrammatically in Text-figure 1.

Almost all of the cells emigrating were neutrophils, although occasional lymphocytes and red blood cells were seen. No distinct changes were noted in the white cells. An amorphous substance similar to the cement substance on endothelial plasma membranes was also present on the surface of leukocytes.

Discussion

The sequence of events occurring during the emigration of white cells in acute inflammation has been lucidly outlined by the Clarks[1] and by Allison, Smith and Wood[2] from studies utilizing transparent ear chambers in rabbits. In normal uninjured capillaries, blood flows smoothly with no tendency of white cells to stick to endothelium. Subsequent to injury, a temporary period of "sticking" of white cells is followed by a prolonged period of margination and then actual emigration through the vessel wall. In similar preparations, Florey[3] has described roughening of endothelium in areas of inflammation. Cells caught on the roughened endothelium were deformed by the force of the blood stream. Florey[3] interpreted this endothelial roughening to represent projections or spikes on which leukocytes were caught. The endothelial processes revealed by electron microscopy may indeed represent these spikes. Roughening and interdigitation of cytoplasm occasionally observed in the area of contact of leukocytes and endothelium in the absence of such processes could also produce the same picture.

In electron microscopic studies of leukocytic emigration in the rat mesentery, Marchesi and Florey[5] observed no changes in the endothelium. Moreoever, we have observed no endothelial changes in studies of acute inflammation in rat skin. In other acutely inflamed tissues in the dog, endothelial alterations have not appeared with the frequency observed in the pancreas. These observations may be related to differences in species and organ reaction to inflammation or to the nature of the inflammatory agent. The true significance of these endothelial processes and what role, if any, they play in the localization of leukocytes are therefore still open to question. Certainly leukocytic emigration is not dependent upon the development of such processes in the rat. Their character and appearance in the present study suggest that under these

experimental conditions endothelial cells participated actively in the localization of white cells. That this is a highly selective process is indicated by the paucity of red cells and lymphocytes participating in the process.

Allison and co-workers[2] observed a striking decrease in sticking of leukocytes in cortisone-treated rabbits after trauma. In the light of the present observations, it is interesting to speculate what effect, if any, cortisone might have on the development of endothelial processes and the roughening of endothelial plasma membranes.

Only rarely were white cells observed sticking to endothelium in the absence of endothelial processes or roughening. Subsequent margination would appear to be associated with the envelopment of white cells by cytoplasmic processes. Although it was difficult to ascertain whether or not leukocytes were contained completely within the cytoplasm of individual endothelial cells, many of them unquestionably occupied an intercellular position. Serial-section reconstructions would be required to prove the former condition.

In most instances the luminal border of endothelial cells was reformed by approximation of endothelial processes before leukocytes reached the opposite side. Leukocytes emerging from the extra-luminal margin of the capillary were situated between the endothelial cell and its basement membrane. By the time they were separated from the endothelial cell by a space of approximately 200 to 300 Å, a new basement membrane, continuous with the original basement membrane on either side, was formed between them. The outermost basement membrane then apparently melted away, releasing the white cell into the perivascular space. By these processes white cells reached the perivascular space without any continuous defect or communication between vessel lumen and extravascular space. Thus the functional integrity of the vessel wall was maintained while white cells passed through it.

The development of large vesicles within endothelial cytoplasm is suggestive of an increased rate of fluid transport across the vessel wall. It is of interest that similar intra-endothelial vacuoles have been observed in many organs in rabbits given hypertonic fluids intravenously, with resultant diuresis and a net transfer of fluid from the outside to the inside of the vessel.[12] Since edema is a well-established component of acute inflammation and represents an accumulation of extravascular fluid in inflamed tissues, the vacuoles observed in the present study may represent active transport of fluid to the outside of the vessel wall.

No distinct quantitative or qualitative changes were noted in the amorphous "cement substance" on the endothelial surfaces or in similar material on the plasma membranes of leukocytes. This is in contrast to

Zweifach's *in vivo* observations in rats [11] of the elaboration of considerable amounts of gelatinous material by endothelium after micro-trauma. In agreement with the observations of Florey, Poole and Meek,[13] scarcely any cement substance was discernible between endothelial cells. Moreover, in keeping with the observations of Allison and Lancaster,[14] no fibrin or fibrin-like substance was seen on the endothelial surface.

Summary

Acute inflammation was produced in dogs by ligation of pancreatic lobules. The earliest changes observed were vacuolation of endothelial cytoplasm and the development of numerous cytoplasmic processes projecting into the vessel lumen. Leukocytes, predominantly neutrophils, appeared to become enmeshed in these processes and were subsequently completely enveloped by endothelial cytoplasm. As leukocytes emerged from the extra-luminal margin of endothelial cells and began to separate from them, a new basement membrane formed between the two. The outermost layer of basement membrane then disappeared, permitting release of the leukocytes into the extravascular space.

By these mechanisms, leukocytes passed through both the endothelium and the vascular basement membrane without any evidence of a mural defect communicating between the vessel lumen and the extravascular space. Under the experimental conditions employed, endothelium appeared to participate very actively in these activities and a striking specificity for neutrophils was manifested.

References

1. Clark, E. R., and Clark, E. L. Observations on changes in blood vascular endothelium in the living animal. *Am. J. Anat.*, 1935, **57**, 385–438.
2. Allison, F., Jr.; Smith, M. R., and Wood, W. B., Jr. Studies on the pathogenesis of acute inflammation; inflammatory reaction to thermal injury as observed in the rabbit ear chamber. *J. Exper. Med.*, 1955, **102**, 655–676.
3. Florey, H. W. General Pathology; Based on Lectures Delivered at the Sir William Dunn School of Pathology, University of Oxford. W. B. Saunders Co., Philadelphia and London, 1957, ed. 2, pp. 47–66.
4. Williamson, J. R., and Grisham, J. W. Leucocytic emigration from inflamed capillaries. *Nature, London*, 1960, **188**, 1203.
5. Marchesi, V. T., and Florey, H. W. Electron micrographic observations on the emigration of leucocytes. *Quart. J. Exper. Physiol.*, 1960, **45**, 343–348.
6. Dalton, A. J. A chrome-osmium fixative for electron microscopy. *Anat. Rec.*, 1955, **121**, 281.
7. Finke, E. Personal communication.
8. Palade, G. E. Fine structure of blood capillaries. (Abstract) *J. Appl. Physics*, 1953, **24**, 1424.
9. Moore, D. H., and Ruska, H. The fine structure of capillaries and small arteries. *J. Biophys. & Biochem. Cytol.*, 1957, **3**, 457–462.

10. BENNETT, H. S.; LUFT, J. H., and HAMPTON, J. C. Morphological classifications of vertebrate blood capillaries. *Am. J. Physiol.*, 1959, **196**, 381–390.

11. ZWEIFACH, B. The exchange of materials between blood vessels and lymph compartments. In: Connective Tissues. Transactions of the 5th Conference, Josiah Macy, Jr., Foundation, New York, 1954, pp. 38–77.

12. LUSE, S. A. Personal communications.

13. FLOREY, H. W.; POOLE, J. C. F., and MEEK, G. A. Endothelial cells and "cement" lines. *J. Path. & Bact.*, 1959, **77**, 625–636.

14. ALLISON, F., JR., and LANCASTER, M. G. Studies on the pathogenesis of acute inflammation. II. The relationship of fibrinogen and fibrin to the leucocytic sticking reaction in ear chambers of rabbits injured by heat. *J. Exper. Med.*, 1960, **111**, 45–64.

The authors wish to thank Dr. W. S. Hartroft for much helpful advice and criticism.

[*Illustrations follow*]

Legends for Figures

FIG. 1. A normal capillary in the dog pancreas. The endothelium is continuous and surrounded by a basement membrane (BM). The nucleus (N) of the endothelial cell bulges into the lumen, and several vesicles (V), mitochondria (M), and Golgi bodies (G) are seen in the cytoplasm. Extravascular space, ES; acinar cells, A; basement membrane, BM. × about 9500.

FIG. 2. An acutely inflamed capillary exhibits numerous cytoplasmic processes (CP) and large vesicles (LV). Nucleus, N; vesicles, V; basement membrane, BM; extracellular space, ES. × about 9500.

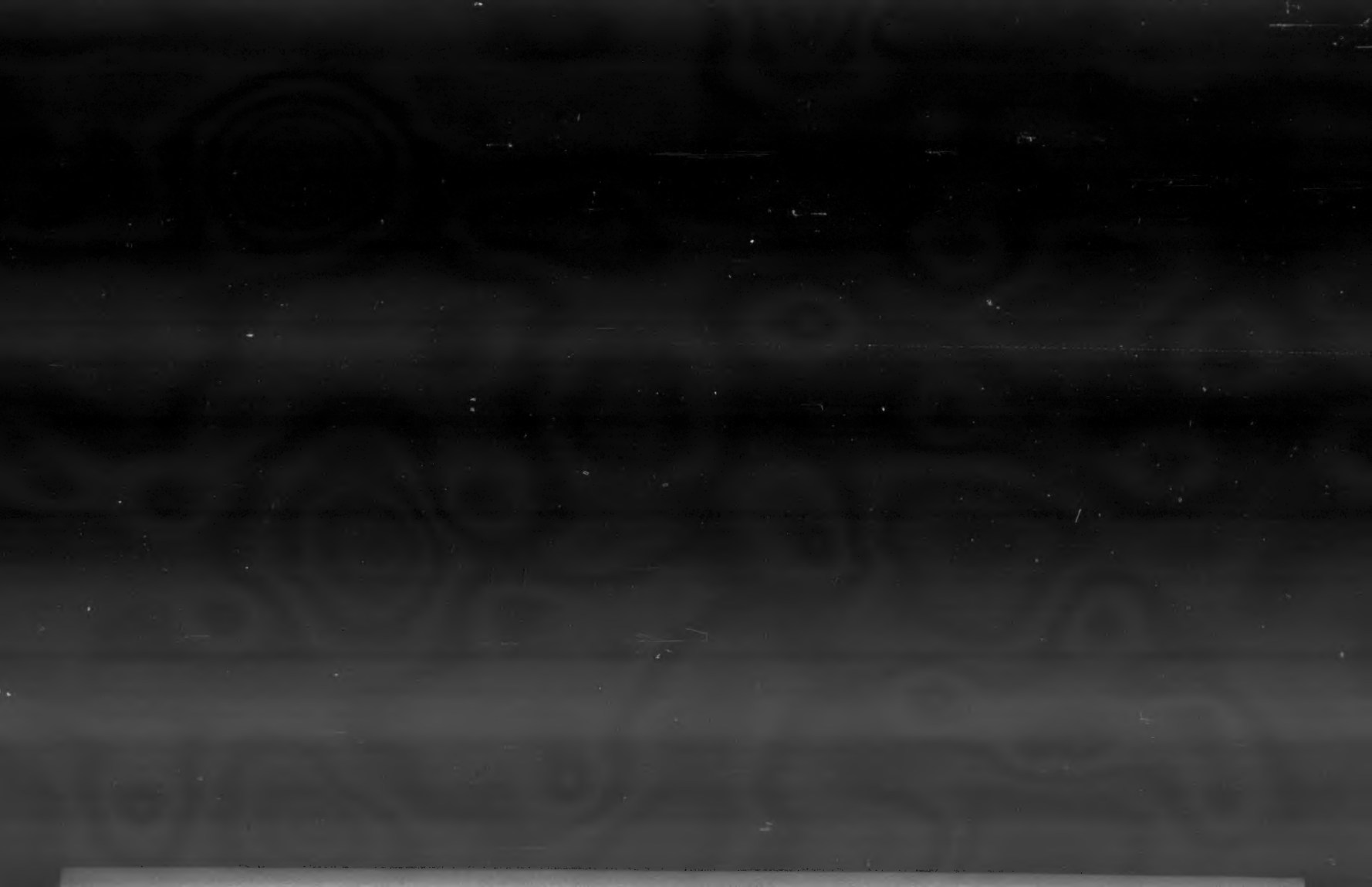

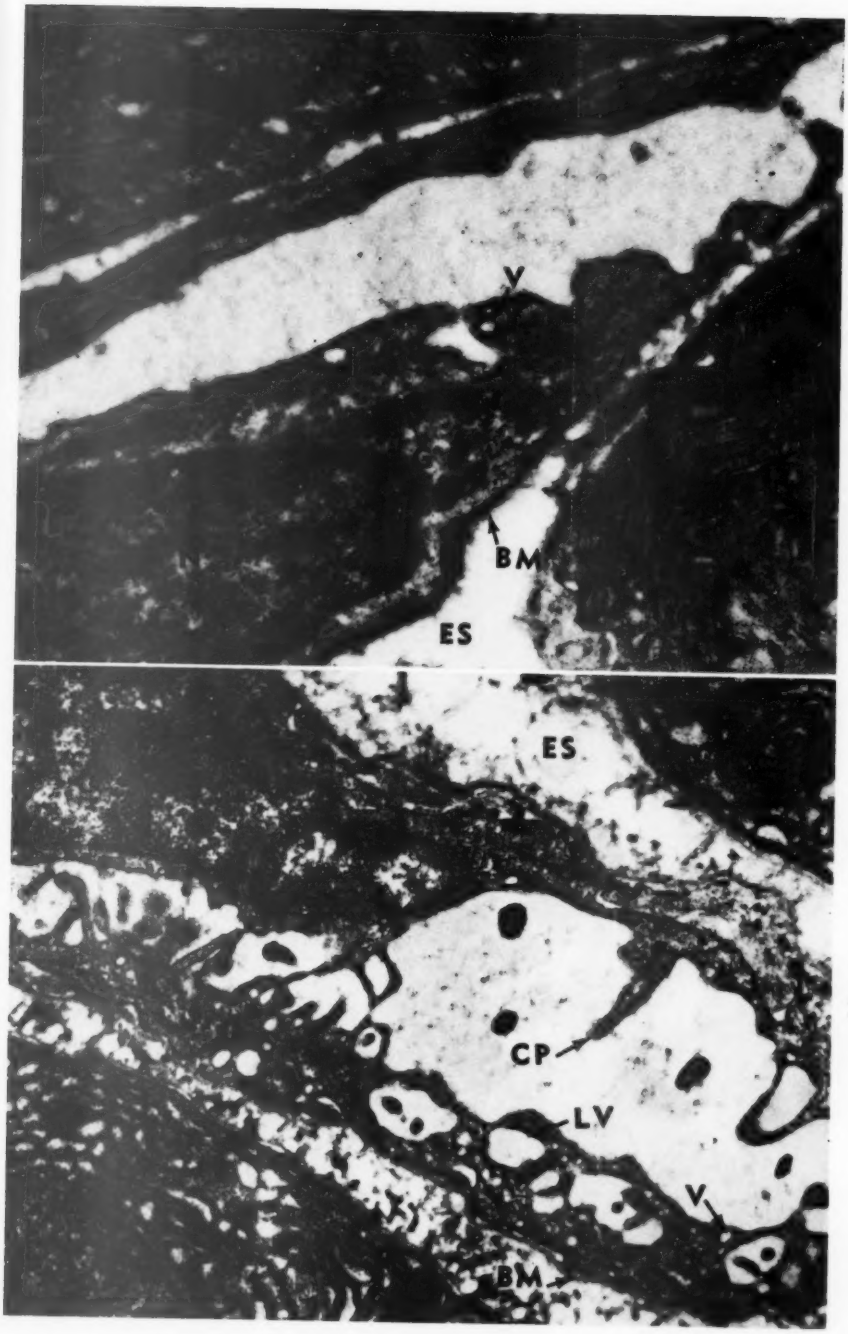

1

2

FIG. 3. Acute inflammation of a pancreatic vessel with many leukocytes in the lumen and the vessel wall. Hematoxylin and eosin stain. × 590.

FIG. 4. A composite electron photomicrograph of an acutely inflamed vessel in which many leukocytes (L) are enmeshed in the endothelium, giving the appearance of margination. Erythrocyte, E; extravascular space, ES. × about 2600.

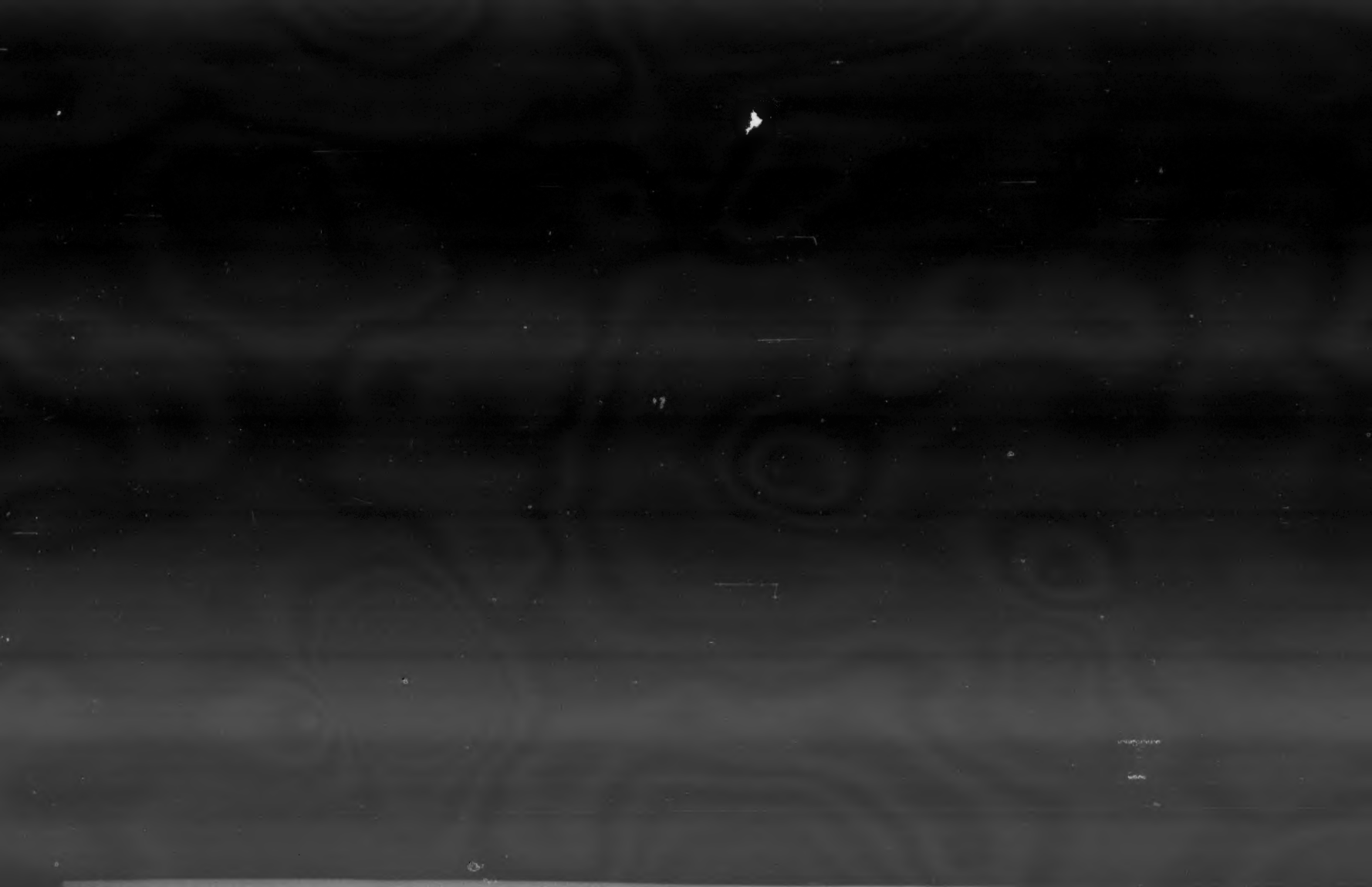

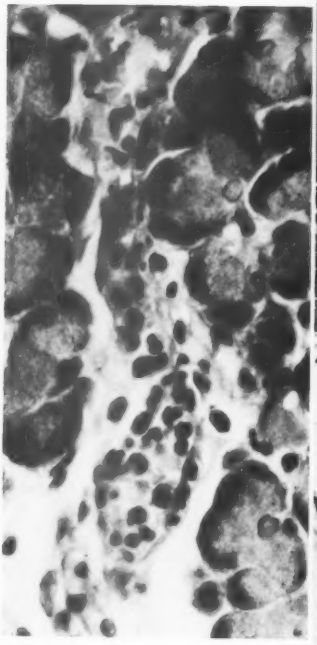

3

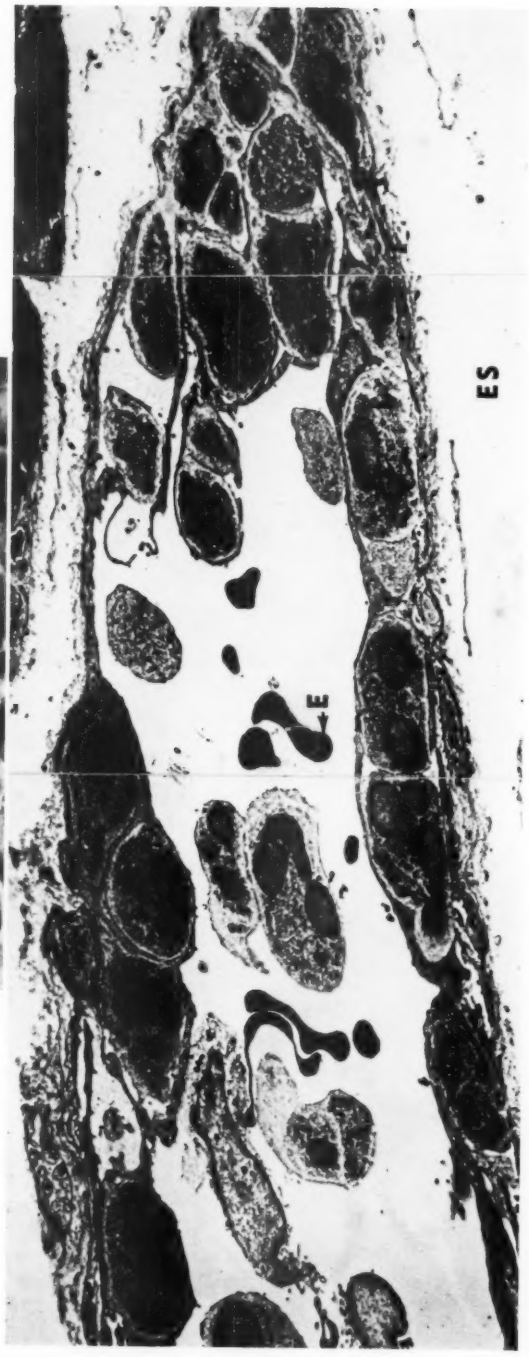

4

FIG. 5. An acutely inflamed vessel in which several neutrophils (L) are trapped by long endothelial cytoplasmic processes (CP). Capillary lumen, CL. × about 9500.

FIG. 6. A leukocyte (L) is almost completely enveloped by endothelial cytoplasmic processes (CP) except for a very narrow segment (S). Nucleus of leukocyte, N; capillary lumen, CL. × about 18,000.

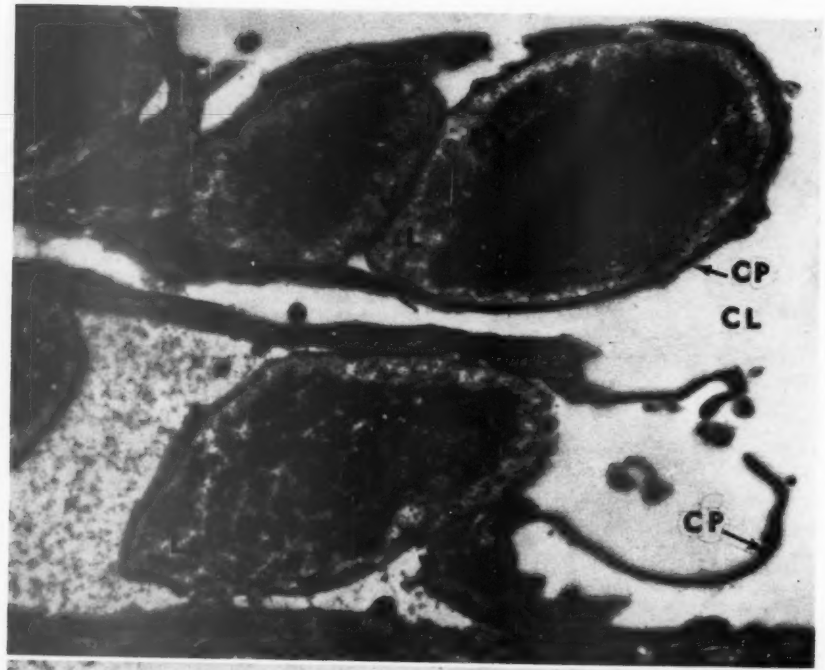

5

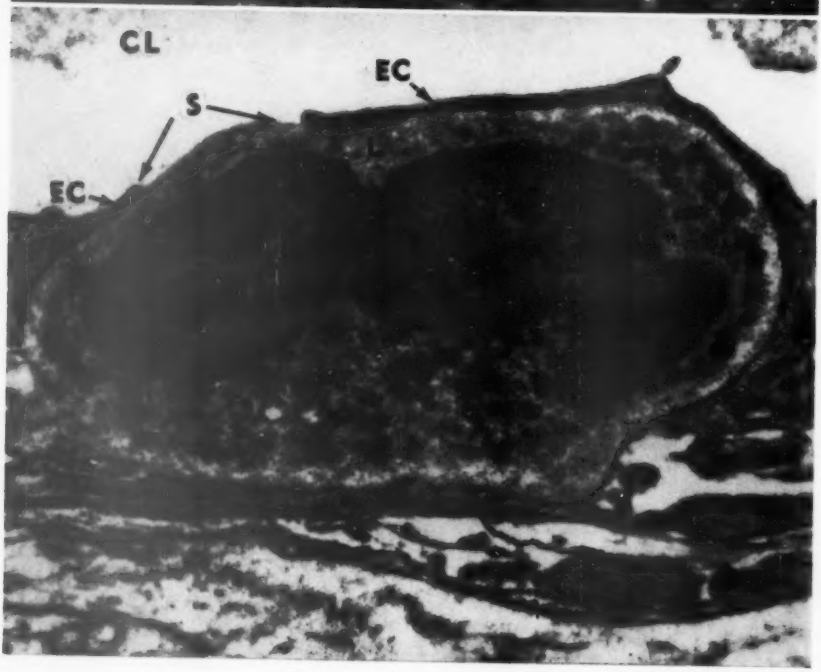

6

FIG. 7. A leukocyte (L) is stuck to an endothelial cell (EC), with roughening and interdigitation of cytoplasm of both cells in the area of contact. × about 18,000.

FIG. 8. Portions of several leukocytes (L) are situated between endothelial cells (EC). Capillary lumen, CL; extravascular space, ES. × about 9800.

7

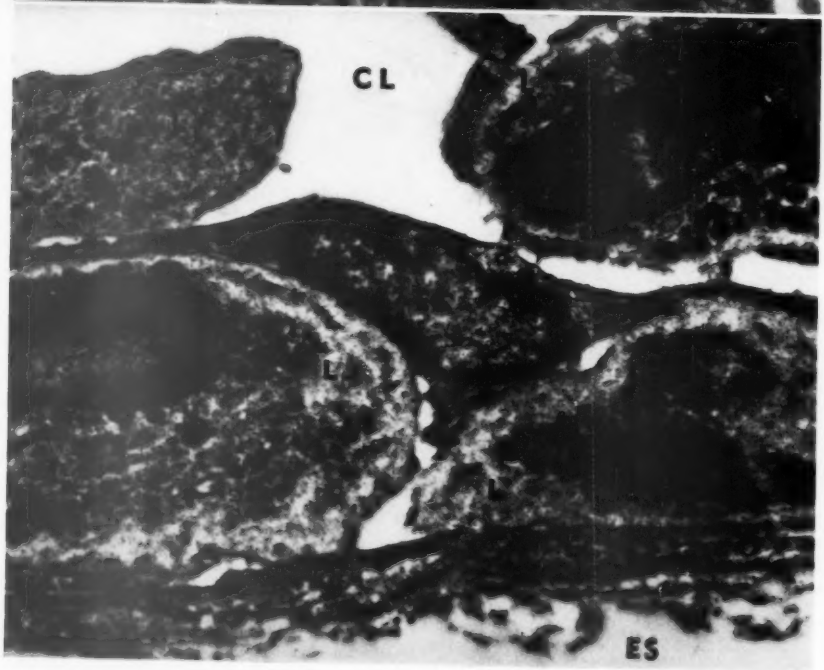

8

FIG. 9. Portions of two leukocytes (L) are completely enveloped by endothelial cytoplasm (EC). In the lower left corner the leukocyte is separated from the extravascular space (ES) only by basement membrane (BM). Nucleus of endothelial cell, N; capillary lumen, CL. × about 10,000.

FIG. 10. A leukocyte (L) is situated between endothelium (EC) and vascular basement membrane (BM). In the lower right corner, only basement membrane separates the leukocyte from the extravascular space (ES). Segments of a new basement membrane (NBM) are forming between the endothelial cell and the leukocyte. Capillary lumen, CL. × about 14,000.

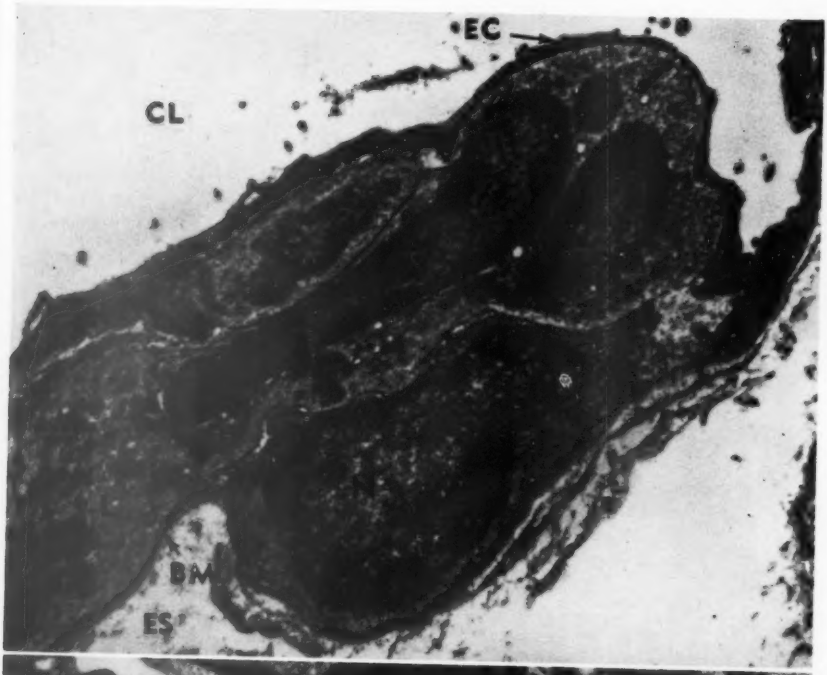

9

10

11

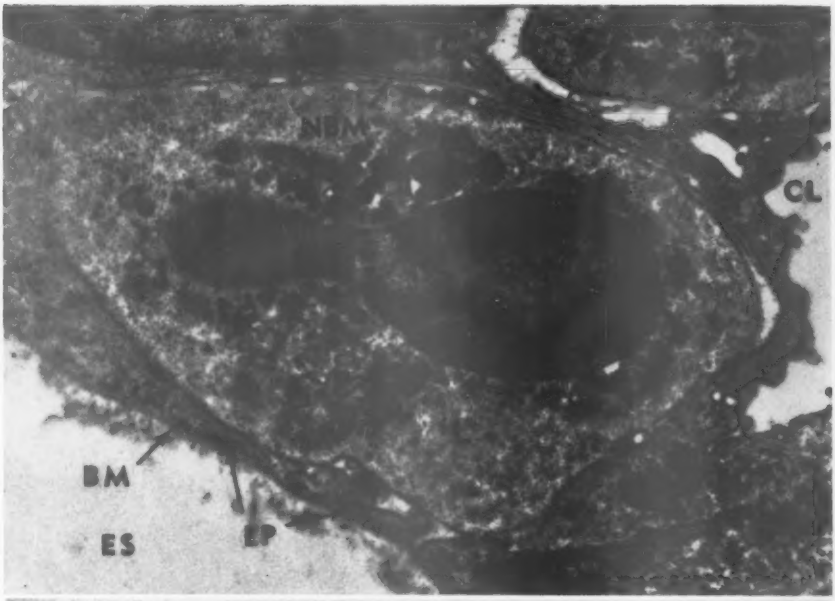

12

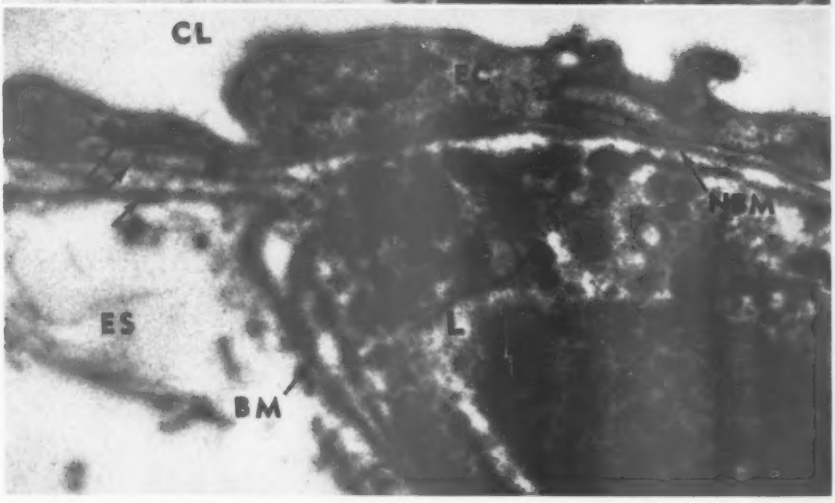

FIG. 11. A leukocyte (L) lies situated between two endothelial cells (EC) and is separated from the extracellular space (ES) only by basement membrane (BM) and endothelial processes (EP). A newly formed basement membrane (NBM) is present between the leukocyte and the endothelial processes. Capillary lumen, CL. × about 15,000.

FIG. 12. A portion of a leukocyte (L) is situated with basement membranes on both the extravascular margin (BM) and the endothelial cell margin (NBM—a new basement membrane). To the left of the leukocyte, 3 distinct layers of basement membrane (arrow) are discernible. Capillary lumen, CL; endothelial cell. EC; extravascular space, ES. × about 33,000.